THICK BRAIN SLICE CULTURES AND A CUSTOM-FABRICATED MULTIPHOTON IMAGING SYSTEM: PROGRESS TOWARDS DEVELOPMENT OF A 3D HYBROT MODEL

A Thesis
Presented to
The Academic Faculty

by

Komal Rambani

In Partial Fulfillment
of the Requirements for the Degree
Master of Science in the
School of Biomedical Engineering

Georgia Institute of Technology
MAY, 2007

THICK BRAIN SLICE CULTURES AND A CUSTOM-FABRICATED MULTIPHOTON IMAGING SYSTEM: PROGRESS TOWARDS DEVELOPMENT OF A 3D HYBROT MODEL

Approved by:

Dr. Steve M. Potter, Advisor
School of Biomedical Engineering
Georgia Institute of Technology

Dr. Ravi V. Bellamkonda
School of Biomedical Engineering
Georgia Institute of Technology

Dr. T. Richard Nichols
School of Physiology
Emory University

Date Approved: 3rd January, 2007.

To my Grand Parents and my Family

ACKNOWLEDGEMENTS

There are several people to whom I would like to acknowledge for their support and help for my M.S. thesis research. First of all, I would like to thank my advisor, Dr Steve Potter, for giving me opportunity for my graduate research work in such an interesting research field. I wish to acknowledge his tremendous support for my education and excellent guidance for my research work. Under his supervision, I learned fine instrumentation and experimental skills that will prove to be great assets to my future career. I would like to acknowledge that as a result of the fine instrumentation training that I acquired under his supervision, I was invited to present in conference (invited talk) and teach a hands-on workshop which is a great honor for a student. Next, I would like to thank my thesis committee members Dr Ravi Bellamkonda and Dr Richard Nichols for their marvelous guidance and support. I gratefully acknowledge the NIH, NSF, CBN, and the Whitaker funding to support this research work.

I am indebted to my Bioengineering Research Partnership (BRP) collaborators for accommodating me as a team member, and for helping and advising me on my research work. I especially thank Professor Ari Glezer and Jelena Vukasinovic for superb collaboration and support for “thick brain slice cultures” project. It is a fantastic experience to work with them. My special thanks also go to Maxine McClain and Eno Ekong for teaching me brain slicing. I acknowledge Kacy Cullen and Zenas Chao for helping me with the statistical analysis of my data. I am grateful to NIH for distributing an excellent software “ImageJ” for free that is very helpful for several image processing and imaging data analysis applications. I acknowledge Johnafel Crowe for providing me

training on multiphoton imaging, and also to accommodate my long imaging or multiphoton construction schedules without which my projects would not have come to completion in a timely manner.

I would like to thank excellent administrative staff for their help. My special thanks to Amber Burris, Bryan Williams, Chris Ruffin, and Beth Bullock Spencer for several helpful events and their support to students. I gratefully acknowledge excellent Georgia Tech student services. I realized how warm and supportive the Georgia Tech community is, when they supported me in my crisis times and helped me to bring my smiles back.

I especially thank to Maxine McClain, Jelena Vukasinovic and Yoonsu Choi. I will always remember all the good laughs and support you gave me in my good and bad times! I thank to Potter group members for their constant support. I am thankful to Zenas Chao and Douglas Bukkam from whom I learned a lot of things. I also want to thank undergraduate researchers who worked with me or in Potter group during these projects. I can never forget Bobby Thompson, Ryan Hanes, Herna, Chris Grubb, and Juan Estrada for good times that we shared while working in the lab. You guys are the best and most hardworking undergraduates I have ever met!

I thank to all the people who helped me directly and indirectly in enhancing my personality. Thanks to “natural problem solvers” for teaching me a lot of things and ingraining a new level confidence in me. The laboratory of neuroengineering at Georgia Tech is a great place to get education. Not only one learns about cutting-edge research here; but also it provides a dynamic environment of human behavior and interactions to an observer. I especially am impressed with the skills of people who are not only keenly

engaged their research but also promote responsible conduct in research and teach ethics to younger generations of scientists and engineers. They are doing a great work to teach these to students which helps them to survive and do justice in the advanced level of their career. I feel grateful to opportunities to interact with such great personalities from time to time.

Last but not least, I acknowledge enormous support from my husband and family. I thank to all my friends with whom I shared great times while studying at Georgia Tech. It is really a great experience to be a part of Georgia Tech community.

TABLE OF CONTENTS

LIST OF TABLES

LIST OF FIGURES

SUMMARY

Development of a three dimensional (3D) HYBROT[1] model with targeted *in vivo* like intact cellular circuitry in thick brain slices for multi-site stimulation and recording will provide a useful *in vitro* model to study neuronal dynamics at network level. In order to make this *in vitro* model feasible, we need to develop several associated technologies. These technologies include development of a thick organotypic brain slice culturing method, a three dimensional (3D) micro-fluidic multielectrode Neural Interface system (μNIS) and the associated electronic interfaces for stimulation and recording of/from tissue, development of targeted stimulation patterns for closed-loop interaction with a robotic body, and a deep-tissue non-invasive imaging system. To make progress towards this goal, I undertook two projects: (i) to develop a method to culture thick organotypic brain slices, and (ii) construct a multiphoton imaging system that allows long-term and deep-tissue imaging of two dimensional and three dimensional cultures.

Organotypic brain slices preserve cytoarchitecture of the brain. Therefore, they make more a realistic reduced model for various network level investigations. However, current culturing methods are not successful for culturing thick brain slices due to limited supply of nutrients and oxygen to inner layers of the culture. We developed a forced-convection based perfusion method to culture viable 700μm thick brain slices.

Multiphoton microscopy is ideal for imaging living 2D or 3D cultures at submicron resolution. We successfully fabricated a custom-designed high efficiency multiphoton microscope that has the desired flexibility to perform experiments using multiple technologies simultaneously. This microscope was used successfully for 3D and time-lapse imaging.

Together these projects have contributed towards the progress of development of a 3D HYBROT.

---

[1] A hybrid system of brain slice cultures (brain) and robot (body)

CHAPTER 1

INTRODUCTION

The brain controls our actions by two way communication with the body and its interaction with the environment. Since the past decade, it is becoming more widely accepted that behaviors are encoded in particular activity patterns that underlie the cytoarchitecture of networks of neurons in the brain [18, 25, 27, 32, 33, 34]. However, the correlation between the two properties, the activity patterns and the morphological connectivity underlying a behavior, is not understood. This makes one of the fundamental questions in neuroscience.

At present, current technologies do not allow high-resolution multisite imaging and electrophysiology simultaneously on *in vivo* preparations. Further, use of any of these techniques is limited to restricted, anesthetized, or non behaving model animal preparations. A hybrid system of a living neuronal network interfaced to a robotic body (HYBROT) via an electronic interface may provide a simpler *in vitro* model to study network properties underlying learning and memory using multiple non-invasive technologies simultaneously. Microelectrode arrays (MEA) and multiphoton laser scanning imaging (MPLSM) methods provide the means to study functional and morphometric network properties simultaneously using a HYBROT model.

Brain slice cultures preserve *in vivo* like cyto-architecture and offer several advantages over *in vivo* models due to easy tissue accessibility and controllability of input/output variables while using multiple techniques simultaneously. Development of a

three dimensional neuro-robotic hybrid model (3D HYBROT) with targeted intact cellular circuitry of thick brain slices for stimulation and recording will allow understanding of neuronal dynamics in the brain at the network level underlying learning and memory.

With the current culturing methods one can successfully culture organotypic brain slices [36, 114]. However, the thick brain slice cultures suffer necrosis in the center of the tissue due to insufficient supply of nutrients resulting from these diffusion-based methods [114]. A convection-based perfusion method that allows flow of oxygenated nutrient medium through the thickness of the tissue will ensure nutrient supply to every cell. This may allow enhanced viability resulting from the forced-convection perfusion based restoration of the circulatory system of the tissue.

To test this hypothesis, an infusion-withdrawal type micro-perfusion chamber that can be modified to incorporate three dimensional electrodes, was fabricated, optimized and used to culture 700μm thick brain slices. The perfusion of oxygenated nutrient medium successfully demonstrated enhanced viability of thick brain slice cultures. I further investigated viability of the cultures as a function of flow-rates to determine an optimal range of the non-invasive perfusion rates. Additionally, I investigated qualitatively morphological and electrophysiological properties of the perfused cultures compared to fresh tissue slices and control (unperfused) cultures.

To study long-term morphological dynamics in two- and three- dimensional networks of neurons along with concurrent multisite electrophysiology, it is required to have a flexible, efficient, non-invasive, and high resolution imaging system. Mark Booth and I constructed a multiphoton-only microscope with desired flexibility of design to

accommodate electrophysiology and life supporting fluidic paraphernalia for concurrent imaging, electrophysiology and perfusion. These two projects have contributed towards essential progress in the development of a 3D HYBROT model.

This thesis is organized as follows. The first two chapters provide introduction and background to the projects undertaken. Chapter three provides a framework to briefly introduce the reader to fluorescence microscopy and the advantages of multiphoton microscopy over other (conventional and confocal) imaging modes. Chapters four and five discuss in detail the design, construction and validation of a flexible custom fabricated multiphoton imaging system. I also point towards future directions in the further development and improvement of this system.

In chapter six, the design, working principle, fabrication, and characterization of a novel forced-perfusion based micro culture chamber are described. I used this device to validate our hypothesis that forced perfusion of oxygenated medium may allow enhanced viability of 700μm thick brain slices compared to unperfused sister cultures. Additionally, I characterized the range of flow rates amenable to cultured tissue for enhanced viability.

The chapter seven explicates qualitative characterization of organotypic organization of the cultures, and recording of spontaneous or chemically evoked electrical activity of these cultures using a single electrode. In the last chapter, I make recommendations for future work for further characterization of these cultures, both, morphologically and electrophysiologically. I give directions to elaborate this study with other suggested flow rates and perfusion paradigms to complete flow characterization for enhanced tissue viability. I also discuss possibilities to modify the culture chamber for

larger and thicker cultures that may benefit several other neuroscience investigations requiring thick brain slice or co-cultures.

This thesis has six appendices. Appendix A provides a step-by-step user manual to operate our custom made multiphoton microscope. Appendix B presents a trouble-shooting manual to optimize the multiphoton microscope for its best performance. In Appendix C, a detailed protocol to set up the fluidic system and the details of the culturing method are given. Appendix D provides detailed methods to label and image cultures for viability assessment and organotypic organization. Appendix E describes methods to analyze data using ImageJ software. In the last appendix, abstracts of published works related to these projects are listed.

CHAPTER 2

BACKGROUND

The human brain is a remarkably complex organ. It not only produces and controls one's thoughts, actions, memories, feelings, experiences, and habits, but also plays vital role in voluntary and involuntary control of the vital organs to lead a normal life. How the brain encodes (learning) and reliably retrieves information (memory) underlying various simple and complex behaviors is one of the fundamental questions in neuroscience research.

In the past few decades, scientists have developed several techniques and experimental models, both *in vivo* and *in vitro,* to study various properties underlying the functioning of the brain. From a century of neuroscience investigations, it is evident that every behavior is encoded in a network of several neurons. On one side, several behavioral studies have shown morphological changes underlying learning and memory [25, 32, 39, 52]; on the other hand, several *in vivo* functional recordings have shown characteristic activity patterns related to a behavior [18, 33, 34]. Likewise, other *in vitro* studies show there are morphometric changes associated with activity of neurons [13]. At present, we recognize several mechanisms underlying neuronal plasticity, such as long term potentiation (LTP), long term depression (LTD), spike timing dependent plasticity (STDP), etc. Current technologies do not allow one to study morphological and electrophysiological properties simultaneously on *in vivo* preparations. Understanding

how morphology and activity are correlated will inform much about the network properties of neurons underlying the encoding and storing of information.

An *in vitro* neuronal preparation allows non-invasive multisite electrophysiology and imaging of the neuronal network simultaneously using extracellular microelectrode arrays and multiphoton imaging. Due to controlled inputs/outputs, better accessibility, absence of interference from peripheral inputs, and their amenability to the use of multiple technologies concurrently, *in vitro* preparations provide a much simpler platform to understand neuronal functioning.

Learning is defined as encoding of information that the brain receives from sensory organs when an animal behaves in its environment. However, *in vitro* preparations lack sensory inputs and do not have any meaning to motor outputs. Our laboratory is developing a novel hybrid *in vitro* model of artificially embodied neuronal cultures with robotic bodies (HYBROTS) to study learning and memory at the network level (figure 2.1). This ambitious project requires several technologies to work simultaneously in real time which include development of long-term neuronal cultures, hardware and software for real-time closed-loop recording and stimulation of neuronal networks, pattern recognition in the recorded data and their assignment to motor commands (behavior), translation of robot (or simulated animal[2]) behavior to stimulation patterns to send sensory information to the cultured neuronal network, and a non-invasive sub-micron resolution imaging system amenable to electrophysiology and fluidic equipment. Our current and alumni laboratory members have successfully developed

---

[2] ANIMAT

long-term dissociated cortical neuronal cultures on flat multielectrode arrays (figure 2.2), real-time closed-loop recording and stimulation of neuronal networks (figure 2.3), and electrical stimulation patterns to control activity of the dissociated cultured neurons [20, 21, 97,98,102,103, 121-125]. We are currently working towards pattern recognition in the recorded data and their assignment to motor commands (behavior), translation of robot (or ANIMAT) behavior to stimulation patterns to send sensory information to cultured neuronal networks [14].

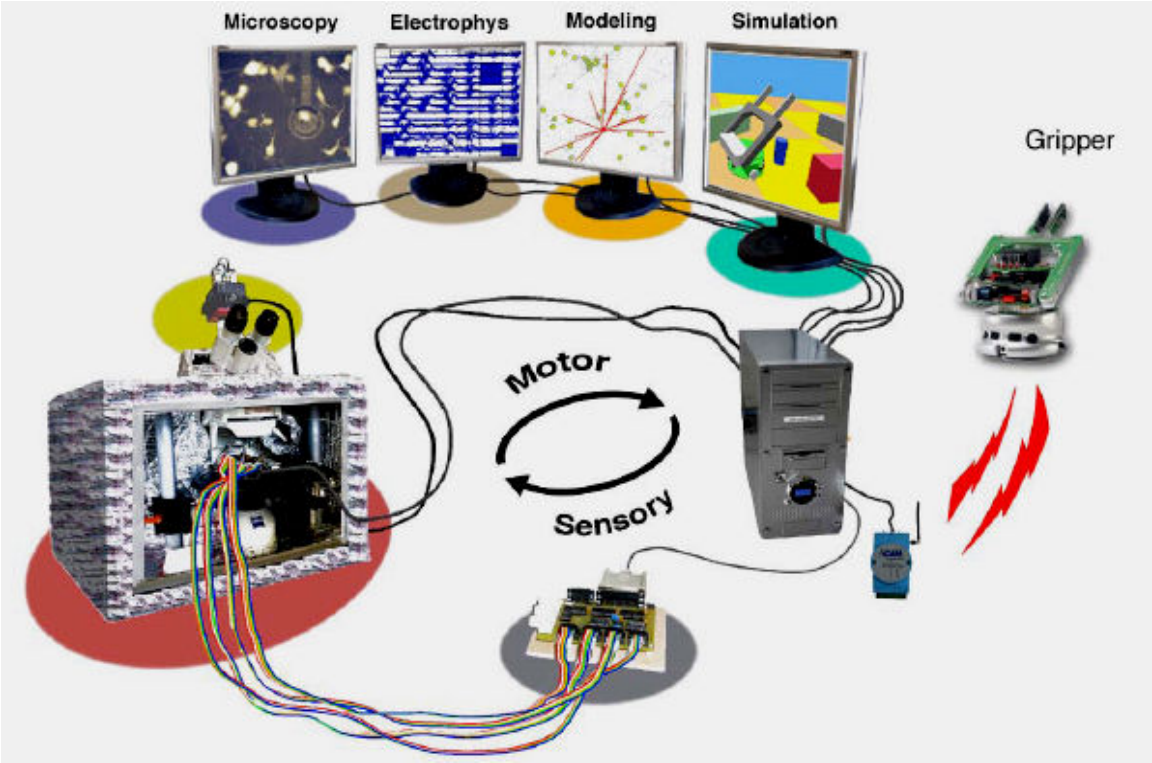

Figure 2.1. A HYBROT Model to study learning and memory *in vitro*.
A dissociated culture of a few thousand neurons plated on a planar multielectrode array (MEA) is interfaced to a robotic body. The activity patterns of the neurons in MEA dish are encoded as simple motor commands that allow robotic body to behave in its environment. The behavior of the robotic body is encoded in stimulation patterns that are delivered to neuronal network using multielectrode array. A closed-loop hybrid embodied system thus created is a simple *in vitro* model to study learning and memory. Along with simultaneous multiphoton imaging, this system provides non-invasive techniques to record activity and morphology of the neuronal network at once. (Drawing: Zenas Chao)

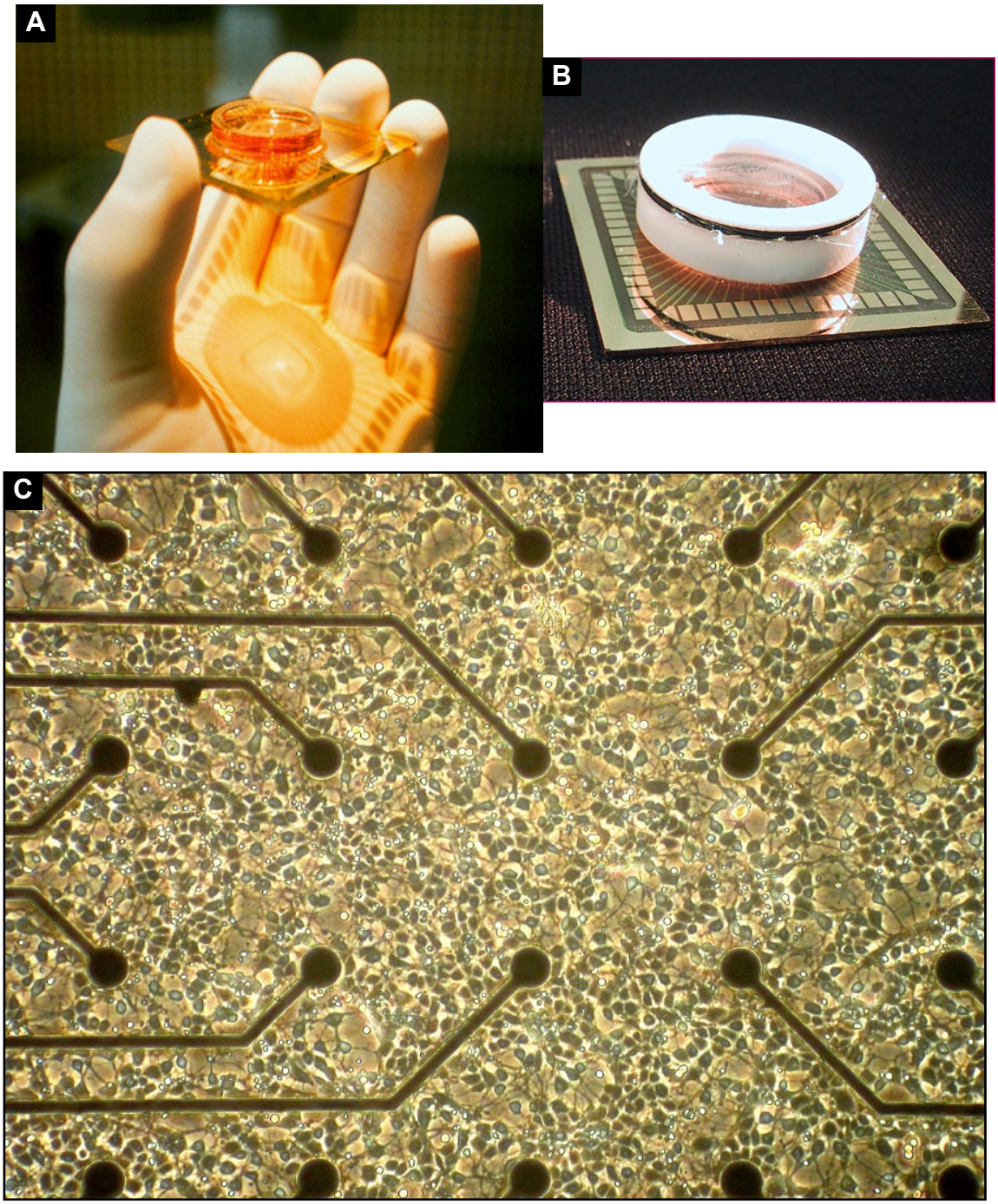

Figure 2.2. Multielectrode Array dish for two dimensional neuronal cultures.
[A] A multielectrode array dish. The central part of the dish contains an 8x8 array of 30µm diameter microelectrodes that are separated by 200µm from each other. The electrode contacts are carried to the outer electrode pads for preamplifier contact. **[B]** A multielectrode array dish sealed with a gas permeable teflon membrane. This enclosed chamber allows long-term viability of culture by preventing bacterial and fungal infections, and maintaining osmolarity by preventing evaporation of medium. **[C]** An image of high density dissociated cortical neuronal culture plated on multielectrode array.

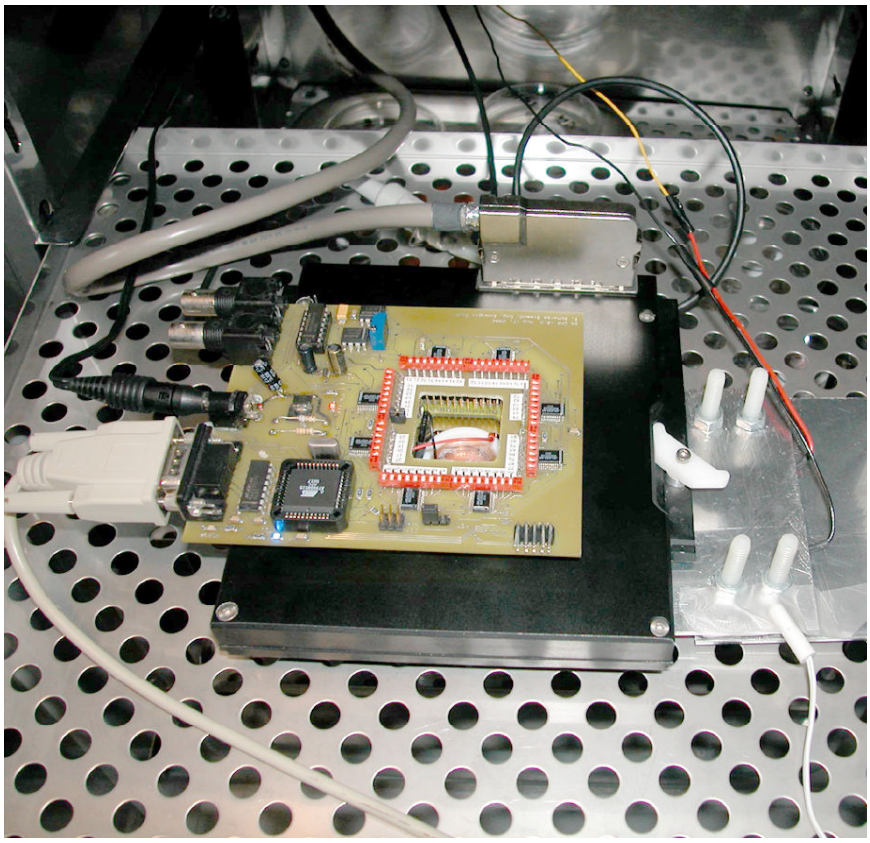

Figure 2.3. Multielectrode electrophysiology recording and stimulation set-up.
This set-up contains preamplifier and custom-made all-channel stimulation system. To perform simultaneous electrophysiology and imaging, microscope should be able to accommodate this system along with microfluidic system (in case of 3D cultures).

Although dissociated flat cultures represent neuronal networks that may encode information, it is argued that three dimensional cultures are a better representation of the *in vivo* like network organization. In fact, it is believed that there is stereotypic network circuitry of neurons underlying an activity pattern. Further, some studies show evidence that activity patterns shape the micro-architecture of these circuits [15, 29].

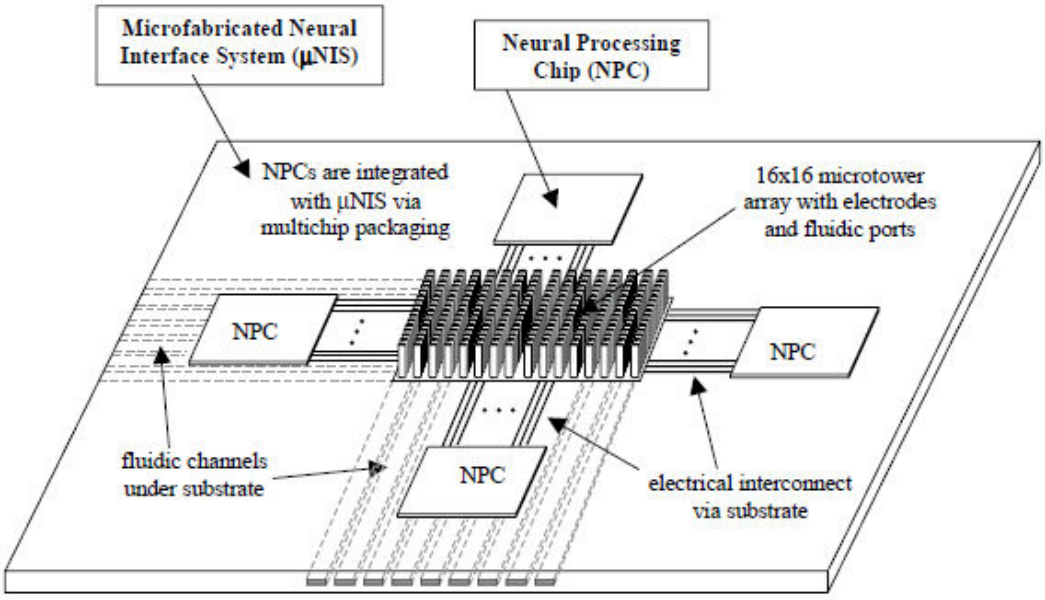

Figure 2.4. Schematic diagram of microfluidic multielectrode neural interface system proposed in a bioengineering research partnership grant.

Organotypic brain slice cultures preserve intact cytoarchitecture of the brain. Thus, a hybrid model that includes an entire cortical thickness slice embodied with a robot (3D HYBROT) would be a more *in vivo* like model of learning and memory. To advance our 2D HYBROT technology to 3D HYBROTS, there are two potential technology developments required: first, a method to culture thick organotypic brain slices, and second, a three dimensional multielectrode array that supports healthy organotypic brain slice cultures. In collaboration with our bioengineering research partners (BRP), we are constructing three dimensional microfluidic multielectrode arrays that will have 1000 electrodes for targeted interface of cortical slices for stimulation and recording from different cortical layers (figures 2.4, 2.5, 2.6). Development of a method to culture thick brain slices and a 3D microfluidic microelectrode neural interface system

will eventually enable us to define stimulation and recording from different cortical layers and would be a more *in vivo* like model.

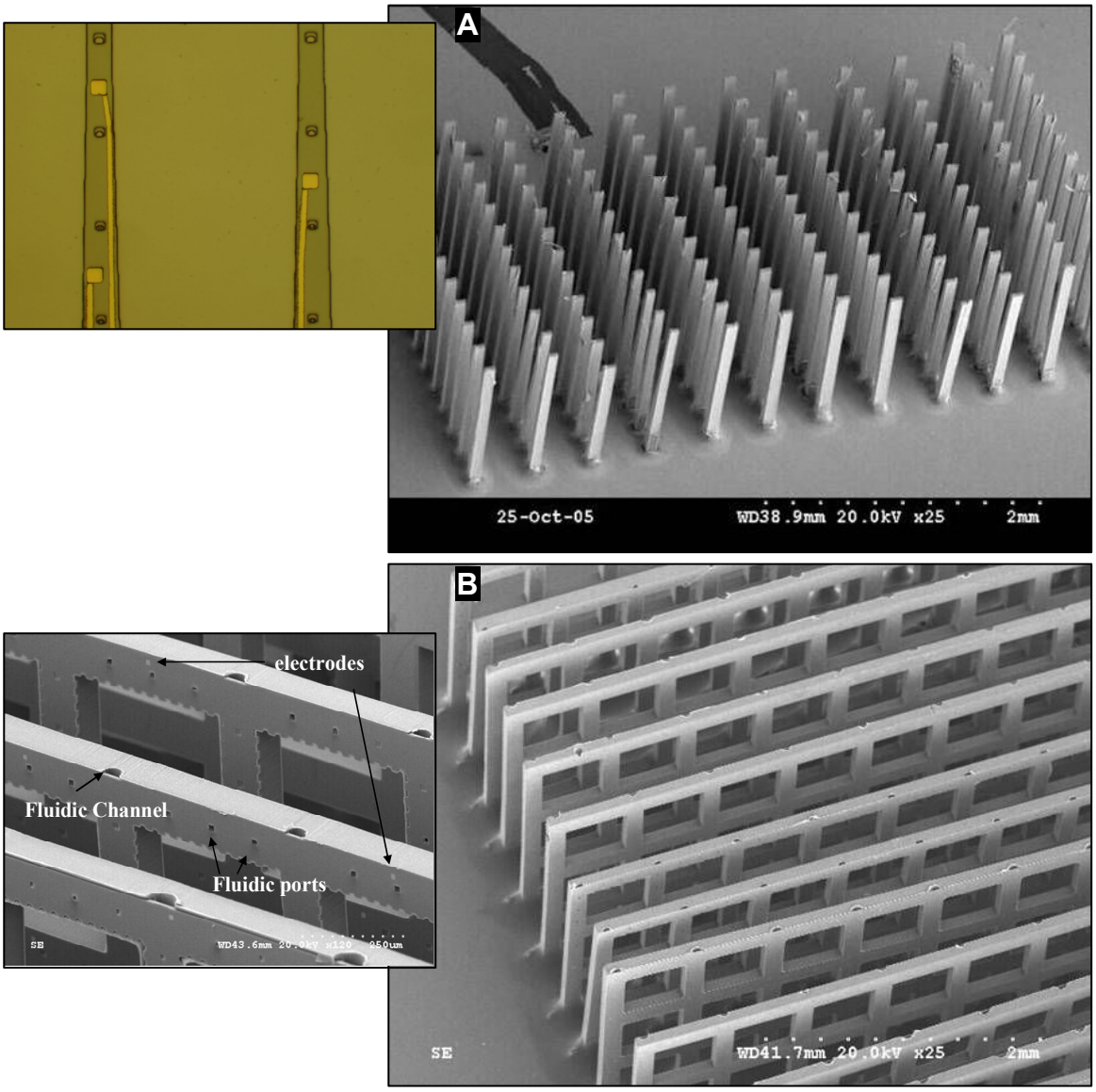

Figure 2.5. Three dimensional microfluidic multielectrode arrays.
[A] Right, Prototype structure of a three dimensional microfluidic multielectrode array for brain slice cultures. Left, picture of two towers with microfluidic ports and microelectrodes. The size of the fluidic ports increases gradually with height of the tower to maintain uniform flow as a result of pressure drop. The fluidic towers are 1mm tall hollow structures that contain fluidic port from bottom to top at every 100µm. The towers taper from bottom to top with tip dimension of 24µmx80µm **[B]** Right, A prototypic structure of a three dimensional microfluidic multielectrode array with cross-bars to support three dimensional dissociated neuronal cultures in bioactive gel scaffolds. Left, enlarged microtowers showing fluidic side ports, fluidic channels and microelectrodes. (Image courtesy: Laura Rowe, BRP collaborator.)

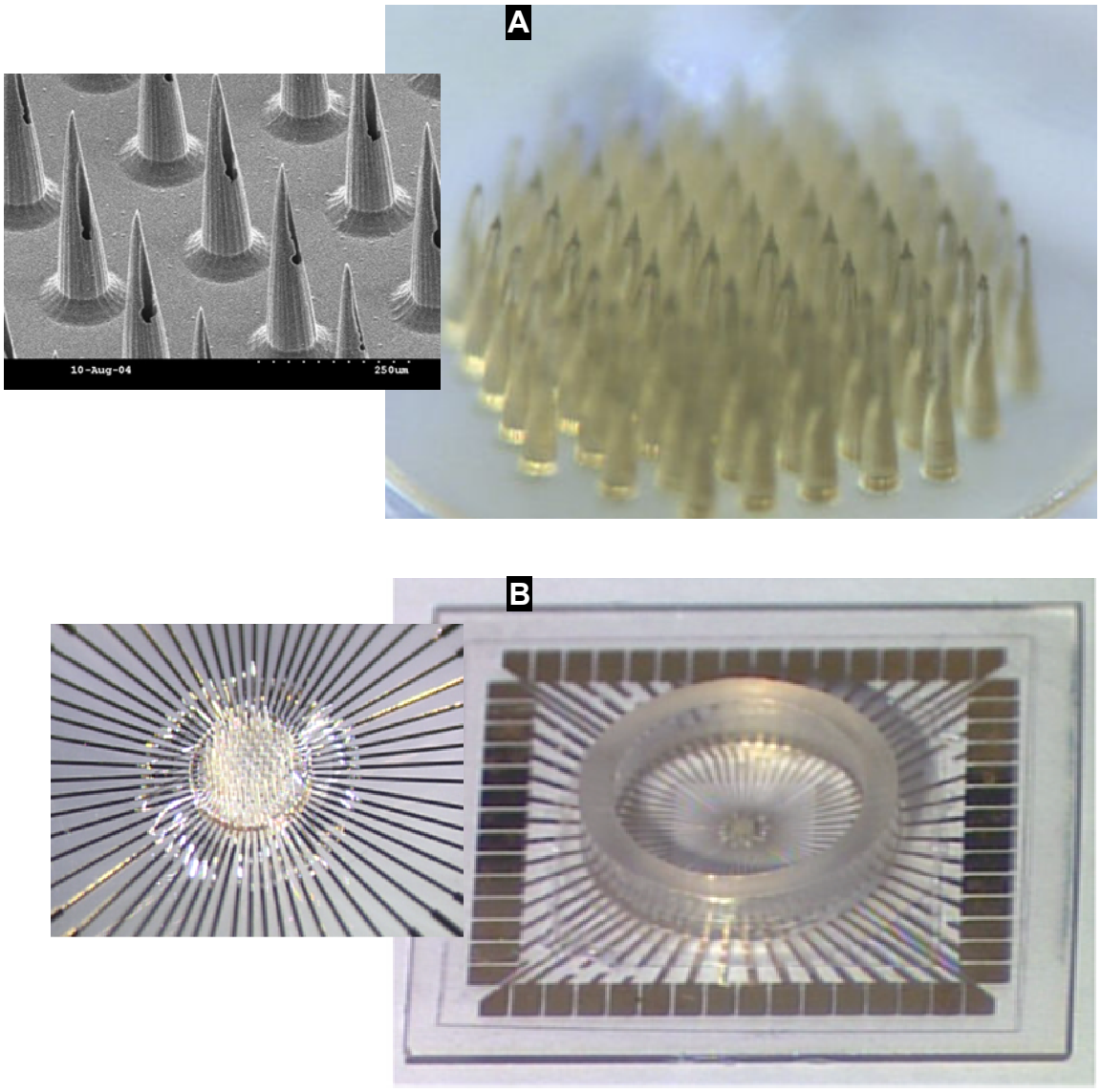

Figure 2.6. Pyramidal three dimensional microfluidic multielectrode arrays.
[A] Right, prototypic structure of tapered microfluidic array with one oval shaped fluidic port. Left, SEM picture of towers showing oval microfluidic port. **[B]** Prototypic structure of three dimensional multielectrode arrays. (Image courtesy: Yoonsu Choi)

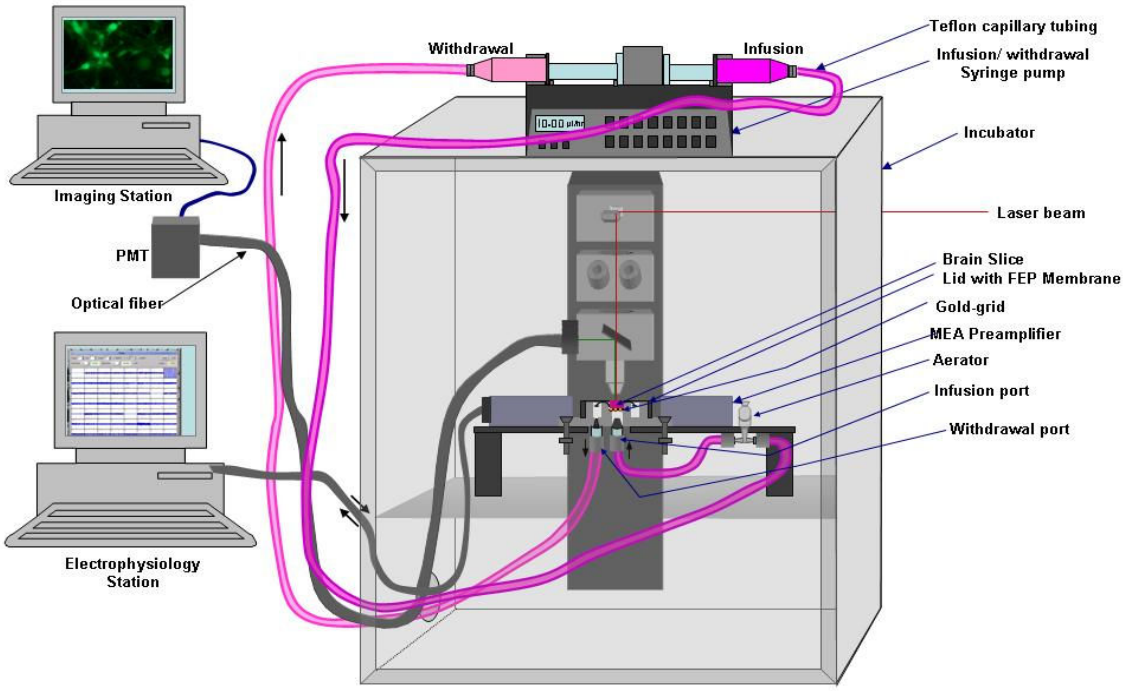

Figure 2.7. Schematic diagram of experimental setup for simultaneous imaging and electrophysiology on three dimensional organotypic brain slice cultures. This is possible with the flexible design of our custom fabricated multiphoton microscope that can accommodate other experimental setups, too.

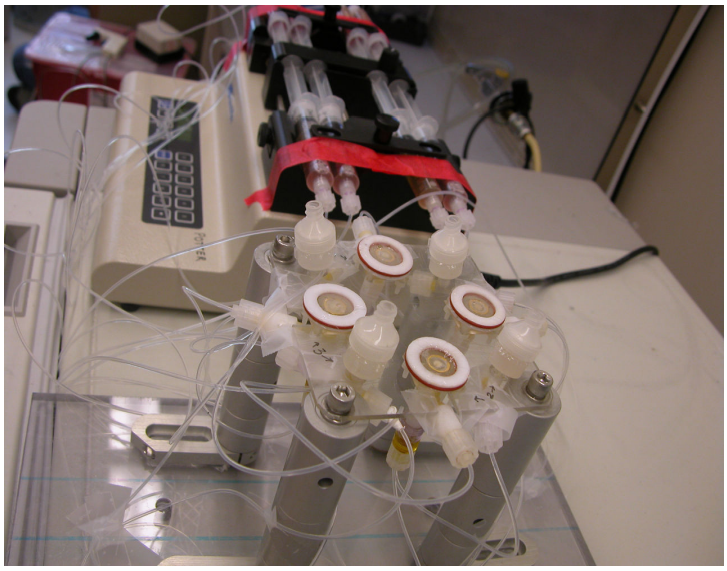

Figure 2.8. An experimental fluidic setup to culture organotypic thick brain slices.

The other side of the HYBROT learning project involves the ability to image the network morphology at sub-micron level non-invasively along with electrophysiology. A multiphoton microscope is ideal for such needs. As a BRP team member, my contribution to 3D HYBROT project involved :(i) development of a flexible custom fabricated multiphoton imaging system that can accommodate other technology platforms like multielectrode electrophysiology recording/stimulation platform and microfluidic setup while imaging, (figure 2.7) and (ii) development of a method to culture thick organotypic brain slices.

Currently, the commercially available multiphoton microscopes have a compromised optical design because they retain their one photon confocal imaging mode. Additionally, these microscopes have inflexible designs which do not allow accommodation of other technical platforms needed for an experiment requiring simultaneous electrophysiology and/or fluidic delivery to the tissue culture. I have custom designed and fabricated a multiphoton-only imaging system with flexible design based on Tsai et al [118]. This system will allow us to image deeper in the thick specimens and perform long-term live cell imaging in future.

The circulatory system of brain tissue gets destroyed during the slicing process, thus hindering supply of sufficient nutrients to cells to meet their metabolic needs. Thin organotypic brain slices can be cultured using the roller tube method and the static membrane insert method [35, 114]. However, these methods provide diffusion-limited supply of nutrients and oxygen to the interior layers of cells of the tissue resulting in necrosis of cells in the center of the slice. We have developed and optimized a novel microfluidic device for convection based forced-perfusion of oxygenated nutrient

medium through the thickness of the brain slice. This method allowed us to optimize 700µm thick cortical slice cultures (figure 2.8). We further characterized these cultures by morphological and electrophysiological activity of these cultures. We anticipate that thick organotypic brain slice cultures will also benefit several other neuroscience and neuroengineering studies.

CHAPTER 3

INTRODUCTION TO FLUORESCENCE MICROSCOPY

ABSTRACT

Today, fluorescence imaging spans wide spectrum in modern biological investigations from molecular to network level at submicron resolution. To take advantage of full potential of advanced fluorescence imaging techniques, it is important to understand some underlying physical principles. This chapter provides a framework to understand basic principles underlying fluorescence, fluorescence microscopy, one-photon and multi-photon laser-scanning microscopy, and advantages of multiphoton imaging of live tissue over single-photon imaging.

INTRODUCTION

Knowledge of various experimental techniques is an important factor for performing successful research in the interdisciplinary biomedical research. Fluorescence imaging is one of the great tools for various biological investigations. Over the past century, fluorescence microscopy has evolved from linear to various non-linear imaging methods because of its recognized power in biological (and non biological) research requiring submicron resolution of imaging. These imaging methods have revolutionized various investigations from molecular to cellular to network level in modern biological and biomedical research due to its advantages over other techniques or as a complementary method to other techniques.

Multiphoton microscopy is a relatively new, non-linear fluorescent imaging method that is gaining popularity with every passing day in various research investigations due to its several advantages over other fluorescence imaging methods in some key areas of biological investigations. In this chapter, there is a brief introduction to basics concepts of fluorescence microscopy, various fluorescence microscopes and differences in the various fluorescent imaging methods, and advantages of multiphoton microscopy over the confocal microscopy. This chapter is designed to introduce some fundamentals for understanding of fluorescence microscopy that will aid in understanding terminology used in the next two chapters of this thesis.

THE ELECTROMAGNETIC SPECTRUM

Human eyes are sensitive to only a subset of the entire electromagnetic spectrum that is known as the visible spectrum. The wavelengths of the visible spectrum range from ~ 400 – 700nm (figure 3.1).

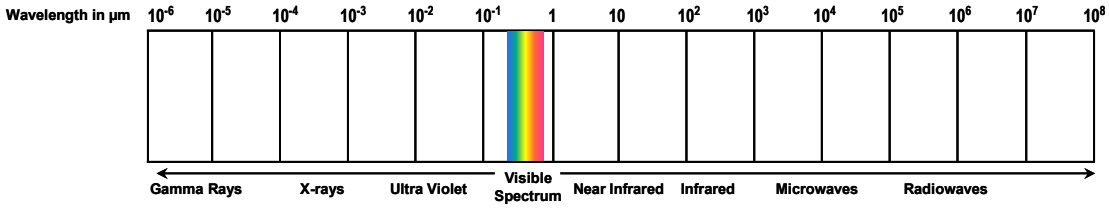

Figure 3.1: The entire electromagnetic spectrum and the visible spectrum.

There are two fundamental laws of the electromagnetic radiation, Planck's law and Rayleigh's scattering law, that are related to the topics explained in next two chapters. Planck's law states that the energy of a photon is inversely proportional to its wavelength λ.

$$E = h.\nu = h.\frac{c}{\lambda}$$ Equation 3.1

where h = Planck's constant and c = speed of light in vacuum. Therefore, shorter (bluer) wavelengths have higher energy than longer (redder) wavelengths. The Rayleigh scattering principle states that the intensity of the scattered photons, I, is inversely proportional to the fourth power of their wavelengths, λ.

$$I\alpha\frac{1}{\lambda^4}$$ Equation 3.2

In other words, the scattering of blue light is ~ 9.4 times as great as that of red light for equal incident intensities.

PHYSICS OF FLUORESCENCE

In accordance with its electronic configuration, every molecule or atom has a ground state of its electrons and the singlet or triplet excited states. The ground and excited energy levels are separated by a characteristic energy difference called band gap energy. Each molecule or atom can absorb incident photons of energy equivalent to its energy band gap to reach one of its excited states, and emits longer wavelength photons to come back to its ground state. The molecules that can absorb in ultra violet (UV), visible, or near infrared (IR) spectra and can emit photons in the visible regime are called fluorophores. The process of emission of photons in visible regime, after the excited molecule or atom returns back to its ground state is called fluorescence.

More formally, the fluorescence activity can be schematically illustrated with the classical Jablonski diagram (figure 3.2). These schematic diagrams were first proposed

by Professor Alexander Jablonski in 1935 to describe absorption and emission spectra of light. Under normal conditions, the electronic configuration of the molecule is described to be in the ground state in these diagrams. The ground state and the excited states are separated by the characteristic band gap energy of the molecule. Due to vibrational spectra, these states are further split into different energy levels. When a photon of energy equal to band gap energy of the molecule hits electrons in the ground state, there is high probability that these electrons can absorb the energy of the impinging photons and are raised to a higher electronic energy states (excited states), a process that may only take a femto-second (i.e.10^{-15} seconds). The electrons in the higher energy states can transition to other higher vibrational singlet energy states or triplet states by non-radiative energy loss depending on their quantum states. Eventually, they release the excessive energy in the form of photons of longer wavelength and return to the ground state of the molecule (atom). The emitted photons in the visible regime are called fluorescent signal. Due to transition of electrons to different vibrational energy states from ground to excited levels, each fluorophore has excitation and emission spectra (figure 3.3).

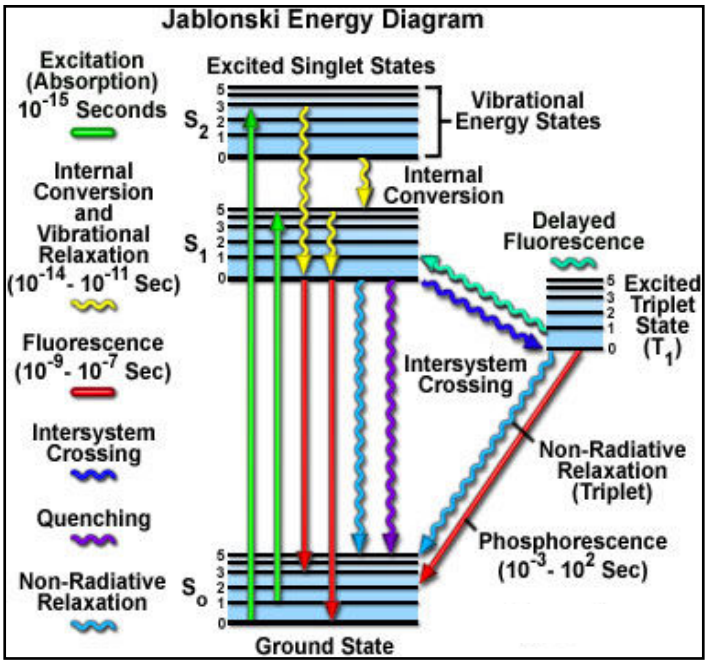

Figure 3.2: Jablonski Energy diagram to show fluorescence fundamentals. A fluorescent molecule has ground state (S0) and excited singlet states (S1, S2) and triplet states (T1). The singlet and triplet states have several vibrational energy states. Several closely located electronic transitions are possible from different vibrational energy levels of ground state to different vibrational energy level of excited states and vice versa. These possibilities result in the spectral bandwidth of the excitation and emission spectra of the molecule. (Picture Courtesy: Prof Michael Davidson)

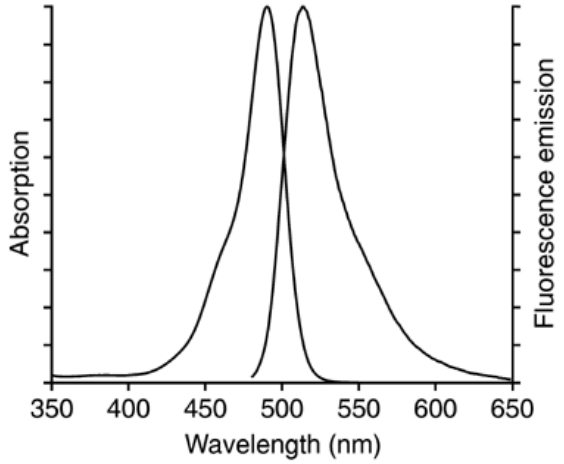

Figure 3.3: An Example of Excitation and Emission spectra of a fluorophore. Each fluorophore has an excitation and an emission spectra. Generally, in one photon excitation, the excitation wavelengths are smaller than the emission wavelengths. (data courtesy: Invitrogen. Data: Fluorescein molecule).

ONE-PHOTON VERSUS MULTIPHOTON EXCITATION

In one photon excitation, the electrons in the ground state absorb the impinging photons of energy equivalent to the energy band gap to reach the excited state. These electrons eventually come back to ground state by releasing excess energy as photons of longer wavelengths (figure 4B). In 1930, Nobel Laureate Maria Goeppart Mayer first predicted in her theoretical calculations the possibility of fluorophore excitation by absorption of multiple photons of total (sum) energy equal to energy band gap (figure 4B) [44]. The absorption of two photons simultaneously by the electrons in the ground state of fluorophores requires very high density of photons. Owing to this condition, the excitation of the fluorophore occurs only at the focal volume of the specimen compared to overall excitation of the specimen illuminated in one-photon excitation (figure 3.4).

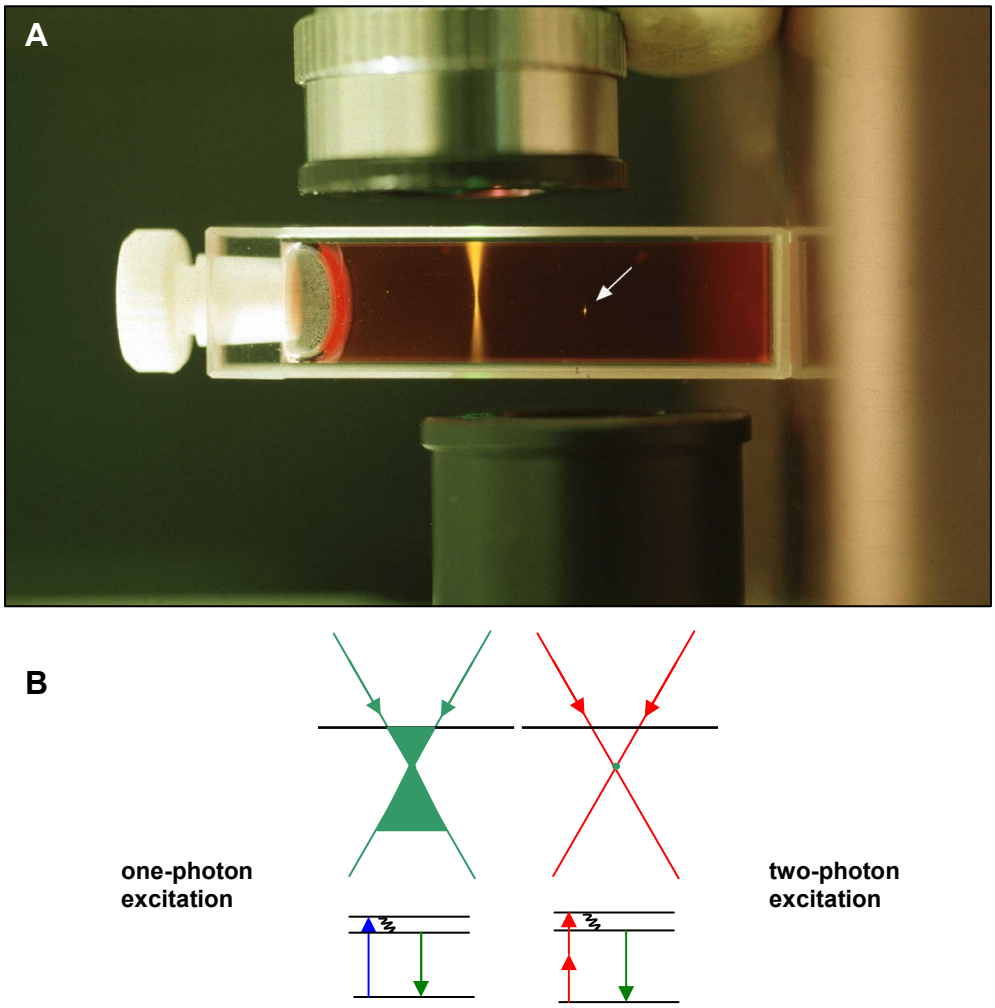

Figure 3.4: One-photon and two-photon excitation.
[A] Picture showing excitation of a fluorescent solution in a cuvette with one photon and two photon (white arrow) excitation. (Picture Courtesy: Brad Amos).
[B] A cartoon depicting the excitation region of specimen with one-photon and two-photon excitation. (Cartoon: by Author).

PULSED LASER FOR MULTIPHOTON EXCITATION

Two-photon excitation requires two photons, of half the excitation energy (double wavelength) of the fluorophore, to impinge on its electrons concurrently and get absorbed. With a continuous wave (CW) laser, the probability of two photons striking together simultaneously on an electrode is very little even at the focal spot, due to low photon density.

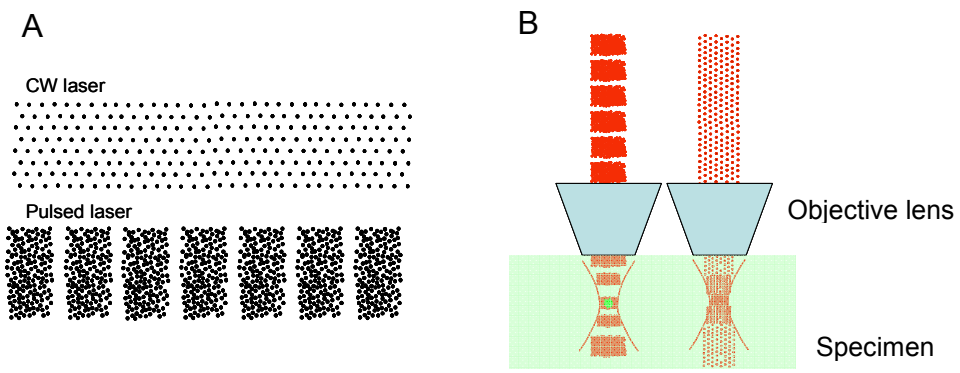

Figure 3.5: Pulsed laser is required for two-photon excitation.
[A] Cartoons of photons density in CW and Pulsed lasers **[B]** Two-photon excitation occurs with pulsed laser (green spot) and not CW laser due to low photon density of CW laser.

A femtosecond pulse laser carrying high photon density pulses ensures simultaneous impinging of two photons on an electron of fluorophores in the focal volume resulting in two-photon absorption (figure 3.5). After the invention of pulsed lasers, the first two photon laser scanning microscope (TPLSM) was made and patented by a team of researchers at Cornell university (W. Denk, J.H. Strickler and W.W. Webb) lead by Prof. Watt W Webb in 1990 [22].

GROUP VELOCITY DISPERSION (CHIRPING)

Femtosecond pulses have spectral (~9 nm) and temporal width (100-200fs for multiphoton imaging) with all the wavelengths distributed around the central wavelength (frequency). The phase velocity of different wavelengths depends on the refractive index of medium in which they travel. In air (refractive index, n=1), phase velocity of all the wavelengths is same; however in the materials with refractive index higher than air (n>1), it varies for different wavelengths. This results in non-uniform distribution of different

frequencies (wavelengths) in the pulse, called group velocity dispersion (GVD) or chirping (figure 3.6). Group velocity dispersion can be linear or complex [1, 45].

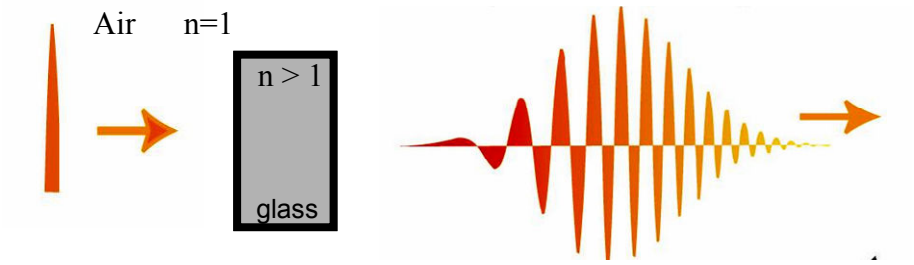

Figure 3.6: Laser pulse andGroup Velocity Dispersion (GVD) of laser pulse after passing through glass.
Femtosecond laser pulses have spectral width. Different wavelengths travel at different speeds inside a medium of refractive index different from air. Therefore, pulses get distorted. (Picture Courtesy: Prof .Rick Trebino)

FLUORESCENCE MICROSCOPY

In the past few decades, fluorescence microscopy has evolved from conventional to confocal and multiphoton laser scanning type microscopes (LSM) for three dimensional imaging. Table 3.1 shows a brief comparison of few factors among conventional, confocal and multiphoton imaging modes.

TABLE 3.1: COMPARISON OF MULTIPHOTON AND SINGLE-PHOTON IMAGING

MICROSCOPY MODE	CONVENTIONAL	CONFOCAL	MULTIPHOTON
EXCITATION SOURCE	Usually halogen/ arc lamp, could be CW laser	CW, Ar, He:Ne, UV	PULSED IR, tunable
3D IMAGING	No	Yes	Yes
RESOLUTION	Average	High (Slightly Better than multiphoton)	High (Slightly poorer Than confocal)
PHOTOTODAMAGE	High	High	Much less
SIGNAL/NOISE RATIO	Poor	Good (function of pinhole size)	Best
IMAGING DEPTH	Poor	Good	Best (better than confocal)
SIMULTANEOUS MULTIPLE LABEL EXCITATION AT SAME EXCITAITON WAVELENGTH	May be	May be	Most probably
PIN HOLE SETTINGS	Not present	Required	Not present
TIME LAPSE IMAGING	Detrimental	Detrimental	Longer-term

Multiphoton microscopy has several advantages over confocal microscopy as a result of localized excitation and use of IR laser as the excitation source. Both, advantages and disadvantages of the multiphoton microscopy over confocal microscopy are listed briefly in Table 3.2 [99].

TABLE 3.2: ADVANTAGES AND DISADVANTAGES OF MULTIPHOTON MICROSCOPY OVER CONFOCAL MICROSCOPY

ADVANTAGES	DISADVANTAGES
Longer excitation wavelengths are scattered much less (Rayleigh's scattering law), so with infrared (IR) laser, one can achieve deeper imaging of specimen.	Pulsed lasers are expensive.
Due to localized excitation, the photobleaching and photodamage is dramatically reduced.	Complicated instrumentation due to pulsed laser.
Since no pinhole is required in multiphoton imaging, more fluorescent signal can be collected from the same focal plane with a given objective lens compared to the confocal imaging. This results in brighter image.	Slightly poorer resolution than confocal imaging due to longer excitation wavelengths (Snell's law of refraction, and diffraction).
Since there is no excitation at out-of-focus planes in specimen, there is much less background signal. This improves signal-to-noise ratio.	Tunable lasers can not achieve long enough wavelengths to excite fluorophores requiring red excitation wavelengths.
Excitation and emission spectra are separated better so more signal could be collected using wider band-pass filters or no filters at all, Hence, more information about fine details of specimen is obtained.	
Two-photon excitation spectra are usually broader than one photon excitation spectra, so it is easier to excite multiple fluorophores with a single laser wavelength, attributing to much less photo-damage to the tissue.	
Pulsed laser is not monochromatic like CW lasers. Pulses contain ~ 10 nm spectral bandwidth. This property, together with broader two photon excitation spectra, contribute to get brighter images at the same laser power.	
Biological tissues absorb less in IR regime of spectrum than UV and visible regime, hence multiphoton microscope causes lesser thermal damage to specimen.	
Only one tunable laser is required for entire range of fluorophores.	
Above mentioned properties makes multiphoton imaging really advantageous for repeated imaging of a specimen, live cell imaging, deep-tissue imaging and long-term live tissue imaging.	

In fluorescence imaging, there are several factors that may affect the quality of images acquired with any of the microscopy (conventional, confocal, and multiphoton) modes. Some of these factors are listed in table 3.3.

TABLE 3.3: FACTORS AFFECTING LASER SCANNING FLUORESCENCE IMAGING

FACTOR	HOW DOES IT AFFECT?
EXCITATION WAVELENGTH	Shorter wavelengths cause photodamage and thermal damage to the specimen.
NUMERICAL APERTURE	Larger numerical aperture can collect signal from larger cone, resulting in more signal collection even from scattering specimen
FLUOROPHORE QUALITY, PREPARATION AND CONCENTRATION	Expired or light-exposed fluorophores do not fluoresce to maximum efficiency or at all. Choice of the right fluorophore, that is stored and prepared as per instructions, guarantees good fluorescent signal yield with an appropriate excitation wavelength. Concentration of the fluorophore also determines amount of fluorescent signal and image quality.
EFFICIENCY OF MICROSCOPE	Efficiency of microscope to excite fluorophores sufficiently and collect the maximum amount of emanating fluorescent signal (photons) translates to quality of the images and the photodamage to the specimen. (The more the excitation laser power required to collect a desired intensity of an image, the more the photodamage is to the specimen and fluorophores, which results in faster photobleaching).
FILTERS	Transmittivity and spectral properties of excitation and emission filters of microscope also decide image quality and authenticity of images (especially in overlapping excitation and emission spectra or overlapping emission spectra of two fluorophores and the choice of appropriate spectral bandwidth of filters)
PIXEL DWELL TIME	Longer pixel dwell time allows more fluorophore molecules to get excited and collection of more photons per pixel, resulting in cleaner and brighter images.
DETECTOR SENITIVITY	Detector sensitivity to the emission spectra of the fluorophore determines the brightness/contrast of images. Uniform sensitivity across visible spectra allows equal amount of signal collection from different color fluorophores excited with the same laser power.
BACKGROUND/AUTOFLUORESCNCE	Some specimens contain molecules that fluoresce with the excitation wavelength used. Depending on application it can be useful signal or count towards background noise. For such applications, appropriate choice of excitation wavelength and emission filters is necessary.
MODE-LOCKING OF LASER	Multiphoton imaging is not possible without mode-locking of the pulsed laser.
ALIGNMENT OF SYSTEM	Misaligned system may lead to poor excitation and emission efficiency of the microscope in addition to non-uniform illumination of specimen across the field of view.

The 3D sectioning properties of laser scanning microscopy methods make them special for various investigations. Some of the commonly used applications in biomedical research include, live or fixed tissue imaging, deep tissue imaging, time-lapse imaging,

Spatiotemporal imaging, Fluorescence Recovery After Photo-bleaching (FRAP), Fluorescence Resonance Energy Transfer (FRET), and photo-uncaging. Knowledge of these basic fundamentals, principles and methods may prove to be helpful in imaging and troubleshooting for basic problems that naïve fluorescent imagers may encounter.

CHAPTER 4

CONSTRUCTION OF A DEEP-TISSUE MULTIPHOTON LASER SCANNING IMAGING SYSTEM

ABSTRACT

Multiphoton microscopy is a relatively new imaging modality with submicron resolution that is becoming popular in a wide spectrum of investigations in life sciences due to its several advantages over confocal and conventional fluorescence microscopy. Some of the featured advantages of multiphoton imaging include localized excitation of specimen, dramatically reduced photobleaching and photodamage, and greater imaging depth. These features make multiphoton microscopy especially suitable to study living and thick biological specimen. We are optimizing thick organotypic brain slices to extend our current 2D dissociated culture studies to 3D to understand mechanisms underlying learning and memory. To keep our 2D and 3D cultures alive for long-term studies, it is necessary to protect them against photodamage. At the same time, we need a flexible microscope design to use multiple techniques on our specimen for example, multielectrode array (MEA) set up and fluidic equipment. We have constructed a custom-designed multiphoton microscope based on design of Tsai et al [118]. The microscope is optimized for two-photon imaging to collect the maximum possible fluorescent signal using the minimum excitation laser intensity. Special attention is paid to get uniformly illuminated images and the ability to use the entire bandwidth of the pulsed laser (700-1000nm) with the same set of optical components. Flexibility of the design will allow us to easily change or incorporate other optical components suitable for different experimental needs. Further, this microscope will allow us to perform electrophysiology and imaging studies concurrently while maintaining the optimum temperature and CO_2 levels using a life supporting environment chamber.

INTRODUCTION

Since the invention of the multiphoton microscope in the past decade, multiphoton microscopy has revolutionized live-cell imaging experiments to explore dynamic processes at molecular, cellular, and tissue level in the biology world. With confocal microscopy, both *in vitro* and *in vivo* imaging of living tissue is limited to a small number of scans of due to deleterious effects of photodamage resulting from repeated exposure to multiple lasers. Multiphoton microscopy is a great tool to perform live cell imaging experiments. It has several advantages over confocal microscopy which include reduced photodamage due to localized excitation of fluorophores in the specimen, no need to focus the emitted fluorescent signal, deeper imaging of scattering tissue due to lesser scattering of long wavelengths used for multiphoton excitation, and imaging using UV excitable fluorophores without using expensive quartz optics and harmful UV light [99].

In our laboratory, we combine multiple technologies to investigate the basic mechanisms underlying learning and memory. These technologies include multielectrode arrays (MEAs), embodiment of 2D and 3D neuronal cultures with animats or robots, and multiphoton microscopy [100, 117]. For long-term morphological dynamics investigations and thick brain slice viability studies we need an efficient microscope with special features. Some of these features include deep tissue imaging, flexibility of the design to accommodate our electrophysiology and fluidic systems; reduction in unnecessary exposure of specimen to the lasers; flexibility to change the frame size, field of view, and ability to zoom in on a region of interest on the fly, both optically and digitally; and most importantly, the ability to efficiently detect very small fluorescent

signals from micron-sized features such as dendritic spines in spite of noise. Currently none of the commercial multiphoton microscope systems have all these features as they often include design compromises that retain the microscope's ability to also perform visible confocal microscopy. This fact motivated us to fabricate a custom designed microscope optimized solely for long-term multiphoton imaging. In this chapter, I describe design criteria chosen for our microscope based on the desired features, selection of optical and mechanical components, and construction of the microscope from these parts.

DESIGNING A MULTIPHOTON MICROSCOPE

Desired features of microscope

A good multiphoton microscope design allows the instrument to closely approach theoretical limits of efficiency while having flexible features to be user friendly. Our research goals include simultaneous imaging and electrophysiology investigations on cultured dissociated neuronal networks. Our near future goals are to conduct these studies on thick brain slices as well. Thus taking into account near- and long-term imaging goals, we require a multiphoton microscope that has following features:

- flexible opto-mechanical design to accommodate multiple experimental techniques such as electrophysiology and fluidic platforms, and *in vivo* preparations
- allows long term time-lapse live cell imaging
- allows deep imaging of thick specimen

- easy access to optical components for quick changes for different experimental needs
- Fine precision XYZ stages for repeated imaging of different regions of interest of the same specimen during long-term experiments
- ability to zoom in on interesting parameters during time-lapse imaging by quickly changing the objective lenses
- sub-micron resolution
- high optical efficiency to cover entire range of Ti:saph laser and collect fluorescent signal from dim structures

To achieve these goals, I adopted the basic optical design of Tsai et al and modified it to meet our needs [118]. Unlike confocal microscopes, the multiphoton microscope needs a pulsed laser which has a peak power of the order of few kilowatts required for the multiphoton excitation and an average power of a few milliwatts that reduces the damage due to heating of the specimen. Multiphoton excitation is a nonlinear process, which involves absorption of two or more photons by the fluorophore with sum (total) energy equivalent to the energy required to excite the fluorophore [22, 44]. The probability of absorbing two photons simultaneously requires a very high density of photons, which is achieved by using pulsed lasers with low duty cycle and high peak power.

Challenges posed by a pulsed laser: Group Velocity Dispersion

As opposed to continuous wave lasers used in confocal microscopy, a pulsed laser is not monochromatic. The pulses of a laser have a spectral width $\Delta\lambda$ and a temporal length τ_p that are related as:

$$\Delta\lambda \propto \frac{\lambda_0^2}{\tau_p}$$

Equation 4.1

where λ_0 is the central wavelength of laser pulse. Thus a shorter pulse has greater spectral width. In an ideal pulse, all its spectral components are uniformly distributed across its temporal length. A pulse with small temporal length and large spectral width is ideal to achieve the maximum fluorescence intensity resulting from multiphoton excitation of a fluorophore. The limitation in the instrumentation of a multiphoton microscope arises due to dependence of the refractive index of a medium on the wavelengths. The uniform distribution of spectral components of a pulse is distorted when it passes through a piece of glass (refractive index, n, glass= 1.3-1.5 compared to air =1). This distortion of pulse spectra is called group velocity dispersion (GVD), or "chirping" and results in reduced the peak power (figure 4.1). Generally, 100-200 femtosecond-long pulses in the infrared wavelength regime experience less chirping than shorter pulses and are best for good multiphoton excitation [118]. The Ti:saph laser is a good choice as an excitation source for multiphoton microscopy [113] as it provides a tunable range of wavelengths across the near IR regime.

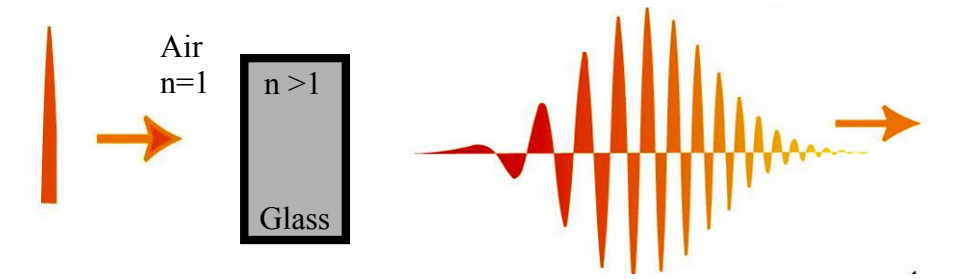

Figure 4.1: Group velocity dispersion of a laser pulse.
Laser pulses have spectral width. Speed of light depends on its wavelength and refractive index of medium. Thus, different wavelengths travel at different velocities in glass resulting in group velocity dispersion of pulse. (Picrture Courtesy: Prof Rick Trebino)

In ideal conditions, a pulse should have no chirping at the focal plane of the objective lens. However, in the real world, chirping is unavoidable because of distortion of the laser pulses by lenses and multilayer dielectric coated mirrors used in the microscope. Imaging with chirped pulses will result in more laser power required for the multiphoton excitation of the fluorophore, with more one-photon heating.

To counter this problem, there are two solutions: (i) to use minimum number of optical elements, and (ii) use a pre-chirping unit (figure 4.2). The chirping could be of two types: positive and negative. If all the components of the microscope are chosen such that they chirp in the same direction, a pre-chirp unit, made up of two prisms having the opposite chirping direction can be used to compensate for this non-uniform stretch in the pulses at the focal plane of the objective lens [54, 113].

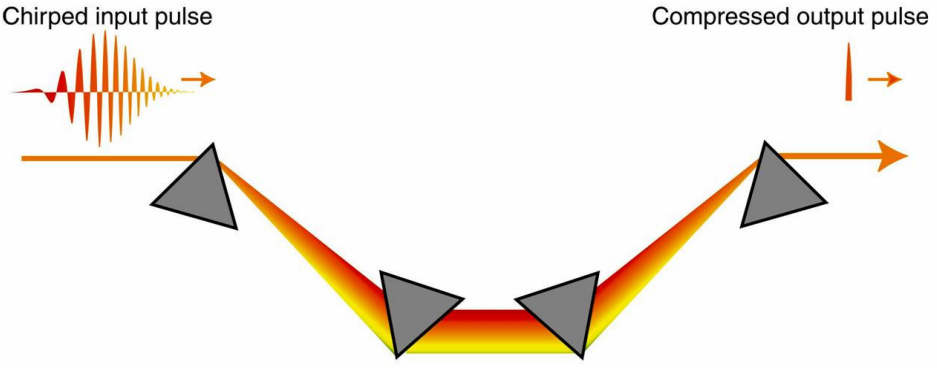

Figure 4.2: Pulse compressor or pre-chirp unit.
The velocity of different wavelengths is refractive index dependent other than air (refractive index n=1 for air, 1.3-1.5 for glass). The velocity of all wavelengths is same in the air but is wavelength dependent in media having other refractive index. The wavelengths with faster velocity in glass (higher refractive index) compared to slower moving wavelengths travel larger area of glass (prism), while the slower wavelengths travel smaller glass areas (tip of the prism) thus optical path length that results in compressing of the chirped pulse. (Picture courtesy: Prof Rick Trebino)

Apart from chirping, other challenges to construct a good multiphoton microscope are: to obtain optically efficient excitation and emission pathways, to meet the requirement of the excitation of fluorophore with minimal laser power; the ability to cover the entire wavelength range of the laser with the same set of optics; to achieve a good spatial resolution and a high imaging frame-rate and to obtain uniform intensity of the image across a frame scan.

Optical design

An upright microscope design along with careful selection of optical components would meet most of these desired features (figure 4.3). To obtain optically good imaging data while minimizing the photodamage to specimen, it is required to have efficient excitation and emission pathways. Since biological specimens are highly scattering media and absorb less in infrared regime of the electromagnetic spectrum than the visible, the longer wavelength regime of the tuning range of the Ti:saph laser is more suitable for

imaging these specimens, especially when repeated imaging of a specimen is desired. Further, it is required to have minimally chirped pulses of laser light at the focal plane and high transmission of the laser light. By using as few optical elements as possible, we minimize light losses due to reflections and chirping. The excitation path includes a pump laser (Coherent Verdi 10W, 532nm), pulsed IR laser (Coherent Mira 900 Ti:saph) , laser beam routing mirrors, laser beam reshaping unit, pre-chirp unit, Pockels cell, scanning mirrors, scan lens, tube lens, dichroic mirror and objective lens. The excitation and emission paths share a path containing objective lens and dichroic mirror. Along with these two, the emission path also includes the collection optics and a detection unit.

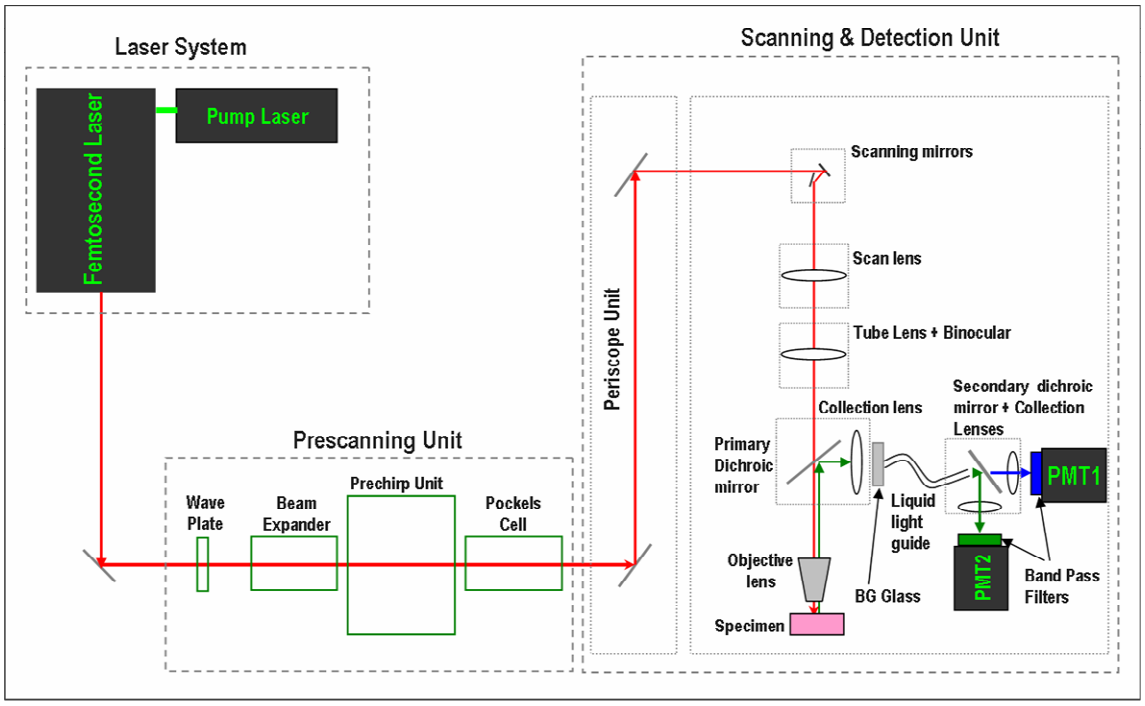

Figure 4.3: Optical Diagram of the multiphoton microscope design.
The system has three units: laser system, prescanning unit, and scanning and detection unit.

SYSTEM CONSTRUCTION

Laser system

Each fluorophore has two-photon excitation cross-section. Shorter pulses could have spectral width extended beyond the two-photon cross-section, resulting in reduced excitation of the fluorophore at a given power. A powerful laser system with broader tunable wavelength range promises multiphoton microscopy of broad range of fluorophores. It is generally accepted that a Ti:saph femtosecond laser has optimal wavelength tuning range and laser pulse properties for two-photon excitation [113]. We use the Coherent Mira 900 laser, which has a tuning range of 700-1000nm, with 100-200fs pulses of ~9 nm full width at half maximum (FWHM) spectral bandwidth.

Currently, we are sharing a laser system (Chameleon, Coherent, Inc.) with a commercial, inverted-type, two-photon microscope. A flip-out mirror or a beam splitter is used, depending on the use of commercial two-photon microscope, to route the laser beam to our system on the same optical table. Due to our preference to use longer wavelengths of laser from its tuning range, an efficient excitation pathway of the microscope is required. The power curve of the laser falls off at these wavelengths (figure 4.4). To make use of all the power available at the extremes of the tuning range, it is important to have good excitation efficiency. To meet this requirement, we use multilayer dielectric coated mirrors between the laser and the microscope (Coherent, Inc.) which can reflect > 98% at 45 degrees and >99.7% at zero degrees for p-polarized laser light ranging from 675-1000nm wavelengths.

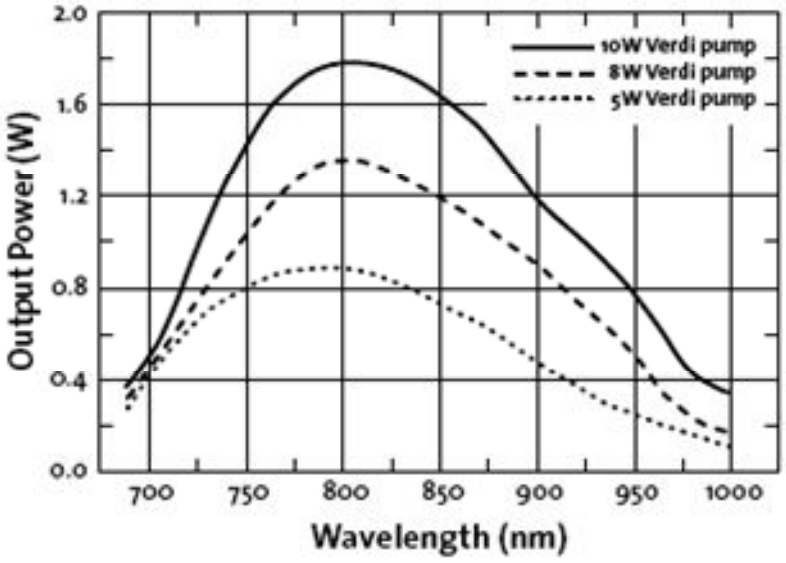

Figure 4.4: A typical Power curve of a Ti:saph Mira900 laser across its entire tuning range when pumped with pump lasers (Verdi) of different powers.
Ti:saph lasers lave peak power around 800 nm wavelength that falls rapidly towards the extreme ends of its tuning range. (Data courtesy: Coherent,Inc).

Scanning and detection unit

The frame rate depends on the speed of the scanning mirrors. Ideally, in a 2D scanning mirror system, the centers of both the mirrors should be imaged to the back-focal point of the objective lens. The deviation from this condition leads to vignetting. To meet the optimal condition, intermediate optics are required between the X and Y mirrors (for example, as in the Biorad scanhead design). This makes alignment of the system cumbersome, and additional optical elements add to chirping of the laser pulses. These intermediate optical elements can be safely eliminated by using 2D orthogonal scanning mirrors mounted with a very small separation distance. These two mirrors could be imagined as a single mirror moving in the XY direction with its center at the mid point of

these two mirrors. To scan the laser beam fast in a raster pattern, we have chosen a top-of-the-line 2D scanning mirror system (Model 6215H, Cambridge, Inc., including driver boards). These mirrors have small size (x-scan mirror =3mm and y-scan mirror = 5mm), and the separation between them is only 5.2 mm. Their small size translates to less mass which helps them to move faster.

A scan lens is a critical optical element which determines the uniform delivery of laser pulses across the raster scan. A plan-apo stereomicroscope objective lens with a large (~8cm) diameter would offer an equal thickness to the pulses of the laser beam moving in a raster pattern [118]. This would stretch the laser pulses to almost the same extent across the raster pattern for more uniform excitation. Currently, we are using (F=60mm; D=25.4mm) near-IR achromatic doublet (AC254-060-B, Thorlabs, Inc.). An 80mm stereoscope objective lens from Zeiss might be an appropriate option in the future, due to its longer focal length (~ 63.5cm) compared to the scan mirror separation. Its large diameter will allow only the central, almost constant thickness region, for the scanning laser beam. A tube lens is required to collimate the laser light going to the objective lens. A binocular is also required to visually inspect the specimen during experimental setup. We have use a trinocular head (Zeiss, Inc.) whose lens is used as the tube lens in our microscope system.

Ideally, the fluorescent light collected from the focal plane of the objective should appear collimated at its back aperture. In reality, this is not true for highly scattering specimens, especially living brain tissue. A good objective lens with high numerical aperture collects the scattered emitted photons from a wider angle. We use a set of four high numerical aperture (10X, NA=0.30; 20X, NA=0.50; 40X, NA=0.80; 63X,

NA=0.95), Zeiss water immersion objective lenses with long (~1mm) working distance. These lenses allow for deep imaging in the specimen while collecting more scattered photons.

A very important optical element, which bridges the excitation and emission paths in a fluorescence microscope, is the dichroic mirror (DM). It separates the excitation light from the fluorescence signal. In our upright microscope, it transmits the laser light and reflects the fluorescence signal. Fluorescence signal collected from a scattering specimen via a 20X objective lens spreads to a bigger area (~ 45mm) by the time it reaches the dichroic mirror. To get a bright image, it is important to collect this entire signal. We purchased a custom made dichroic mirror (Chroma, Inc.) with 4cm x 5cm dimensions. This dichroic mirror has a sharp cut-off at 700nm wavelength such that the entire bandwidth of the laser is transmitted and the fluorescence signal (<700nm) is reflected at > 99%. The transmission and reflection properties of our dichroic mirror are shown in figure 4.5.

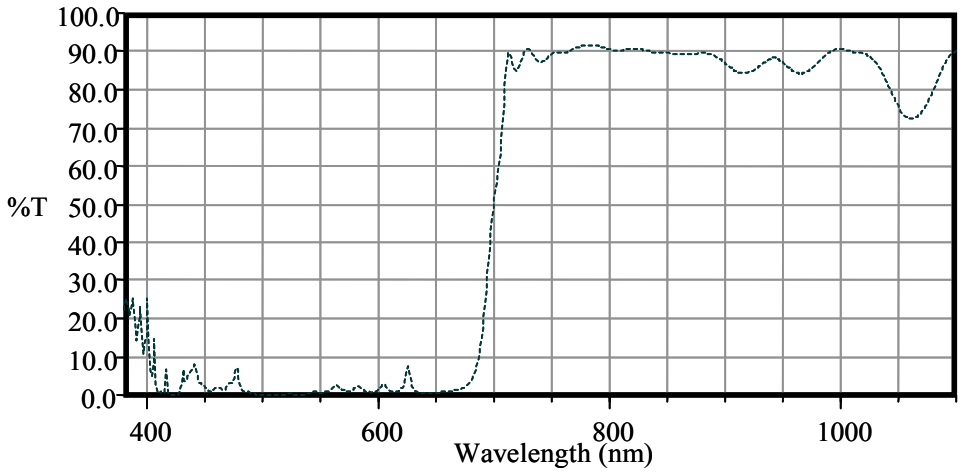

Figure 4.5: Transmission curve of custom made dichroic mirror with a sharp cut-off at 700 nm wavelength.
This allows to transmit the laser light to the specimen and to redirect the fluorescent signal (< 700nm) towards the collection pathway. (data courtesy: Chroma, Inc.)

In our system, a pair of collection lenses along with a liquid light guide helps to transport and focus the fluorescent signal on the active area of the detector. A collection lens with large diameter, placed as close to dichroic mirror as possible, ensures maximum collection of fluorescent signal. We use an aspheric lens with a 50.8mm diameter (Oriel, Inc.) which focuses the fluorescent signal on the 8 mm diameter aperture of a liquid light guide (Oriel, Inc.). The liquid light guide transmits ~ 90% of the collected fluorescent light to another aspheric lens with numerical aperture of 0.7. This second lens helps to focus the signal onto the active area of the photomultiplier tube (PMT).

To detect the collected signal, we have selected a side-on PMT with large active area of 8mm x 24mm (Model R3896, Hamamatsu, Inc.). This PMT has high quantum efficiency and a relatively flat plateau of sensitivity over the entire visible range of wavelengths as shown in figure 4.6. It is desirable to cool the PMT in a custom liquid-cooled housing (Photocool, Inc.) to reduce the detector thermal noise to detect the small

fluorescent signal emanating from tiny morphological structures. A high sensitivity PMT requires blocking of any residual laser light collected along with the fluorescent signal. For this purpose, an IR blocking BG39 glass is placed in front of the PMT. Additional band-pass filters can be mounted in a quick-release mount to achieve enhanced contrast. A careful selection of highly regulated power supplies for the PMT and a custom-fabricated preamplifier along with cooled housing makes it an efficient, low-noise detection system.

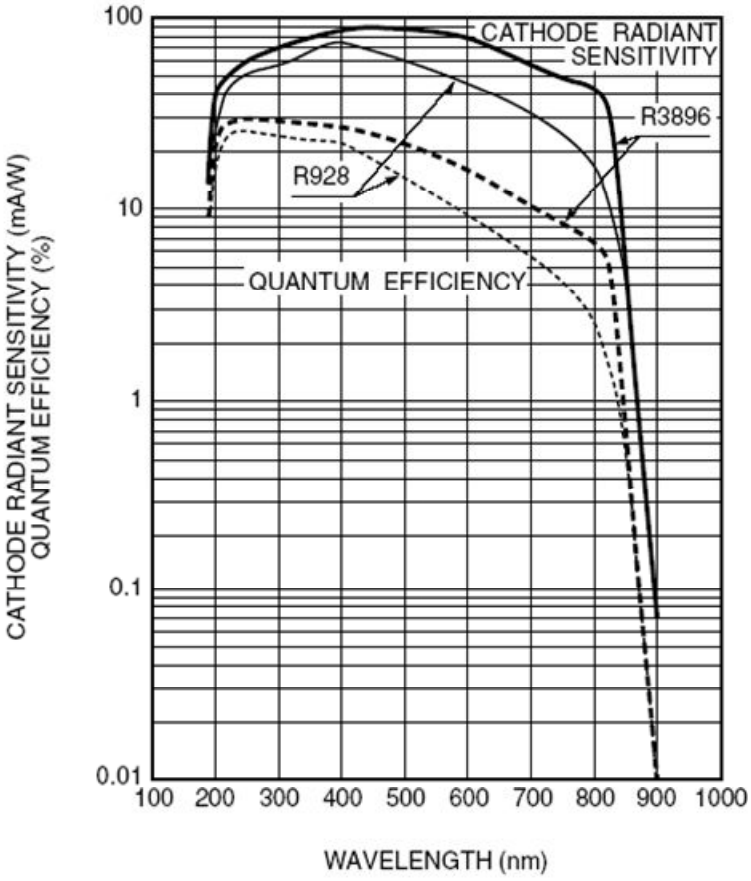

Figure 4.6: Sensitivity of the detector.
A nearly constant sensitivity across the visual range of spectrum ensures detection of all color photons equally. An efficient detector unit translates to lower laser power to excite the specimen (data: Hamamatsu, Inc.)

Laser Beam Shaper

The laser beam of the femtosecond laser (Coherent MIRA900) is 0.8mm in diameter and diverges (1.7 mrad) slightly which translates to increasing beam diameter as a function of distance from the laser exit-aperture. The smaller size of the scanning mirror (3mm) and the requirement to overfill the objective lens back aperture makes it necessary to reshape and collimate the laser beam along its excitation path. This is achieved by a two-lens telescope (beam-expander focal length 100mm, and 80mm) before, and two lens telescope (the scan lens tube lens) after the scanning mirrors. Further, a Pockels cell is required to modulate or block the laser intensity to avoid any unwanted exposure of specimen to the laser light during the raster scan regions where signal is not collected. Together, these additional but essential optical elements introduce group velocity dispersion of the pulses of laser. Multilayer dielectric coatings on reflecting mirrors and antireflection coatings on the transmission optics also introduce chirping of laser pulses. The pre-chirp unit is a two-prism and a retrograde mirror system (SF10 glass, CVI Lasers, Inc.) that will be used to compensate for GVD caused by the optical elements in the excitation pathway.

For four dimensional (XYZ, t) imaging, it is required to move the objective lens or the specimen in the z-direction. We prefer to move the objective lens in the fine z-steps because our specimens are coupled to heavy electrical recording and stimulation hardware. A coarse motorized Z-translator quickly moves the objective up and down to facilitate the placing and focusing of the specimen with 1μm precision. To capture finer 3D details of the specimen, it is important to image the specimen at smaller z-increments, for which a piezo-controlled fine z-translator mount for the objective lens is required. A

practical problem with the commercially available z-focuser is that it covers most of the objective length with its motor and would collide with our MEA recording and stimulation hardware. For such spatially constrained conditions, it would be advantageous to be able to use the entire length of objective lens. To meet this requirement we decided to mount a fine z positioner (PI, Inc.) upside down using a custom quick-release mounting plate.

For repeated imaging of the different regions of interest (ROI) in the specimen in a long term experiment, it is required to move the specimen repeatedly to those regions at desired times. We use a computer controllable XY stage, which can repeatedly go to the same ROI (±1μm) when used in closed-loop mode (Phytron, Inc.). In addition to these features in our system, while a small optical zoom in the region of interest can be obtained by decreasing the scan angle of the scanning mirrors, a comparatively bigger optical zoom can be obtained by quickly changing the objective lens via the custom-fabricated quick-release objective lens mounting plate.

Software control: Scanning, Data Acquisition Control, XY stage and Focal Control

Custom software written in LabView 7.1 controls the synchronized movement of scanning mirrors and data collection from the PMT. Since digital-to-analog cards have only one FIFO memory available, to exploit the fastest scanning speed of the scanning mirrors, I chose two digital-to-analog cards (Model PXI-6733, National Instruments, Inc.) to control the motion of the scanning mirrors. The scanning mirrors are driven using custom waveform developed by Tsai et al to optimize the speed of the raster scan. A real time system integration (RTSI) bus is used to synchronize commands using counters and clocks (pixel clock, line clock and frame clock) of the digital-to-analog cards to each

scanning mirror, collect data information as time series through data acquisition card and update position of z-controller (figure 4.7). The data is collected only in the linear part of the driving waveform to avoid the non-uniform speed of the mirrors at the corners of the waveform. At the edges of the scanned region, non-uniform velocity will cause non-uniform illumination and a distorted shape of the specimen. The collected fluorescent signal is converted to voltage in the preamplifier circuit which is passed to a data acquisition card (Model PXI-6115 National Instruments, Inc.) from where it is read, displayed and stored as an image using custom-written LabView software. The current version of the LabView user interface includes the following features: image display without storing, line scan, custom frame size of images, different scan speeds, 2D imaging, 3D imaging (z-stack), specimen (XY) stage control, Z-positioner control, 2D and 3D time-lapse imaging, optical zoom by changing scan angle of scanning mirrors, saturated pixel display, and laser power modulation by software control of Pockels cell(figure 4.8). The collected signal is stored as data files that can be converted to readable image files such as *.tiff, *.jpeg, *.bmp, and *.png using custom developed LabView user interface utilities package. A step-by-step microscope operating manual and a trouble-shooting manual are given in appendices B and C.

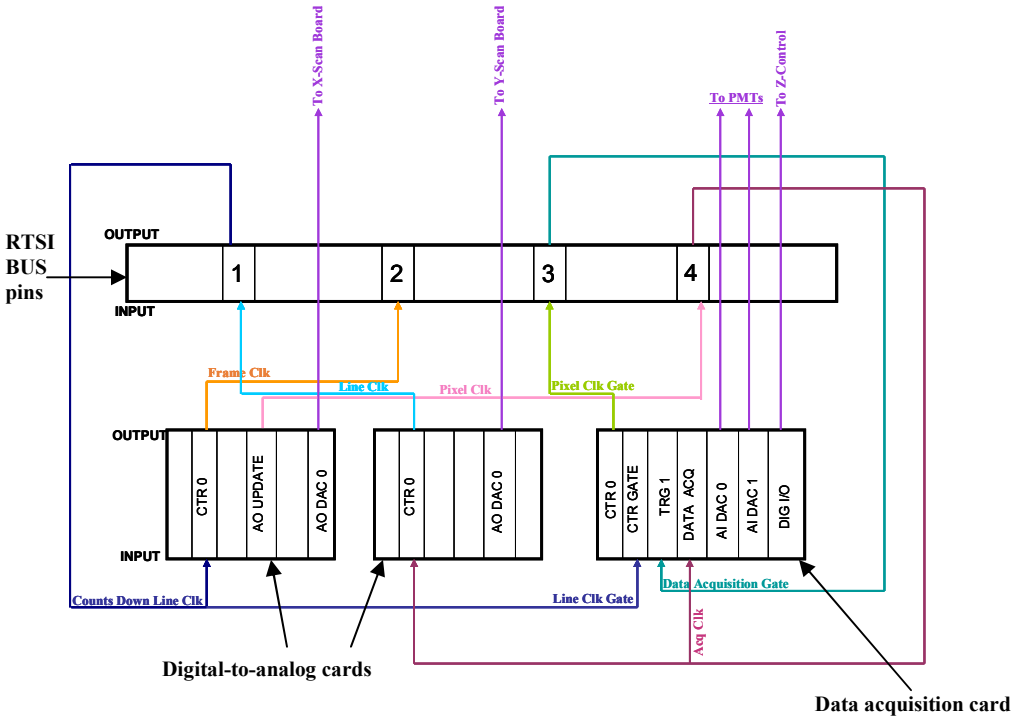

Figure 4.7. Schematic diagram of synchronized scanning and data acquisition control to form basis for software control.

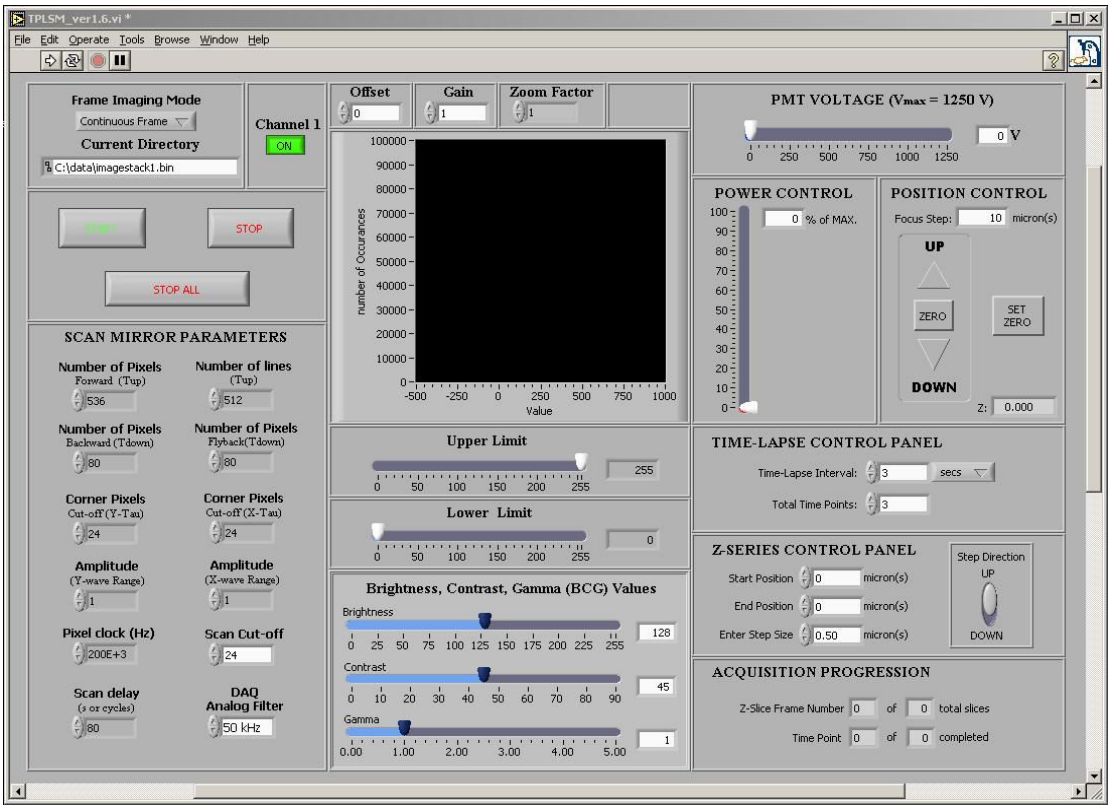

Figure 4.8: Screen-shot of Software User interface to operate the microscope in various imaging modes.
The current version of software allows continuous display of images without saving, 2D (single plane), 3D (z-stack), 2D and 3D time-lapse imaging. Further, it allows controlling image intensity by changing laser power and detector (PMT voltage) gain. This software also allows locating and focusing the specimen using X, Y and Z controls.

Environment chamber

For time-lapse imaging of living cultures, it is desired to keep the tissue healthy while imaging. For this purpose, a controlled environment chamber is constructed around the microscope to regulate physiologic levels of temperature and CO_2. The supporting frame and body of the environment controlling unit was constructed using wooden bars, mylar bubble plastic insulation and metal foil tape (figure 4.9). To make sealable doors and windows, Velcro is used. A common chicken egg incubator is used as a heating

element that heats and maintains the chamber at physiologic temperatures (33ºC -37ºC) by circulating the heated air.

Figure 4.9: Environment control chamber.
[Left] Older version of environment chamber around the custom made multiphoton microscope. The frame work for this chamber was made with coat hangers. There was limited heating due to large thermal loss by the conducting surface of the optical table. The surface of the table was not covered with insulating bubble wrap. **[Right]** Current version of the environment chamber. The frame work is made up of wooden bars and the door is made of plexiglass. This sturdy frame minimizes vibrations transferred from the heater fan. The chamber is made completely double-walled with bubble wrap. The surface of the optical table and the X-95 rail (frame of microscope) are also insulated to prevent any heat loss. Currently, this chamber can be maintained at 20º-31ºC temperature. A higher wattage heater will be required to maintain physiologic temperature (37ºC) inside the chamber. The eye-pieces of microscope were made external for convenient visual inspection without opening the door during long-term time-lapse imaging. Undergraduate researcher scholars, Bobby Thompson and Christopher Grubb, contributed significantly in the construction and optimization of this chamber.

A commercial CO_2 sensor and a CO_2 tank supply is used to regulate CO_2 level in the chamber while imaging. While this chamber serves the purpose as a life support system for the cultures, it also helps to prevent exposure of detectors to stray light in the room that might result in background noise in the images. A complete microscope is shown with and without environment control in figures (4.9, 4.10).

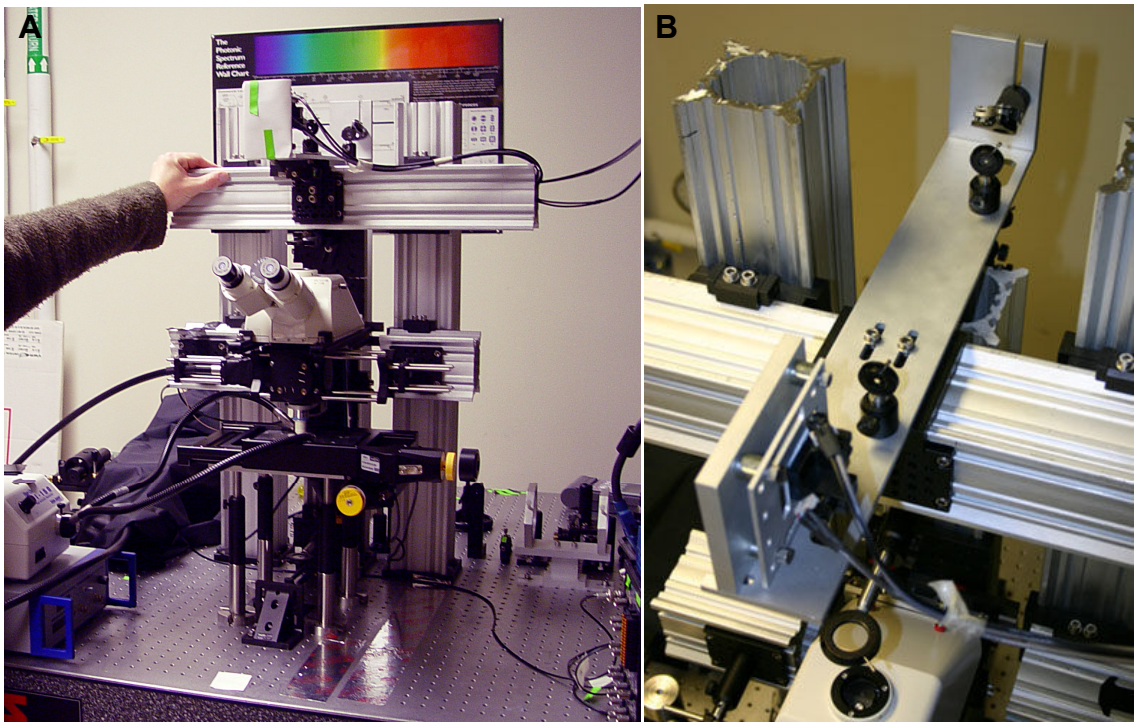

Figure 4.10: Custom fabricated multiphoton microscope.
[A] Full front view of the microscope. **[B]** Scan plate containing upper periscope mirror, alignment pinholes and scanning mirrors. Scanning mirrors are mounted on custom fabricated high conduction and thermal loss aluminum plate to ventilate heat generated during high scanning speeds or long-term scanning.

DISCUSSION

We have described construction of a user friendly and flexible custom made microscope, which will allow us to conduct long term imaging and multi-unit recording and stimulation experiments concurrently to investigate the information processing mechanisms in networks of cultured mouse neurons. While our microscope is designed to achieve optimum excitation and emission efficiency, our design offers a unique blend of features which, when incorporated, will help us and others combine long-term imaging and electrophysiology. These features include programmable XY stage for 4D imaging to investigate an ongoing dynamic phenomenon in the specimen, quick-release objective lens accessory to quickly change the objective to zoom on a region of interest, maximum

collection of isotropically emanating fluorescent signal using a mirror under the specimen and ability to reduce the thermal noise to detect tiny fluorescent signals.

With our system, we can use any wavelength from the entire tunable range of Ti:saph laser efficiently with a single set of optics. Moreover a minimum number of optical elements retain the temporal quality of the laser pulses which translates to efficient excitation of the fluorophore. The small size of the scanning mirrors helps to achieve fast scanning rates and eliminates unnecessary optical elements to attain good alignment of the laser beam path. Along with scan mirrors, a careful selection of scan lens and a custom made dichroic mirror makes the excitation path efficient such that minimum laser power is required to obtain a uniform illumination in the specimen. Collection of photons emanating from the specimen is optimized by using a sensitive detector, efficient collection optics and a transmission path reflection mirror under the specimen. This reduces the power to illuminate the specimen and will allow the ability to image deeper in the specimen by increasing the laser power as a function of depth. If needed, this microscope can be extended to collect second harmonic generation (SHG) signal in the transmission path even while imaging in multiphoton mode [88]. Life support of the cultures during long-term imaging is important; we have built an environmental chamber around the microscope to maintain appropriate temperature and CO_2 levels [101] .

CHAPTER 5

VALIDATION OF THE CUSTOM FABRICATED MULTIPHOTON LASER SCANNING IMAGING SYSTEM

ABSTRACT

An efficient multiphoton microscope with flexible design ought to allow imaging of wide range of experimental specimens and accommodate experimental needs. We have fabricated a high-throughput custom designed multiphoton microscope with desired flexibility and features that is optimized for long term time-lapse and three dimensional (3D) imaging of living specimen. After constructing the microscope, we tested and calibrated its various features. In this chapter, we report validation of our custom made imaging station for two dimensional (2D), three dimensional (3D) and time-lapse imaging. Further, we discuss future directions to add more software and hardware features.

INTRODUCTION

Multiphoton imaging has revolutionized life science investigations requiring live cell imaging to study dynamics properties from molecular to cellular to network level due to its several advantages over confocal imaging [99]. Over the past decade there is an increasing number of revolutionary investigations in life sciences from molecular to systems level that have benefited from multiphoton microscopy, such as protein trafficking on living neurons using quantum dots attached to molecular cues, morphometric network properties of neurons at submicron resolution, calcium imaging

from spine to network level of intact (*in vivo*) or sliced brain (*in vitro*), molecular imaging to unravel molecular interaction and their localization in the cells, effect of pharmacological agents on targeted structures of cells, photouncaging of molecules to study the effect of pharmacological agents, and so on [2, 3, 7, 15, 16, 24, 31, 52, 53, 74, 75, 77, 92, 109, 110].

Because of the non-linear nature of multiphoton excitation that demands high photon density in excitation source, it requires femtosecond pulsed laser. A pulsed laser poses several challenges in the instrumentation of the multiphoton microscope and requires special features of optical components for an efficient microscope. Most of the commercial microscopes have compromised design to use same set of optics for multiphoton and one photon microscopy to retain their ability to perform confocal imaging. To meet our requirements for deep tissue imaging and/or long-term time lapse imaging of neuronal networks in dissociated cultures or brain slices, I have custom fabricated a multiphoton only microscope to meet the desired efficiency and flexibility required for our studies. In this chapter, I report the performance of the microscope for some of these applications such as 2D, 3D and time-lapse imaging.

SYSTEM VALIDATION: OPTICAL PROPERTIES

Achievable scanning-speed

The scanning mirrors can deflect up to range of ±20 degrees, but for our purpose only ±4 degrees of deflection is adequate. The mirrors are driven by a custom made waveform developed by Tsai et al to optimize speed and linearity of scanning during data

collection. The smaller (3mm x 3mm) mirror is driven at a fast rate, which forms the basis for the line scan and the octagonal longer mirror (5mm x 3mm) moves at a much slower rate to move the line scan in a raster pattern. The maximum velocity that can be achieved by our scanning mirrors for different scan angles is given in the figure 5.1.

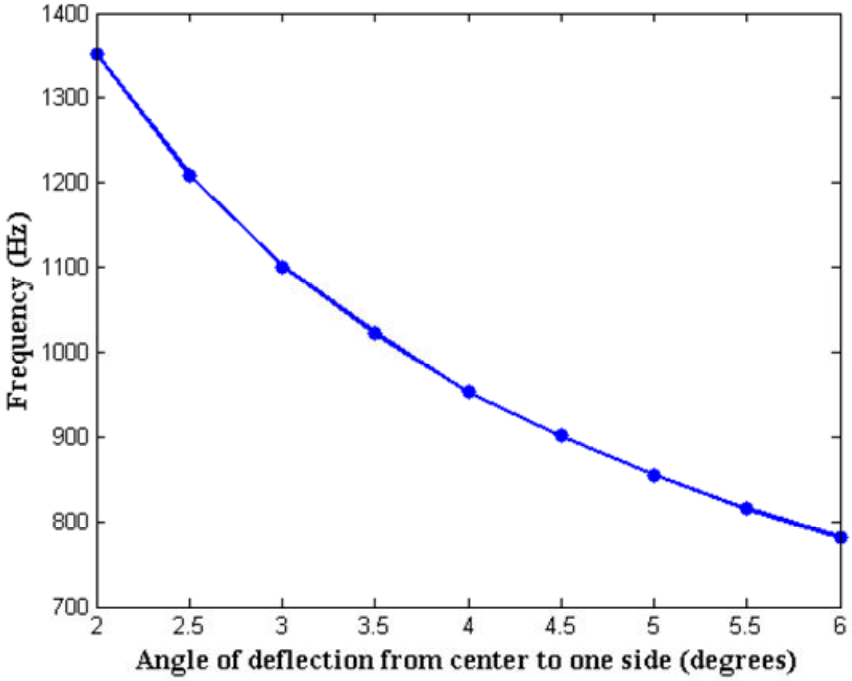

Figure 5.1: Speed of scanning mirrors at different angles of deflection (scan angles).
At smaller angles, higher speed of scanning can be obtained. At higher angles, bigger field of view can be obtained. Only a scan angle up to ±4 is desired for the various imaging needs. The default value is set to ±2 degrees of deflection.

Field of view and Scan angle

The angle of scanning of the laser beam decides the field of view of specimen for a given objective lens. This property could be exploited to optically zoom in or out of the specimen at the expense of scan speed (figures 5.1, 5.2) without changing the objective lens. This property can be controlled from the graphical user interface (GUI). To calibrate the field of view of different objective lenses at various scan angles, a hemocytometer

grid was used to reflect a weak laser beam (<2mW) to the detector. A montage image of images taken at different scan angles with a 20X W (N.A. 0.5) objective lens is shown in figure 5.2. With increasing scan angles, the edges of the raster scan of the laser beam are blocked by the back aperture of the objective lens leading to the vignetting of the image. A complete table of field of view with different objective lenses at different scan angles is given in table 5.1.

TABLE 5.1: FIELD OF VIEW (IN MICROMETERS)

USER PANEL INPUT	SCAN HALF-ANGLE	10X	20X	40X	63X
1.0	2.0	640.00* 640.00	312.20*312.20	162.03*162.03	103.23*103.23
1.1	2.2	775.56*775.56	350.68*350.68	179.02*179.02	113.78*113.78
1.2	2.4	--	387.88*387.88	195.42*195.42	123.67*123.67
1.3	2.6	853.33*853.33	412.90*412.90	211.56*211.56	134.73*134.73
1.4	2.8	914.29*914.29	449.12*449.12	228.57*228.57	143.81*143.81
1.5	3.0	984.62*984.62	474.07*474.07	243.81*243.81	153.28*153.28
1.6	3.2	1024.00*1024.00	512.00*512.00	258.59*258.59	164.10*164.10
1.7	3.4	1113.04*1113.04	533.33*533.33	278.26*278.26	175.34*175.34
1.8	3.6	1163.64*1163.64	568.89*568.89	290.91*290.91	186.86*186.86
1.9	3.8	1219.05*1219.05	609.52*609.52	304.76*304.76	195.41*195.41
2.0	4.0	1347.37*1347.37	640.00*640.00	--	208.13*208.13
2.1	4.2	1422.22*1422.22	673.68*673.68	345.95*345.95	216.95*216.95
2.2	4.4	1505.88*1505.88	731.43*731.43	360.56*360.56	226.55*226.55
2.3	4.6	1600.00*1600.00	752.94*752.94	376.47*376.47	239.25*239.25
2.4	4.8	1706.67*1706.67	775.76*775.76	387.88*387.88	248.54*248.54
2.5	5.0	--	825.81*825.81	406.35*406.35	258.57*258.57

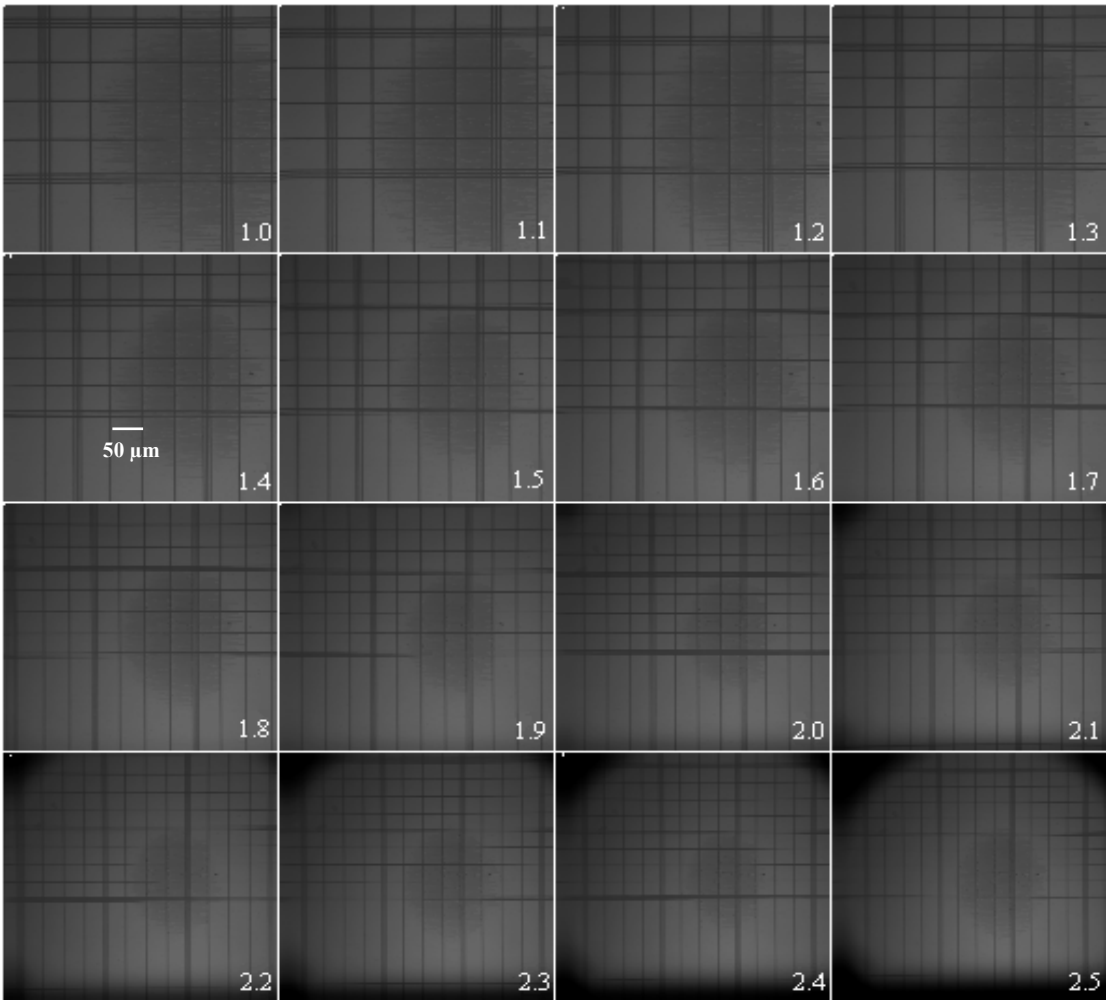

Figure 5.2: Montage of 512x512 pixel images of hemocytometer grid taken at different scan angles with the Achroplan 20X NA 0.5 water immersion objective lens. The scan angle can be changed from the user panel in single digit decimal increments. The input from the graphical user interface is voltage that is delivered to driving boards of the scanning mirrors. The default value is set at 1 (V) which translates to ±2 degrees of scan angle from the central position (zero position). The voltage increments are set to one decimal place. 0.1 V of increase in voltage (input from the front panel) translates to ±0.2 degrees of scan angle increment. Ability to change scan angle from front panel allows small change in field of view and hence magnification to capture details of image without changing the objective lens. With 20X W (NA 0.5) objective lens, the scan angles larger than 3.8 degrees (1.9 input from user control panel) lead to vignetting of the raster scan of the laser beam at the corners of the image due to blocking of laser beam at back aperture (0.8 mm standard) of objective lens. An increase in the scan angle reduces the scanning speed.

Excitation pathway efficiency

The excitation pathway efficiency depends on four factors: (1) diameter of laser light transported by optical components, (2) reflection at each optical component due to refractive index mismatch, (3) chirping of the laser pulse and (4) absorption. If the cross-sectional intensity profile of the laser beam is gaussian, over 90% of the laser intensity (power) is located at its full width at half maximum (FWHM) length. To make maximum use of laser power, the laser should be mode-locked in the gaussian mode and the aperture of various optical components should be as big as or greater than the diameter of the laser beam. We use a two lens (f =100mm, and 80mm) telescope to reshape the laser beam to fit on the aperture of the small mirror (3mm). Secondly, we minimized the number of optical components (mirrors and lenses) on the laser beam excitation pathway. The lenses (transmission optics) are coated with antireflection coatings (except the scan lens) and the mirrors are coated with multilayer dielectric coatings to avoid 4% loss of laser power at each air-optics interface. The laser was tuned at 800 nm wavelength and the laser power was measured before the microscope and at the focal plane of the objective lens (figure 5.3).

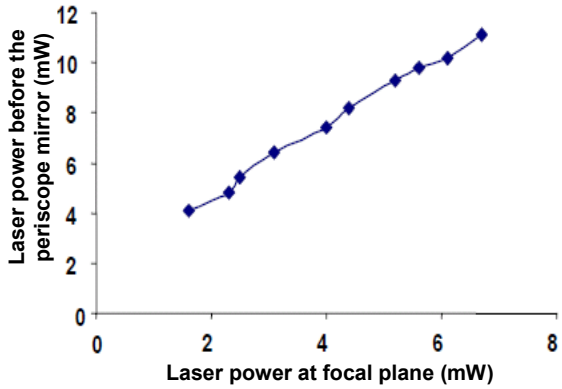

Figure 5.3: Efficiency of excitation pathway to transport laser power at the focal plane.

Chirping of laser pulses

Laser pulses are not monochromatic. They possess spectral bandwidth of ~ 9 nm with a temporal length of 100-200 fs with all the wavelengths gaussian distributed across the central wavelength. Attributing to different velocities of different wavelengths in a medium of refractive index different than air (n=1 for air), the pulses get distorted due to group velocity dispersion. The chirped pulses reduce the excitation efficiency of the system. To counter this problem, we chose a minimal number of optical lenses on the laser beam path. Using a novel device, the Grenouille, constructed by our collaborators (Prof Rick Trebino and Group), we measured pulse properties of a 80fs pulse before the microscope and at the focal plane at 800 nm wavelength [1, 44]. Without the Pockels cell in the beam path, the pulses got elongated by only 15% by the current optics which ensures high efficiency to excite the fluorophore (figure 5.4).

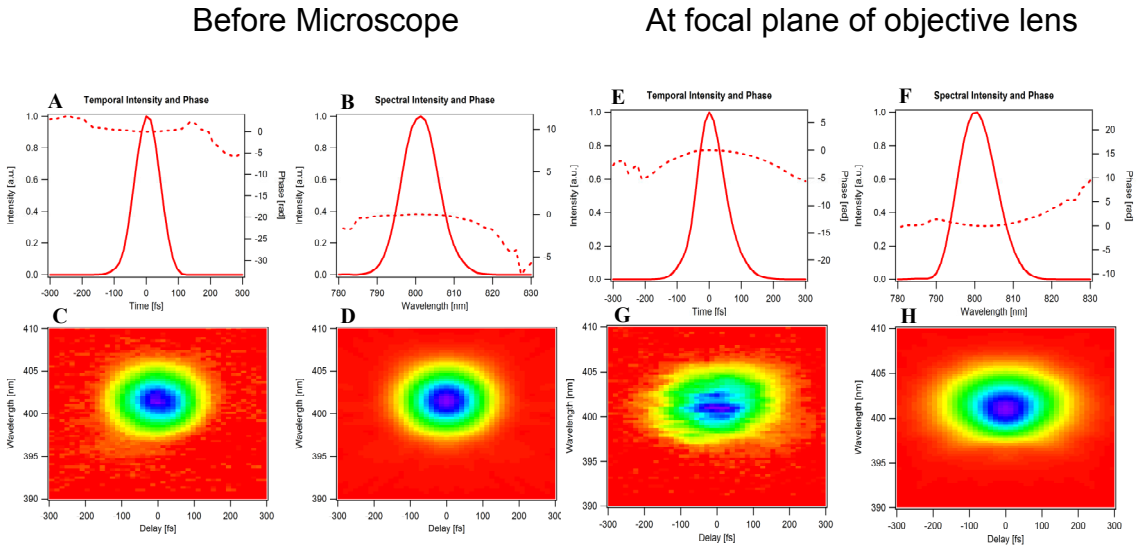

Figure 5.4: Spatial and temporal properties of laser pulse before the microscope (left) and at the focal-plane of objective lens (right).
[A, B] temporal and spectral properties of pulse before the microscope **[C,D]** measured raw data, and cleaned data. **[E, F]** temporal and spectral properties of pulse after the microscope (at focal plane of the objective lens) **[G, H]** measured raw data, and cleaned data. There was no Pockels cell in the beam path. Few elements in the excitation pathway introduced chirping only unto 15% for a 80 fs pulse of laser tuned at 800nm wavelength.

Illumination of the image across the field of view

For several imaging applications requiring studies of morphological dynamics of micron-level structures, it is important to illuminate the specimen uniformly across its field of view. Fluorescent plastics have homogeneous fluorescent properties. I used a piece of green fluorescent plastic to image this property. The specimen was imaged with a 20X W (N.A. 0.5) objective lens at scan angle ±2 degrees. The image was normalized and a contour plot was obtained using Matlab. I observed a gradual decrease of intensity from center to periphery. The difference in the intensity from center to edges is up to 15% (figure 5.5). The difference in illumination intensity across the field of view could be due to non-uniform thickness of the scan lens or tube lens across the raster scan resulting in different level of stretching of pulses at different scan angles.

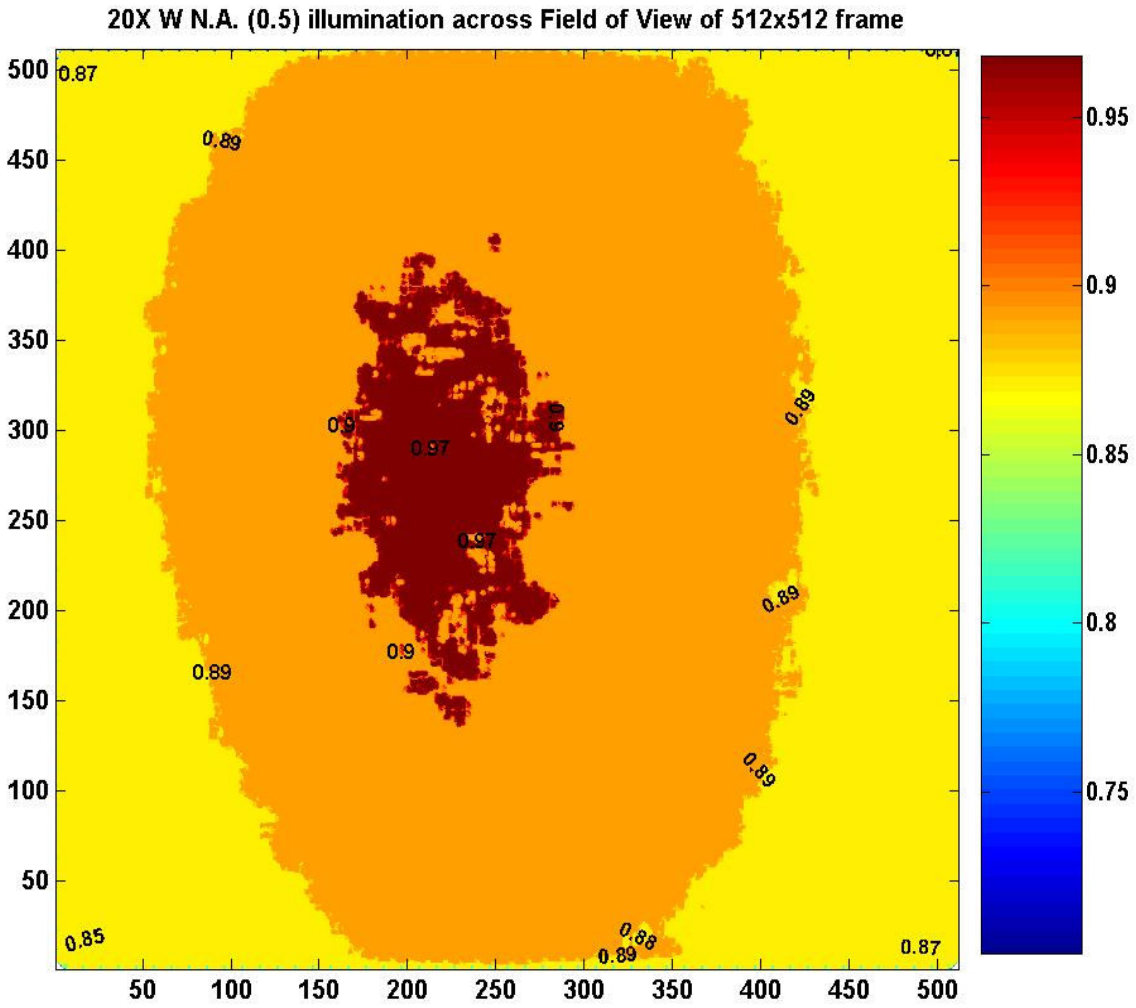

Figure 5.5: Percentage of illumination across the field of view.
A green fluorescent plastic was imaged with 20X W (N.A. 0.5) lens to estimate the illumination of the specimen across the field of view. The image intensity is normalized and a contour plot is obtained using MatLab. It is evident that the illumination is inhomogeneous across the field of view with more illumination in the center that falls by 15% towards the edges of the image.

SYSTEM VALIDATION: IMAGING

Two Dimensional (2D) Imaging

We tested this system for 2D two-photon imaging with specimen labeled with various fluorescent labels. Figure 5.6 is an image of neuronal culture that was fixed after 16 days *in vitro*. The culture is labeled with Alexa488 that is attached to antibodies

against microtubule associated protein (MAP2). Figure 5.7 is image of living dissociated mouse cortical neuronal cultures (2 DIV) that was labeled with Calcein AM fluorescent indicator. The culture was imaged alive with 800 nm excitation wavelength. These images indicate the ability of the microscope to image fine dendritic and tiny spine structures.

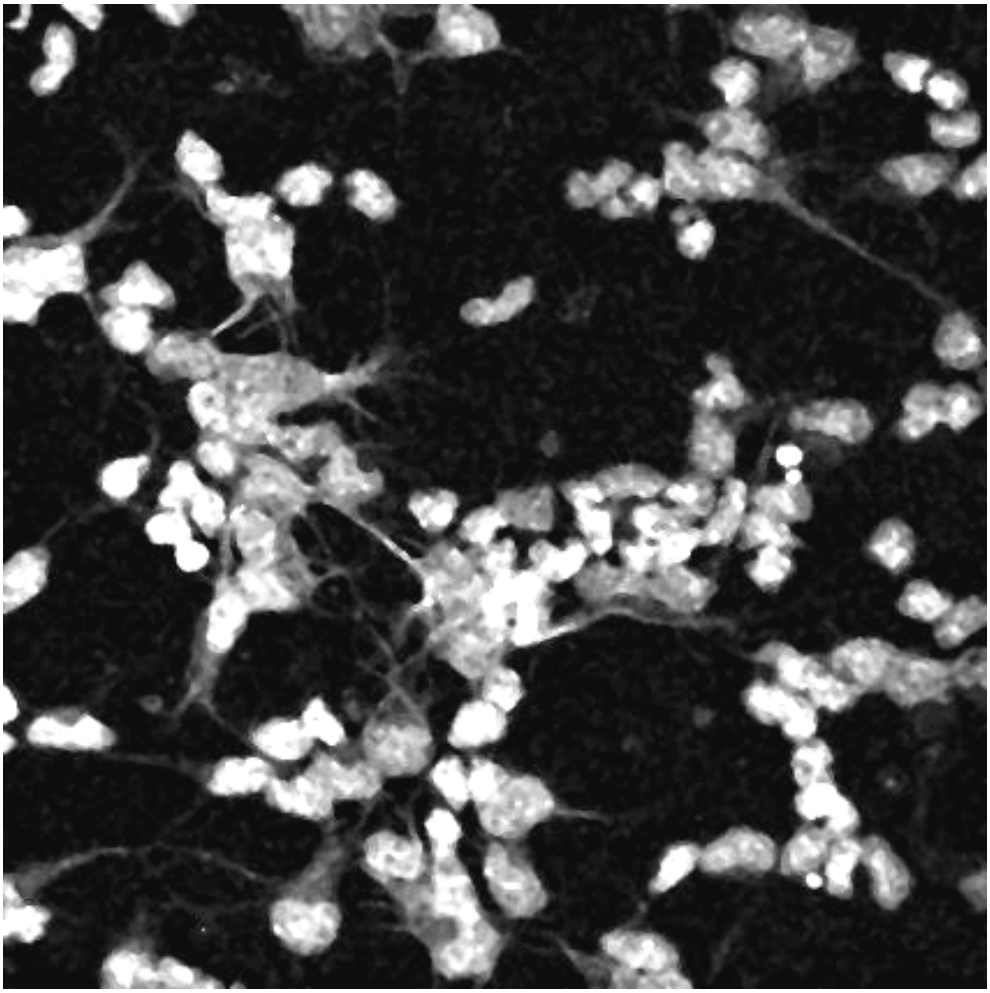

Figure 5.6: Multiphoton image of fixed dissociated rat cortical neuronal network. The network of dissociated neurons is fixed and labeled with Alexa 488 to MAP2 with water immersion 40X lens (N.A. 0.8). (Image courtesy: Mark Booth)
40x W, 0.8 NA, excitation wavelength 800 nm.

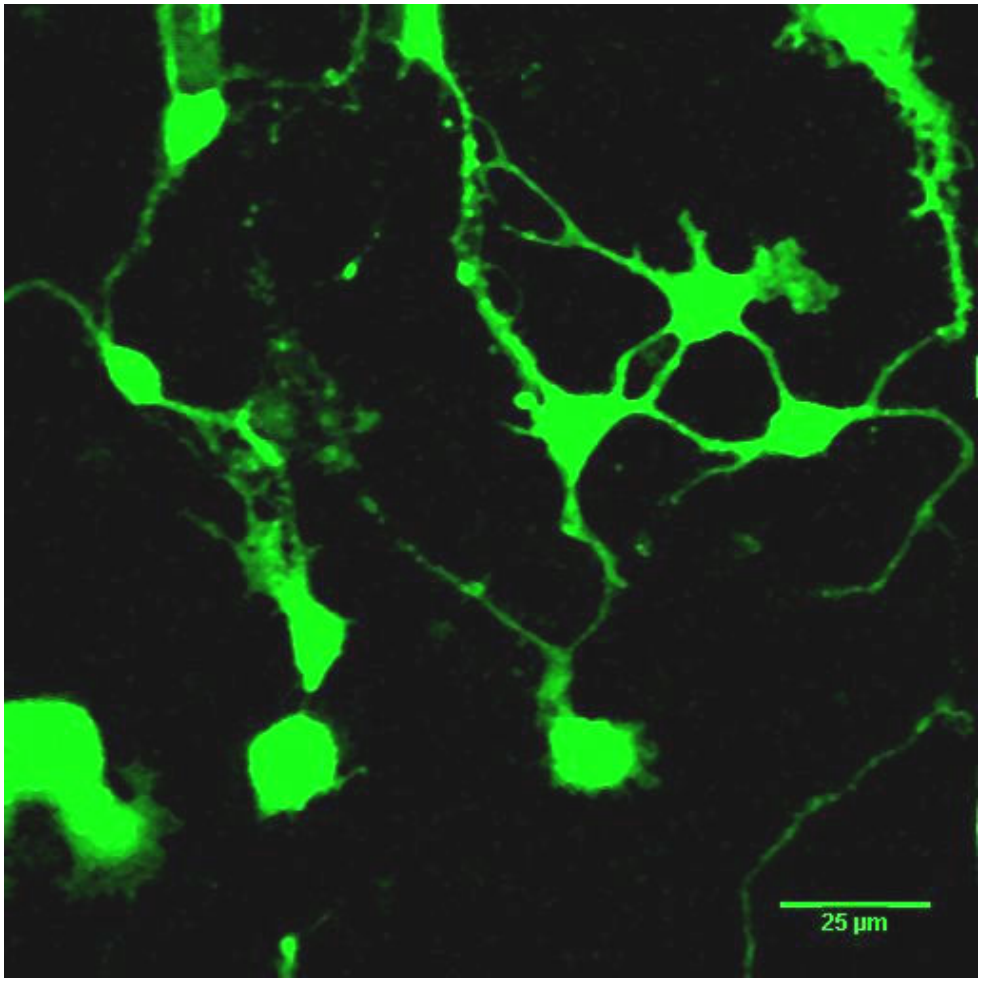

Figure 5.7: Multiphoton image of living mouse cortical neuronal network labeled with Calcein-AM.
The dissociate culture is 2 days *in vitro*. The image is taken with a 40x W, N.A. 0.8, objective lens. The frame size is 512x512 pixels. The laser was tuned to 800 nm wavelength.

Three dimensional (3D) Imaging

Further, we tested the system for three dimensional imaging. A pollen-grains slide was used to image auto fluorescence of pollen grains. The specimen was excited at 800 nm wavelength and images of a spiny pollen grain were captured at increasing z-level using a 40X water immersion lens (N.A. 0.8). The images were imported into ImageJ software to make a z-projection (figure 5.8). Next, we tested this system to image a living

hippocampal brain slice labeled with nuclear stain Hoechst (figure 5.9). The image shows a z-projection of the entire stack of images.

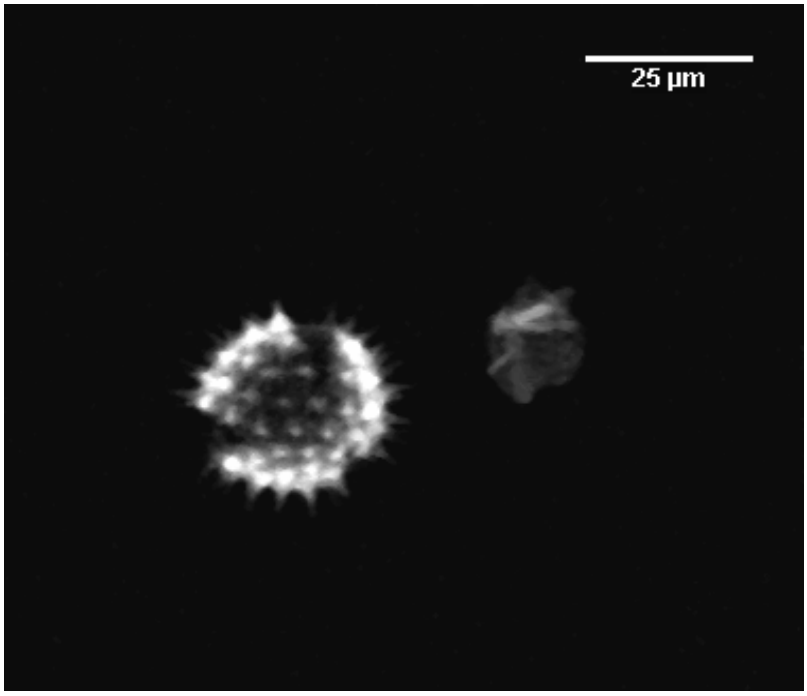

Figure 5.8: Z-projection of a pollen grain.
Pollen grains embedded in agar slide were imaged with 40X W (0.8) objective lens at different z-elevations to obtain 3D image. The images of the z-stack were merged to an average (mean) z-projection using ImageJ utilities. The brightness and contrast are enhanced in imageJ software. The frame size is 512x512 pixels. Shown frame is subset cropped from the original image. This image demonstrates ability of the microscope to image micron level details of the specimen like spines of this pollen grain.

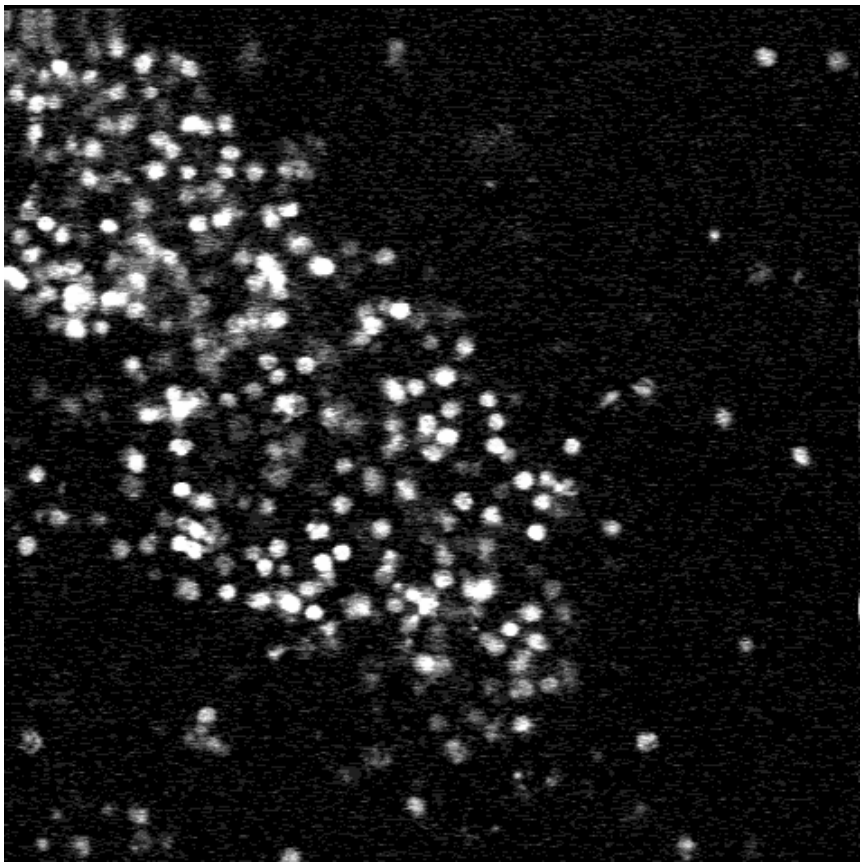

Figure 5.9: Z-projection of Hippocampal slice labeled with nuclear stain - Hoechst.
The images are taken with a 20X W (N.A. 0.5) objective lens at different z-elevations. The frame size is 512x512 pixels. The images were merged to an average (mean) z-projection using imageJ utilities. The different elevations are reflected as difference in intensity level of the nuclei. The image is raw data with background noise.

Time-lapse Imaging

Further, we tested ability of the system for time-lapse imaging. A two day old mouse neuronal network was labeled with Calcein AM in a culture dish sealed with a baggy FEP membrane lid. The images of the culture were captured every 5 minutes for 4 hours. The images were imported in ImageJ software and cleaned to remove background noise. A montage of first 42 time-frames is shown in figure 5.10. The conversion of the

time-lapse images to a movie clearly shows morphometric dynamics of interacting neurons and astrocytes in the developing culture.

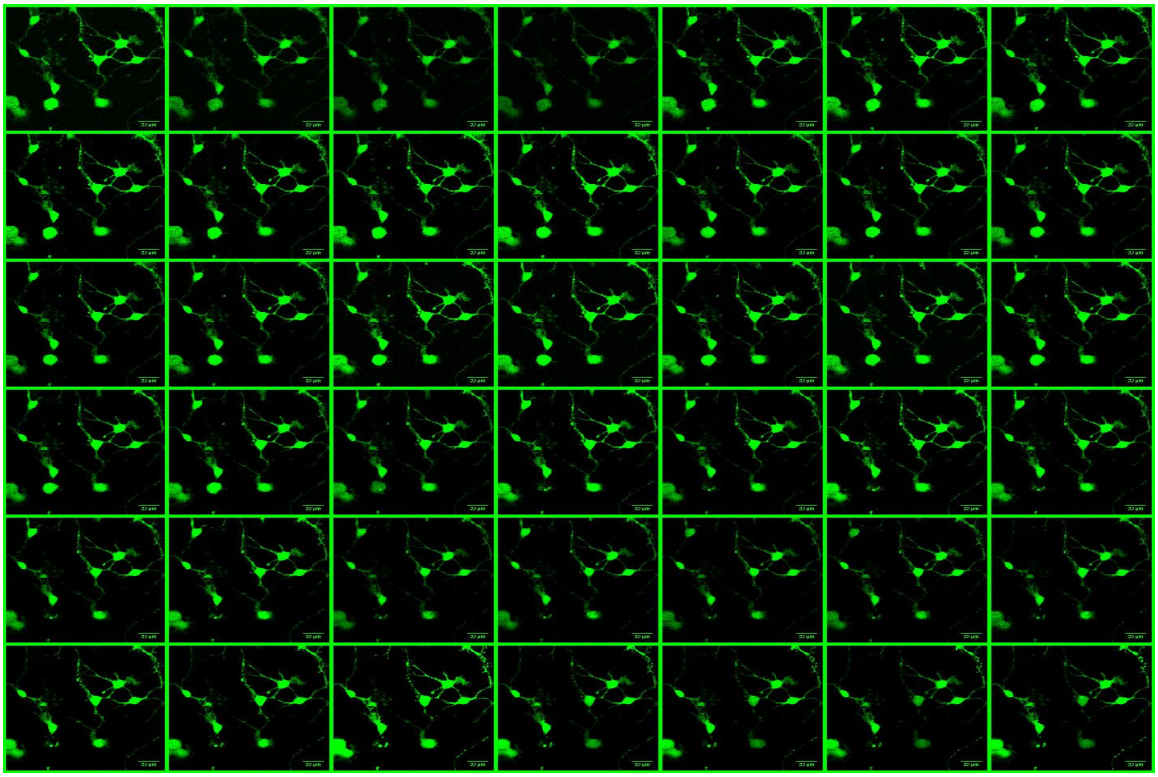

Figure 5.10: Montage of 42 time-lapse images of living neuronal culture (2DIV) labeled with calcein-AM.
The specimen was excited at 800 nm wavelength and fluorescent signal was collect with a band-pass filter. Images were taken every 5 minutes to make a time-lapse movie. Images were taken with 40x W, 0.8 NA objective lens with a 512 x 512 pixel frame size. The laser power was set at 70mW laser power at turning mirror. The scale bar is 20 μm.

Compatibility with Multiple techniques

In collaboration with our BRP partners, Bruno Frazier and group, we are developing a novel three dimensional microfluidic multielectrode neural interface system. We tested the ability of our system to accommodate a complex fluidic set-up to test delicate microfluidic arrays of prototype devices and characterize their fluidic properties.

Figure 5.11 shows an image of such a fluidic array that was tested using dilute solution of 1 µm fluorescent beads being pumped at the rate of 1ml/hr through the device.

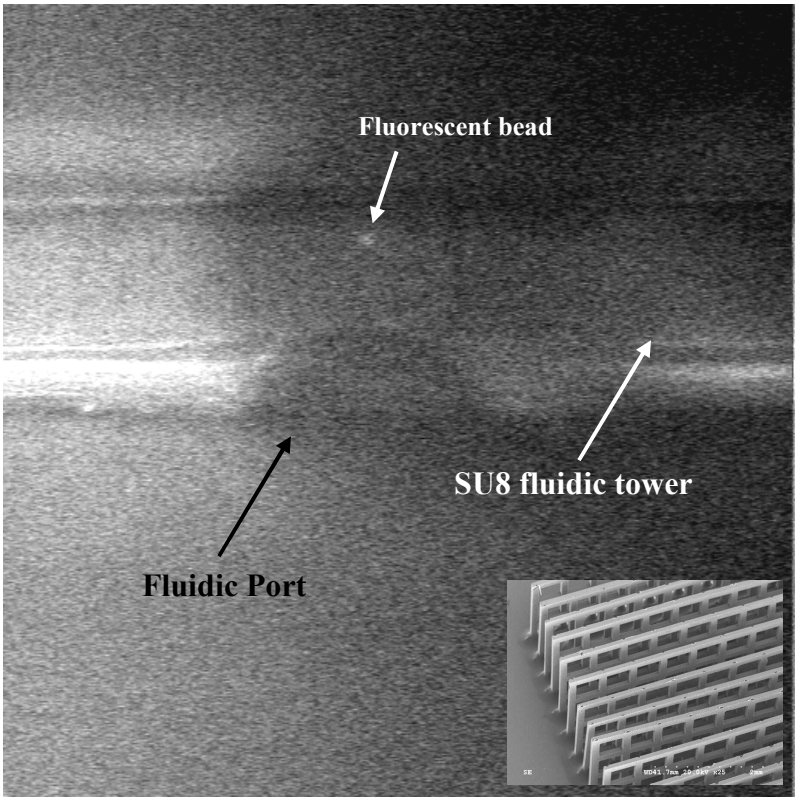

Figure 5.11: A section of fluidic tower of three dimensional microfluidic neural interface device.
The device was tested for fluidic functionality using dilute fluorescent bead solution. The flow rate was set to 1 ml/hr. This experiment demonstrated ability to accommodate complex experimental set-ups and perform simultaneous imaging. Inset, SEM image of the prototypic microfluidic array device.

DISCUSSION AND DIRECTIONS FOR FUTURE WORK

Here we demonstrated several common tests to evaluate the performance of our custom made imaging system. With this system we could successfully image living and non living *in vitro* preparations in 2D, 3D and time-lapse mode. However, many more

features could be improved or added to this system. In near term goals, it is desired to test the system for 4D imaging (X, Y, Z, t).

Large two-photon excitation cross-section of several fluorophores and spectral bandwidth of the laser pulses allow excitation of multiple fluorophores with overlapping two-photon excitation spectrum. A carefully selected combination of such fluorophores allows multicolor (red, green, blue) imaging of specimens during one scan. This feature greatly enhances the ability of long-term time-lapse imaging of living specimens with minimal photodamage to the specimen. Currently, the system is equipped with only one detection channel. Addition of two more detection channels will greatly increase the utility of this microscope for multicolor imaging.

During time-lapse imaging, images are captured only at a fixed interval of time. Ideally, a shutter is required at the excitation port to block unnecessary exposure of specimen to the laser. Also, the scanning of the scan-mirrors should be stopped when the image is not being taken to avoid heat induced damage to their circuitry during long-term time lapse imaging. The current version of the microscope does not have these features. A Pockels cell could be used to block the laser beam during the time when no image is captured. To use a pockels cell in this mode, it would be required to modify the current version of the software by synchronizing the time-lapse interval with the output of the Pockels cell. Additionally, it will be required to modify the software control to stop the scanning of the mirrors during this time-period. The Pockels cell contains a large electro-optic crystal that introduces group velocity dispersion of the pulses. Thus, it will be required to introduce a pulse-compressor in the beam path to counter chirping of the pulse introduced by the Pockels cell and other additional optical components. In addition,

the Pockels cell could be synchronized to the frame clock of the software to increase the laser intensity as a function of imaging depth in the specimen. Addition of this feature in the software will enable hands-off imaging of the thick biological specimen. Further, feedback from the detector to the pockels cell could be used to modulate the power of the excitation laser within the image plane. This feature would allow observation of tiny structures more clearly.

Together, addition of more detection channels, modification of software to synchronize the frame clock to the power modulation by the Pockels cell, and stopping the scanning mirrors during lapsed time of time-lapse imaging will allow automated imaging in time-lapse and deep-tissue imaging modes. Addition of a high numerical aperture objective lens, an appropriate bandpass filter, and a detector in the transmission path will allow collection of second harmonic generation signal along with two-photon imaging.

CHAPTER 6

CULTURING THICK ORGANOTYPIC BRAIN SLICES: A PERFUSION-BASED CULTURING METHOD

ABSTRACT

Brain slices are widely accepted *in vitro* models for wide spectrum of neuroscience investigations today. However, culturing thick organotypic brain slices is a challenge due to necrosis that starts in the center of the tissue as a result of insufficient diffusion-based supply of nutrients. We hypothesize that a convection-based supply of oxygenated nutrient medium through the thickness of the tissue will provide sufficient nutrients to every cell and may result in enhanced viability of the tissue. In this chapter, I report fabrication and optimization of a novel infusion-withdrawal type micro-perfusion chamber to culture 700µm thick brain slices. The results suggest that continuous perfusion of oxygenated nutrient medium through the tissue allows enhanced viability of 700µm thick brain slice cultures. Further, I investigated range of flow-rates to obtain enhanced viability. The results suggest that approximately three culture volume exchanges per hour is the best perfusion rate for enhanced viability of thick brain slices.

INTRODUCTION

The brain has stereotypic/characteristic organization in terms of functional units and pathways with in each species. Brain slices preserve *in vivo* like cyto-architecture and offer several advantages over *in vivo* models due to easy tissue accessibility and controllability of input/output variables while using multiple advanced techniques

simultaneously, e.g., multiphoton imaging and multi-site multielectrode recording. In the past two decades, neuroscience investigations using explants of brain slices have contributed a plethora of information underlying the functioning of the central nervous system. Thus, brain slice cultures are valuable *in vitro* models for various electrophysiological, morphological, pharmacological, ischemic and traumatic brain injury studies.

Development of organotypic brain slice cultures has opened avenues to extend several investigations done on acute brain slices over longer time periods up to several weeks. With current methods, brain slices can be maintained in culture only up to few micrometers thickness due to diffusion limited nutrient supply [35, 36, 51, 114] . Thick organotypic brain slice cultures will offer an advanced *in vitro* model for neuroscience research that requires larger portions of intact laterally and tangentially interacting stereotypic pathways with in or between different sections of the brain [5, 75]. However, it has been a challenge to culture such thicknesses of nervous tissue. It is generally believed that thick (>300μm) brain slice cultures suffer necrosis in the center of the tissue due to diffusion-limited insufficient supply of nutrients. A convection-based perfusion method, that allows flow of oxygenated nutrient medium through the thickness of the tissue, will provide nutrients to every cell in the tissue slice. This may allow enhanced viability resulting from simple forced-convective based artificial restoration of circulatory system of the tissue.

Here, I report a unique convective-flow based perfusion method to successfully culture 700μm thick organotypic brain slices. An infusion-withdrawal type micro-fluidic chamber was fabricated, optimized and used to culture thick brain slices. The results of

my experiments indicated that perfusion of oxygenated nutrient medium through the thickness of the tissue allows enhanced viability of thick brain slices compared to the slices cultured using traditional culturing methods after 2 days *in vitro* (DIV) and 5 DIV. Further, I assessed a range of non-destructive perfusion-rates that results in enhanced the tissue viability.

MATERIALS AND METHODS

Brain slice culture

The brain slices were harvested from P11-P15 mouse pups of strains C57BL/6J and B6.Cg-Tg(Thy1-YFP)16Jrs/J (Jackson Laboratory) and were mounted on the microfluidic infusion chamber. The pups were euthanized using isofluorane in accordance with approved protocols. Under sterile conditions, the euthanized pup was decapitated and brain was removed and immediately stored in chilled pre-oxygenated nutrient medium for approximately 1 minute. The brain was cut into two hemispheres using a micro-knife and each hemisphere was sliced to obtain 700µm thick tangential or coronal cortical slices using a tissue chopper. The sliced tissue was immediately transferred again to chilled nutrient medium and the slices were separated using micro-spatulas under a dissection microscope. This entire procedure, from decapitation to slice separation, took place with in 5-6 minutes. The 700µm thick cortical slices were cut into 3 mm round disks to fit snugly in the infusion chamber using a biopsy tissue cutter. These tissue slice discs were transferred to new sterile culture dish containing 2 ml of chilled nutrient medium and were transferred to a laminin-coated infusion chamber under sterile conditions inside a laminar flow hood. The microfluidic culture chamber was then

enclosed with teflon-sealed lids [97]. The syringe-pump was started and the entire set-up was transferred to culture-friendly controlled environment of a humidified incubator (5% CO_2, 9% O_2, 65% RH and 35ºC temperature) [12].

Adhesion methods

At lower flow rates (≤ 20µl/hr), laminin coating facilitates adhesion of the tissue to the gold grid and the inner walls of the infusion chamber. A FEP-membrane containing teflon lid provides a gas permeable surface from the top of the tissue to hold the tissue down to the chamber while allowing gaseous exchange to equilibrate the nutrient medium with the incubator environment. At higher flow rates, a tissue-culture compatible weight (a Millipore membrane attached to an approximately 6mm diameter gold ring using a thin layer of PDMS) was used to facilitate tissue adhesion to the infusion chamber.

Viability assessment

The tissue viability was assessed using cell permeant and non-permeant fluorescent nuclear labels, Hoescht and Propidium Iodide, respectively. The cultures were labeled with 20µl of Propidium iodide and Hoescht mixed in 200µl of nutrient medium. The cultures were incubated with fluorescent labels for 30-40 minutes while they were being perfused at the regulated flow-rate. The flow was stopped and the infusion and withdrawal ports of the chamber were sealed to avoid evaporation of the nutrient medium during imaging. The z-stack images of dead and living nuclei of tissue were collected using 20X (NA 0.5) Achroplan water immersion objective lens (Zeiss) in two separate detector channels when the specimen was excited and scanned for simultaneous multiphoton excitation of both fluorophores at 800nm wavelength. The viability was assessed by counting dead and live nuclei using ImageJ software (Appendix E).

DESIGN

Convective-flow based culturing method

Brain slices cultures are widely accepted and commonly used experimental paradigms over a century now [17, 26, 35-37, 40, 46, 47, 50, 51, 59-62, 114]. During this time, several techniques were invented to culture viable brain slices. These days, the roller tube method and the membrane insert interface method are the most popular techniques to culture organotypic brain slices for wide gamut of molecular biology, electron microscopy, imaging, electrophysiology, pharmacology, ischemia, neurotoxicology, traumatic brain injury, and immunohistochemical studies [7-11, 13, 16, 19, 25, 31, 59-62, 68, 74, 77-81].

The roller tube method was the first successful organotypic brain slice culturing method pioneered by Houge. It was later refined by Gahwiler [35]. In this process, ~100μm thick brain slices are harvested and glued to a cover-slip using a plasma and thrombin clot. The cover slip is in turn submerged in a test-tube that is half-filled with the nutrient medium. For sufficient gaseous exchange, the tubes are rotated at around 20 revolutions per hour (rph) such that the tissue is submerged in nutrient medium and then exposed to gases to supply oxygen in turns (figure 6.1A, B, C). With this method, the tissue flattens down to monolayer thickness. However, the culture maintains some organotypic structure.

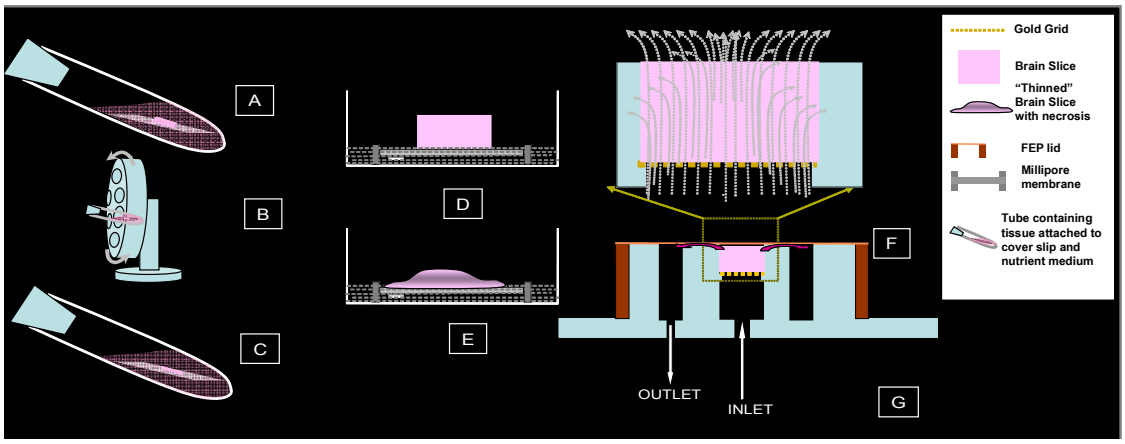

Figure 6.1: Comparison of different culturing methods.
[A,B,C] Gawhlier's Roller-tube method **[D, E]** Stoppini's membrane-insert culturing method **[F,G]** Our perfusion-based culturing method.

Later, in 1990, Stoppini et al [114] invented a simpler interface type method to culture organotypic brain slices on submerged permeable membrane inserts. In this method, ~ 150-450µm thick brain slices are harvested and placed directly on a membrane insert (Millipore). The membrane insert is floated on the nutrient medium inside a small culture dish in such a way that the brain slice gets nutrients by diffusion from the bottom side. The top surface of the tissue is covered with a thin layer of nutrient medium resulting from capillary action; however, it is in direct contact with the air to allow the gaseous exchange from the top surface (fig 6.1D, E). In this method also, the tissue thins down to 5-6 cell layer thickness and spreads laterally [111]. These two methods use diffusion as the primary source of nutrient supply to the tissue and are not successful at culturing thicker (>400µm) brain slices.

Organotypic brain slice cultures thin down significantly from their originally cut thickness. This could be because of two possible reasons: a lack of mechanical support that promotes lateral migration of cells, or cell death due to insufficient nutrients. It is believed that the tissue suffers necrosis in the middle of the slice due to insufficient

diffusion-limited nutrient and oxygen supply. Consequently, the ischemic cells eventually die and the tissue thins down to ~150µm thickness within 2 days in culture [114]. A method that supports active transport and exchange of ample nutrient medium and gases (oxygen and carbon dioxide) throughout the thickness of the tissue may allow one to culture viable thick organotypic brain slices. To test this hypothesis, we have devised a micro-biofluidic chamber in collaboration with Ari Glezer and Jelena Vukasinovic. This device not only allows the convective perfusion of nutrient medium throughout the thickness, but also provides mechanical support to the tissue on its circumferential sides (figure 6.1F, G).

The micro Fluidic chamber and the closed-loop perfusion Set-up

To support 3D flow through the tissue thickness, a coaxial bicylindrical device with common base was designed and constructed by our collaborators Ari Glezer and Jelena Vukasinovic by molding PDMS in wax molds. The wax molds were prototyped using 3D Systems Thermojet printer and a 3D CAD of the device. The inner cylinder, called the infusion chamber, has a gold micro grid (PELCO) on an orifice 700µm deep from the top surface of cylinder. The gold grid is 3mm in diameter and 50µm in thickness with a 54 square micrometer pores forming a total fluid transmission area of 40 % of its total area (figure 6.3A). To allow efficient 3D transport of the nutrient medium inside the chamber volume, there are 350µm deep microchannels in the wall of the infusion chamber that are separated 50µm from each-other [119]. The infused medium from the infusion port located at the bottom of infusion chamber passes through the tissue that is adhered to the gold grid in the infusion chamber, and exits to the outer cylinder, referred as the withdrawal chamber. The used nutrient medium is withdrawn from the outlet port

located in one side of the withdrawal chamber. The sterility in the chamber is maintained using a transparent semi-permeable FEP membrane containing teflon lid [97]. The FEP membrane is permeable to gases but not to liquids, which allows exchange of O_2 and CO_2 gases between the incubator environment and the nutrient medium across the membrane while preventing the evaporation of the medium from the chamber. This helps to maintain pH of the medium and the osmolarity inside the chamber and also prevent infection.

To operate in the infusion-withdrawal function, the chamber is attached to a push-pull type syringe pump (KD Scientific, Inc) using FEP capillary tubing as separate infusion and withdrawal lines and associated micro-connectors. The infusion line contains an aerator close to the input port that serves three main purposes: one, it traps the air-bubbles in the infusion-line and allows them to escape the micro-capillary tubing; second, it acts like a damper for the medium coming in pulses as a result of stepping motor operation of the syringe pump; and last it allows oxygenation of the nutrient medium by exchange of environment across the FEP membrane. The perfusion set-up is such that the amount of infused medium equals the amount of the withdrawn medium to maintain a constant pressure difference across the tissue in the chamber. More details to set up the device for experiments are mentioned in Appendix C.

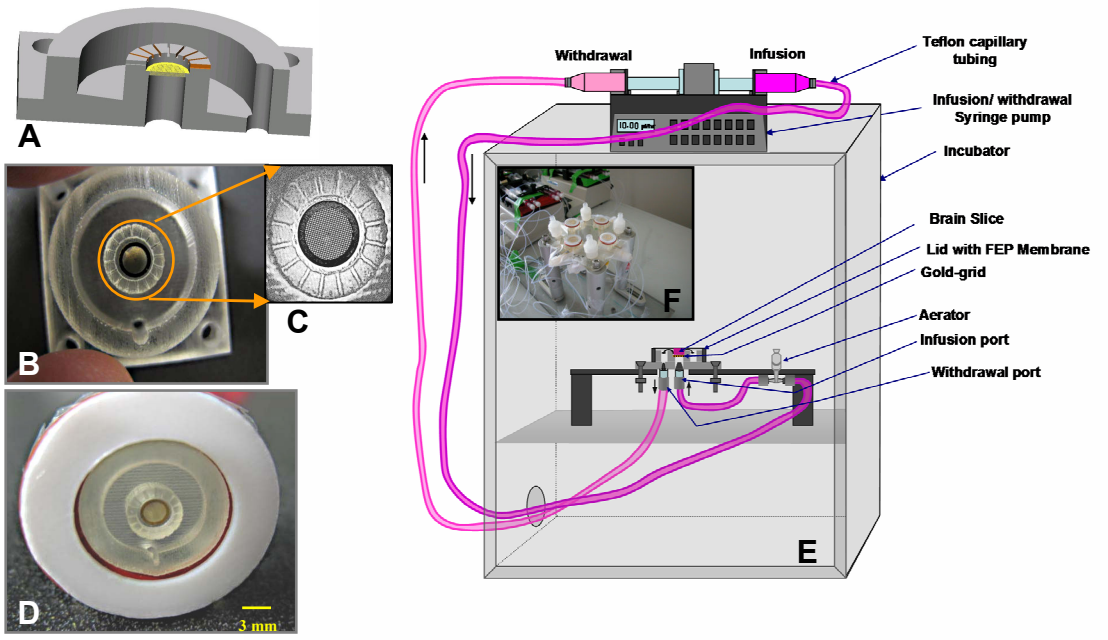

Figure 6.2: Microfluidic culture set-up.
[A] The computer Aided Design (CAD) of microfluidic chamber to mass-produce molds from thermoplastic material. The chamber has two coaxial cylindrical units; the inner cylinder, called infusion chamber is hollow and houses a gold-grid at 700µm depth from top to support tissue. The cylinder contains 150µm wide and 350µm deep channels on its wall to achieve uniform infusion of medium in the deeper layers of the cultured tissue. The bottom of this cylinder is used as a infusion port using micro-capillary tubing. The outer cylinder, called withdrawal chamber, carries the out-flowing medium from the infusion chamber. This chamber contains a small hole on one side of the withdrawal chamber to attach the withdrawal micro-capillary tubing. **[B]** Perfusion chamber made out of PDMS material using thermoplastic mould. **[C]** The infusion chamber holds a 3mm in diameter gold grid usually used for SEM/TEM microscopy. The pore size in the gold grid is 54 x 54 um making up a total of 40% area open for the fluid injection. **[D]** The perfusion chamber is covered with FEP membrane-containing teflon lid. When attached to infusion and withdrawal lines, this chamber provides means to control the tissue environment and helps to prevent infections. **[E]** Perfusion set-up to perfuse oxygenated nutrient medium while maintaining pH, temperature and osmolarity of the culture. **Drawing:** Infusion/withdrawal of medium at the same flow rate maintains the pressure gradient across the tissue. The set-up is kept in a humidified incubator controlled at 5% CO_2, 9% O_2, 65% RH, and 35ºC. The infused medium passes through the aerator and gets equilibrated with the incubator environment before reaching the tissue. The teflon membrane lid prevents evaporation of medium and thus maintains osmolarity of nutrient medium. **Inset:** Experimental set-up for four slices simultaneously using a single syringe pump.

Flow trajectories in the infusion chamber

To ensure nutrient supply throughout the tissue volume (chamber volume), our collaborator Jelena Vukasinovic, conducted micro Particle Image Velocimetry (µPIV) studies at various elevations in the infusion chamber. These studies indicate that the

microjets[3] emanating from each of the gold-grid openings interact with adjacent ones and this interaction increases/intensifies with elevation of the chamber (fig 6.3b-e) resulting in more uniform flow trajectories at higher elevation. The flow direction of infused medium near the periphery of the chamber is biased by the micro-channels in the chamber wall while the infused medium microjets closer to the axis of the chamber penetrate deeper before getting biased by the microchannel openings starting at mid height (350μm from the gold-grid orifice) of the infusion chamber wall (figure 6.3b-f, 6.1f, 6.1g). On the other hand, the microjet trajectories emanating close to the infusion chamber wall, get biased laterally by the microchannel openings. This design ensures the lateral supply of the nutrient medium closer to the wall of the chamber. This geometry of the chamber allows axial and lateral flow of nutrient medium inside the culture volume (infusion chamber). The flow profile of nutrient medium thus achieved ensures ample nutrient supply in the deeper ischemia vulnerable area of the tissue.

---

[3] Microjet : A stream of infused medium from each opening (pore) of the gold grid.

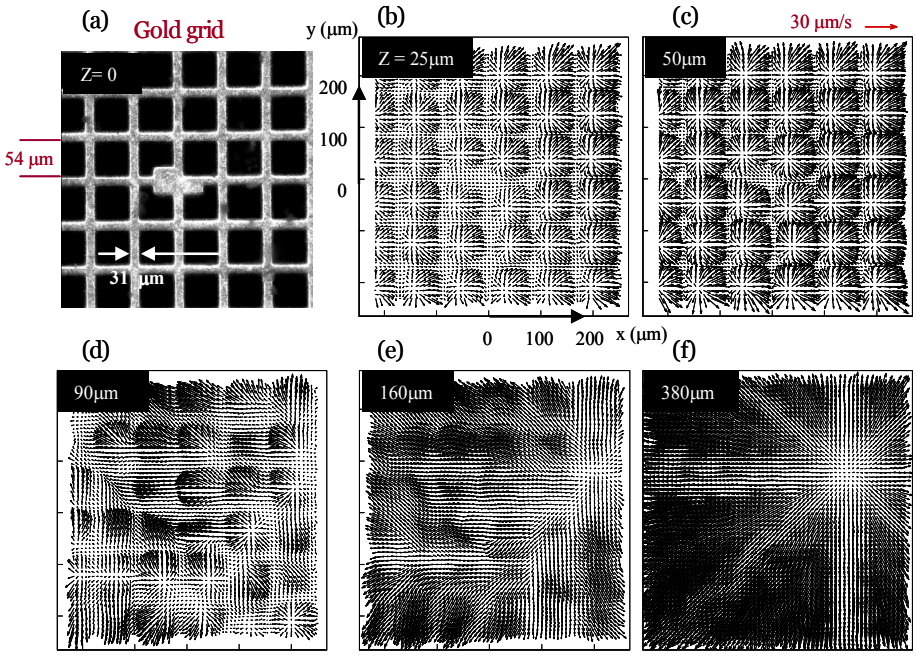

Figure 6.3: Flow trajectory and velocity distribution of micro-jets at various elevations in the infusion chamber at a flow rate of 5 µl/min. **[a]** Magnified view of the gold grid **[b]** The radially spreading infused fluid jets near the surface of gold grid submerged in stationary fluid **[c]** Upon interaction with a relatively stagnant medium within the chamber, radial outflows intensify with elevation as jets broaden and decelerate streamwise (along their axes) **[d]** Concomitant with reduction in streamwise momentum, µjet interactions become apparent with peripheral jets turning at lower elevations **[e]** Peripheral µjets merge and begin vectoring towards the perimeter of the cultured domain influenced by a strong wall jet developing along the membrane **[f]** The exit flow is biased towards the µchannel exits in the infusion chamber wall, and, a strong wall jet originating from the centrally located stagnation zone forms as jets issuing closer to the center (axis) of the chamber penetrate deeper into the cultured domain than those located closer to µchannels. This study ensures ample amount of nutrient supply in the center of the cultured brain slice resulting from convective flow of nutrient medium (Data Courtesy: Jelena Vukasinovic)

RESULTS

Perfusion allows enhanced culture viability

700µm thick cortical slices harvested from the same brain were cultured on membrane inserts using Stoppini's method and microperfusion devices. The perfusion in the experimental microperfusion chambers was started at 10µl/hr infusion/withdrawal rate using a push-pull syringe pump. The cultures plated on unperfused microperfusion devices (control experiments) were placed in a small culture dish containing nutrient medium. In these control experiments, medium supply is diffusion based from the bottom of the gold grid analogous to membrane insert method. After two days of perfusion, the viability of cultures was assessed by multiphoton imaging of the slices labeled with Hoechst and Propidium Iodide fluorescent nuclear labels (Appendix D). The results of my experiments indicate a statistically significant increase in viability of the perfused cultures compared to the unperfused sister cultures (figure 6.4).

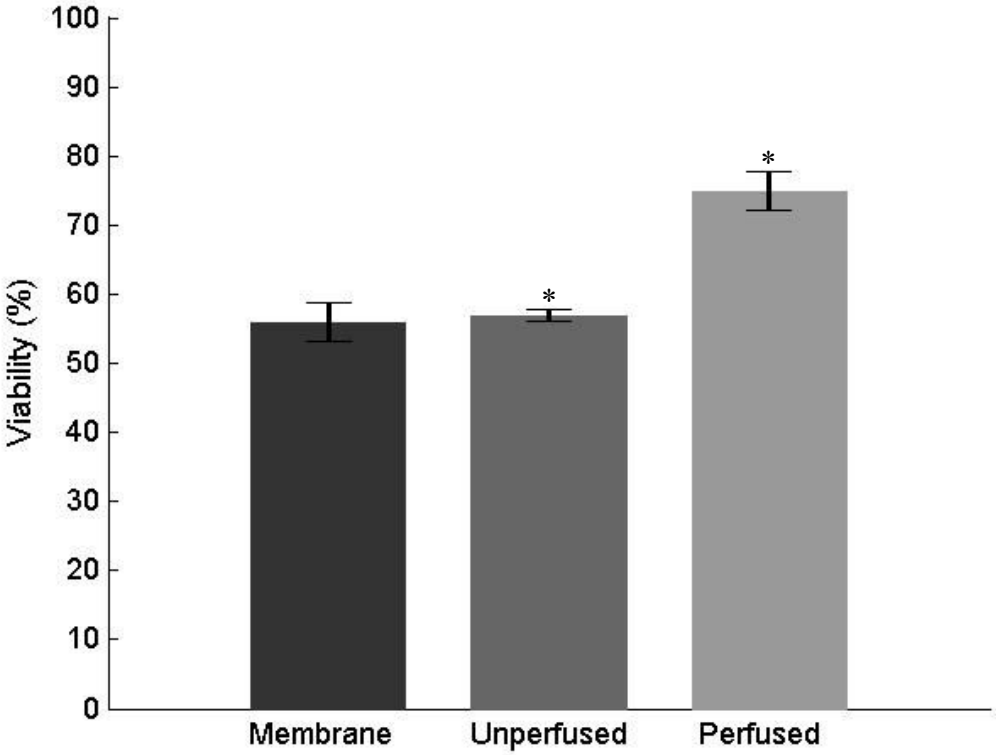

Figure 6.4: **Perfusion of nutrient medium through the tissue thickness results in enhanced tissue viability.**
Cortical slices of 700µm thickness were cultured on microperfusion devices and on membrane inserts using Stoppini's method. The unperfused microperfusion device cultures and membrane insert cultures were taken as control cultures. Figure shows Mean±SEM (n =4 of each case) viability of these cultures assessed after 2DIV. The perfusion rate was 10µl/hr. A generalized linear model ANOVA test, followed by Tukey's multiple comparison test was used to evaluate statistical significance. The perfused cultures showed statistically significant increased in viability compared to the control sister cultures ($p < 0.05$).

Optimal perfusion rates for enhanced viability

To assess the flow-rates for optimal supply of nutrients to the tissue without shear-stress induced damage to the tissue, we performed a series of experiments to perfuse the tissue at different flow rates that include: 5, 10, 20, 30µl/hr. The viability was assessed after 2DIV. The results of my experiments indicate that flow rates 20µl/hr or less result in enhanced viability of the tissue while higher flow-rates turned out to be

detrimental to the delicate tissue structures resulting in formation of channels inside the tissue and reduced overall viability. Thus, I found that a flow rate translating to 3 culture volume exchanges per hour is the optimal flow rate to maximize the viability of the tissue as a result of constant nutrient supply (figure 6.5).

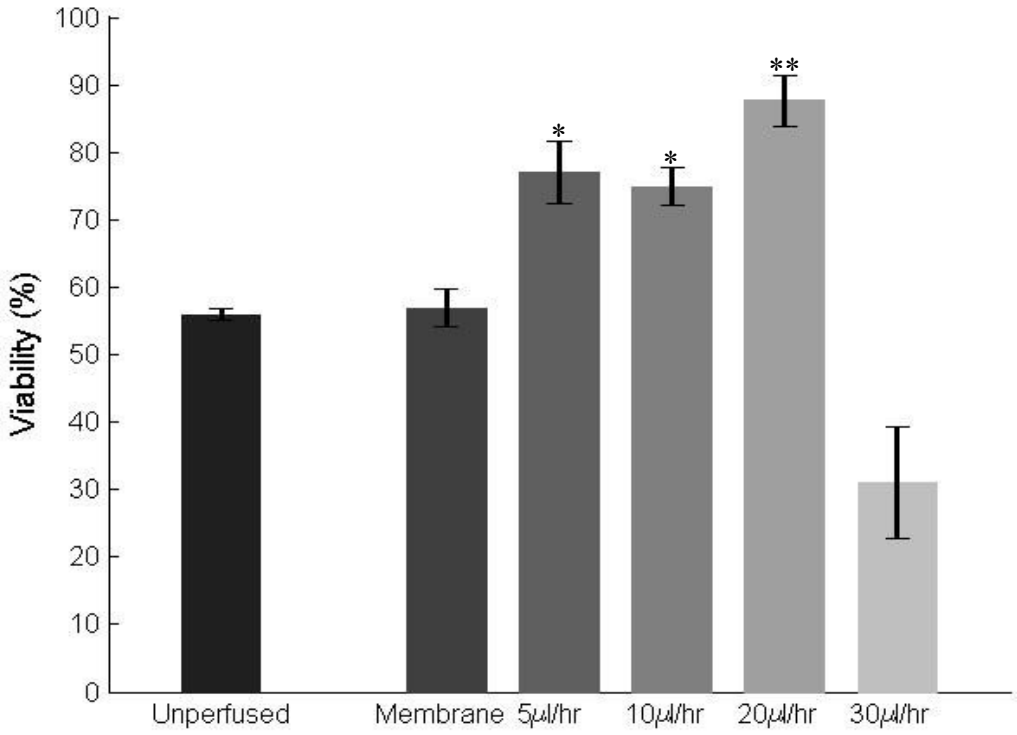

Figure 6.5: Assessment of range of optimal flow rates for enhanced slice culture viability.
Flow rates ≤ 20 µl/hr are non-invasive flow rates for enhanced tissue viability. A flow rate (20 µl/hr) of 3 volume exchanges per hour is optimal for enhanced viability. Higher flow rates (≥ 20µl/hr) are detrimental to tissue. Figure shows viability at each flow-rate (Mean±SEM, n=3-4). A generalized linear model ANOVA followed by a Tukey's multiple comparison test was used to evaluate statistical significance. ** indicates $p<0.01$ compared to membrane and unperfused controls. * indicate $p<0.05$ compared to membrane and unperfused controls.

Viability of organotypic thick brain slice cultures after 5 DIV

I further assessed the viability of the cultures after 5 days of continuous perfusion of nutrient medium at the non-destructive range of flow rates that was determined in the

2DIV series of experiments. The viability was assessed using the same methods as explained in the optimal flow-rate assessment results. The results indicate greater than twice the viability of the perfused cultures compared to the unperfused cultures. Even after 5 days of perfusion, the flow rate 20µl/hr proves to be the most suitable flow-rate for enhanced viability of the culture (figure 6.6). This flow rate translates to three culture-volume exchanges per hour.

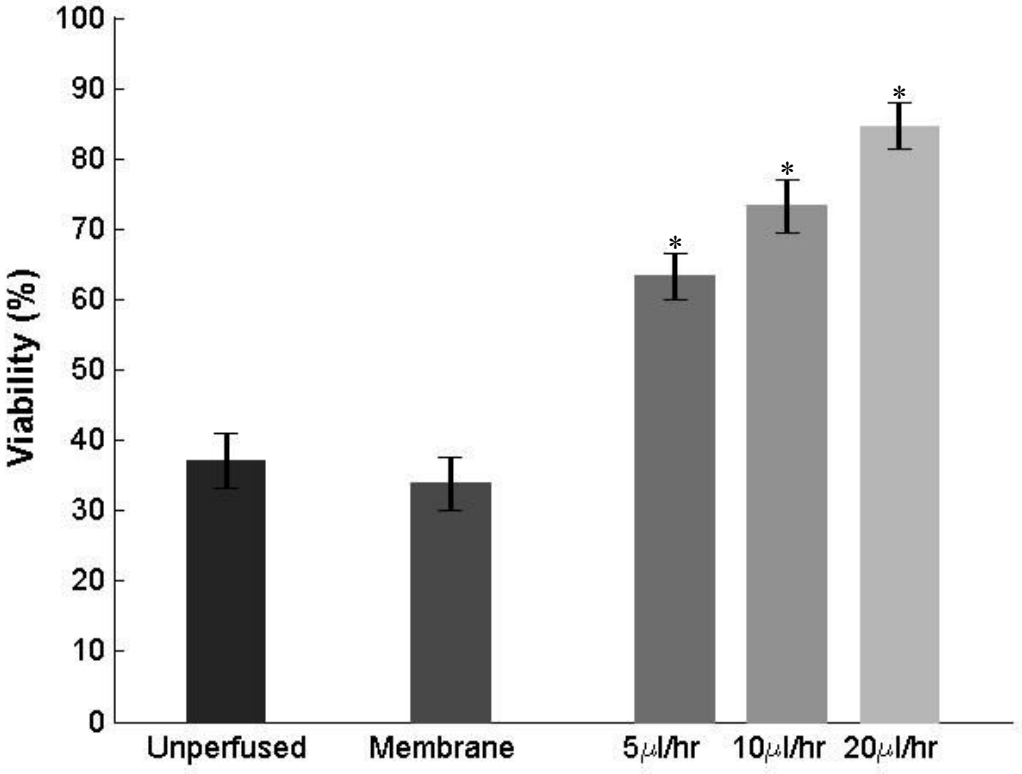

Figure 6.6: Viability of cultured brain slices after 5 days *in vitro.*
Thick brain slices show enhanced viability at various non-invasive flow rates (5, 10, 20µl/hr) compared to unperfused cultures and standard membrane insert based cultures after 5 days of perfusion. At 20µl/hr flow-rate, > 80% viability was observed even after 5 days in culture and proved to be the optimal flow rate for sufficient nutrient supply through the thickness of the tissue. The viability is plotted (Mean±SEM, n= 3-4) for various flow rates. A generalized linear model ANOVA test, followed by Tukey's multiple comparison test was used to evaluate statistical significance. (*) indicates statistical significance ($p<0.01$) compared to unperfused and membrane controls.

DISCUSSION AND CONCLUSIONS

Here I presented a successful technique to culture viable 700µm thick organotypic cortical slices using a novel "through the thickness perfusion" paradigm. To use this method successfully, it is required to anchor the tissue to the gold grid substrate and the inner walls of the infusion chamber to block all the paths of low resistance for fluid flow. In the absence of any path of low-resistance of flow, the infused medium is required to flow through extracellular space of the tissue throughout its thickness before entering the withdrawal chamber. The adhesion of the tissue is achieved by coating the infusion chamber with laminin and incubated for 30-40 minutes. Additionally, the brain slices are cut into 3 mm circular discs using a sterile biopsy tool before transferring to the infusion chamber. The same diameter of the infusion chamber and the brain slice allow perfect accommodation of tissue in the chamber that facilitates adhesion of the tissue to the walls of the infusion chamber via laminin coating, ensuring that no paths of low resistance exist for the flow of infused medium. Further, the FEP membrane containing teflon-lid of chamber also assists in confining the tissue in the infusion chamber by minimizing the space on the tissue surface that might result in tissue floating during the initial adhesion process when the infusion is started.

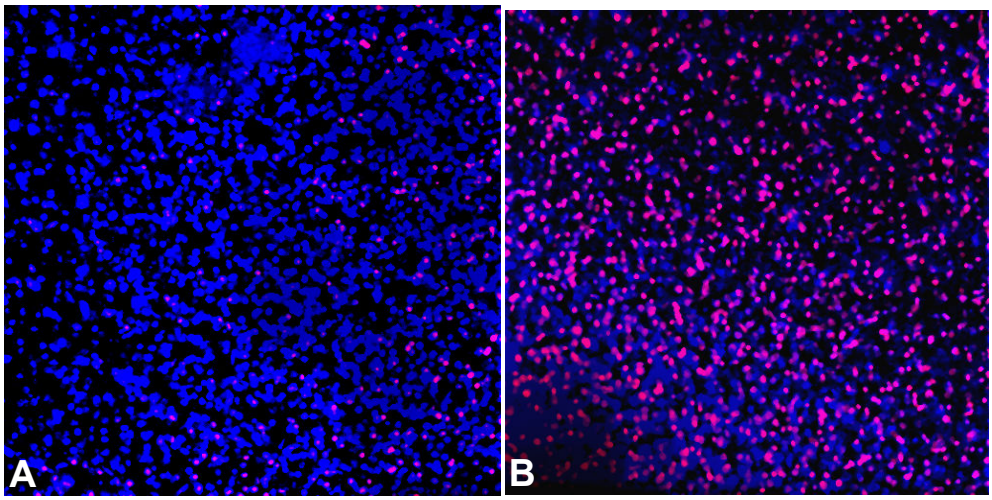

Figure 6.7: Representative micrographs of tissue nuclei labeled with Hoechst and Propidium iodide.
[A] z-stack project of part of perfused tissue thickness indicating significantly higher number of live cells (blue) than the dead cells (red). **[B]** z-stack project of part of control tissue thickness indicating significantly higher number of dead cells compared to perfused tissue.

The results of my experiments indicate that perfusion of nutrient medium allows increased viability of the cultured brain slice compared to two types of control cultures. Further, I examined viability for a series of flow rates (5, 10, 20, 30µl/hr) used to perfuse the tissue for two days in culture. The long-term (5 DIV) perfusion experiments' results suggest there is a linear increase in the viability of the cultures with increase in infusion rates. Additionally, both the 2 day and 5 day perfusion results demonstrate that approximately 3 culture volume exchanges per hour supply ample nutrients to the tissue resulting in over 80% viability of the tissue even after 5 days in culture (figure 6.7). Some percentage of the cell death could be ascribed to the initial injury to the peripheral cell layers of the culture caused by the tissue cutting process.

This novel perfusion paradigm to culture thick brain slice cultures could be extended to culture slices from other parts of the brain as well. With the modified design

and fabrication of the gold grid device, one could extend this technique to culture thick organotypic co-cultures of any lateral dimensions. Further, these devices could be modified to culture even thicker brain slices. We expect thick brain slice cultures will provide an advanced experimental platform to several neuroscience and neuroengineering researchers who are working in the fields of learning and memory, traumatic brain injury, neuropharmacological studies, neurotoxicity studies, ischemia studies, neural implant *in vitro* biocompatibility studies for prosthesis applications, neural implant-glial scan formation studies, and so on.

CHAPTER 7

CHARACTERIZATION OF THICK ORGANOTYPIC CORTICAL SLICE CULTURES

ABSTRACT

Thick organotypic cortical slice cultures might prove to be valuable *in vitro* models in a wide spectrum of neuroscience investigations. Viable 700µm thick brain slices can be successfully cultured *in vitro* by perfusion of nutrient medium through the tissue. In this chapter, we present qualitative characterization of organotypic organization and functional activity of the organotypic 700µm thick brain slice cultures. Further, we demonstrate that our culturing method maintains greater thickness of the tissue compared to the control cultures even after 5 days *in vitro* (DIV) by providing additional mechanical support using the biocompatible walls of the infusion chamber. Together, these results reveal that thick organotypic cortical slices could be cultured successfully that maintain organotypic cellular level morphological organization and are functionally active. Thick organotypic brain slice cultures provide an *in vivo* like platform for the creation of 3D hybrots, an *in vitro* embodied culture model to study learning and memory.

INTRODUCTION

Brain slices are well established *in vitro* experimental models to study mechanisms underlying learning and memory, and several other neuroscience investigations, since they preserve *in vivo* like cyto-architecture while providing easier access to the desired cellular networks and controlled input/output variables compared to

in vivo preparations. Today, most of our understanding of synaptic plasticity and mechanisms of LTP and LTD is attributed to hippocampal and cortical slice studies. Recently, there is flurry of investigations performed on thick cortical, hippocampal or co-culture slices preparations [5, 11, 59, 60, 66]. However, these studies are done on acute slice preparations due to their short life-time and unavailability of a reliable method to culture thick brain slices. Hence, these important investigations are limited to only a few hours. To date, very little information is available on long-term network properties of brain information processing. Organotypic brain slice cultures offer an opportunity to extend these studies over longer time periods to study a wide range of mechanisms that include neurogenesis [105], synaptogenesis [88], regeneration [68], protein expression using viral vectors [30, 56, 72, 73], and simulated traumatic brain insults [62]. Additionally, the accessibility of the preparation permits multiple noninvasive techniques to be applied simultaneously [1, 2, 20, 21, 24, 13, 16, 52, 53, 57, 85, 92, 73, 74, 96, 109, 112], e.g. multielectrode arrays, multiphoton imaging, pharmacological manipulations, etc . However, current culturing methods allow only 5-6 cell thick organotypic cultures for longer term viability [111]. A method to culture thick brain slice cultures will provide a novel platform to extend these studies over wider and deeper areas of neuronal networks for longer time periods.

Here I report successfully cultured 700μm thick cortical slices of 3mm diameter. However, the culture chamber could be easily modified to accommodate any smaller or larger radial dimensions of the tissue. In this study, I qualitatively evaluated organotypic organization of the culture after 5 days *in vitro*. The culture appears to maintain healthy cells of characteristic morphological shapes. Additionally, I found that these cultures

maintain thickness >80% of the actual thickness of the tissue. Further, I was able to record spontaneous or chemically evoked activity in most of the cultures.

Together, these results indicate healthy thick cortical cultures with maintained organotypic morphological organization and functional activity. Thick organotypic cortical slice cultures may offer a novel experimental model for long-term neuroscience investigations. This culturing method is a step closer to advance technology to create a simpler embodied *in vitro* neuro-robotic hybrid model to study long-term learning, memory and drug addiction *in vitro* using multiple non-invasive techniques.

MATERIALS AND METHODS

Brain slice culture and perfusion set-up

The brain slices were harvested from P12-P16 mouse pups of strains C57BL/6J and B6.Cg-Tg(Thy1-YFP)16Jrs/J (Jackson Laboratory) and were mounted on the microfluidic infusion chamber. The pups were euthanized using isofluorane in accordance with approved protocols. Under sterile conditions, the euthanized pup was decapitated and brain was removed and immediately stored in chilled pre-oxygenated nutrient medium for approximately 1 minute. The nutrient medium contains 50% OptiMEM (Invitrogen), 25% equine serum (Hyclone), 25% Hank's Balanced Salt Solution (HBSS) (Invitrogen), 500µl of 0.5mM Glutamax (Gibco) and 0.45 g of D-glucose (Invitrogen) per 100ml of nutrient medium. The brain was cut into two hemispheres and each hemisphere was sliced to obtain 700µm thick tangential or coronal cortical slices. The sliced tissue was immediately transferred again to chilled nutrient

medium and the slices were separated using micro-spatulas under a dissection microscope. This entire procedure, from decapitation to slice separation, took place with in 5-6 minutes. The 700µm thick cortical slices were cut using a biopsy tool into 3mm round disks to fit snugly in the infusion chamber. These tissue slice discs were transferred to a new sterile culture dish containing 2ml of chilled nutrient medium and were transferred to the laminin-coated infusion chamber. The microfluidic culture chamber was then enclosed with FEP membrane-sealed teflon lids [97]. The syringe-pump was started and the entire set-up was transferred to culture-friendly controlled environment of a laboratory incubator maintained at 5% CO_2, 9% O_2, 65% Relative Humidity and 35ºC temperature [12].

Adhesion methods

At lower flow rates (≤ 20µl/hr), laminin coating facilitates adhesion of the tissue to the gold grid and the inner walls of the infusion chamber. An FEP membrane containing teflon lid provides a gas permeable surface from the top of the tissue to hold the tissue down to the chamber while allowing gaseous exchange to equilibrate nutrient medium with the incubator environment. At higher flow-rates, a tissue-culture compatible weight (a Millipore membrane attached to an approximately 6mm diameter gold-ring using thin layer of PDMS) was used to facilitate tissue adhesion to the infusion chamber.

Viability assessment

The tissue viability was assessed using cell permeant and non-permeant fluorescent nuclear labels, Hoescht and Propidium Iodide as explained in the chapter 6.

Tissue Fixing and Haematoxylin and eosin (H&E) staining

Due to limited imaging depth with fluorescence microscopy, the cultures were fixed and sliced along their thickness into thin slices. These slices were stained with H&E stain using the standard protocol and were mounted on gelatin coated slides to obtain the thickness parameters. The tissue was fixed in 2% paraformaldehyde in 0.5X PBS with its pH and osmolarity adjusted similar to that of nutrient medium that is supplied to the cultures. Adjustment of these parameters was crucial to prevent any major changes in tissue thickness. This was ensured by fixing fresh tissue of various thicknesses. The thickness was assessed using bright field images taken with camera operated upright microscope in a calibrated field of view.

Functional Activity recording

Micro-wire electrode set-up

The Axoclamp electrophysiology station was modified to adopt 50µm thin steel wire electrode and a ground electrode. The wire electrode was firmly held using a holder attached to a xyz stage that allowed precise movement of the electrode to facilitate probing of the tissue at various places and depths. The spontaneous signal was measured relative to a ground electrode using commercial software at 10 kHz sampling rate. In the absence or low level of spontaneous activity, the culture was treated with 120 mM KCl solution warmed at incubator temperature to record chemically evoked activity.

RESULTS

Viability of thick organotypic brain slice cultures

Current popular methods to culture brain slices include the roller tube method and the membrane insert method [2, 10]. These methods exploit diffusion as the source of nutrient supply to the tissue throughout its thickness. The tissue eventually flattens down to a monolayer in the roller tube method and 5-6 cells thickness in the membrane insert method [111]. We have invented a novel perfusion method to culture thick brain slices (Chapter 6). Using this method, I evaluated viability of the cultures at non-invasive perfusion rates after 2 days of perfusion and 5 days of perfusion (figure 7.1). The perfusion of cultures showed increased viability as a result of increased perfusion rates both after 2 days and 5 days of perfusion. The viability decreases over time (5days versus 2 days) even for perfused slices. However, the decrease in viability of unperfused slices was much greater than that of the perfused slices.

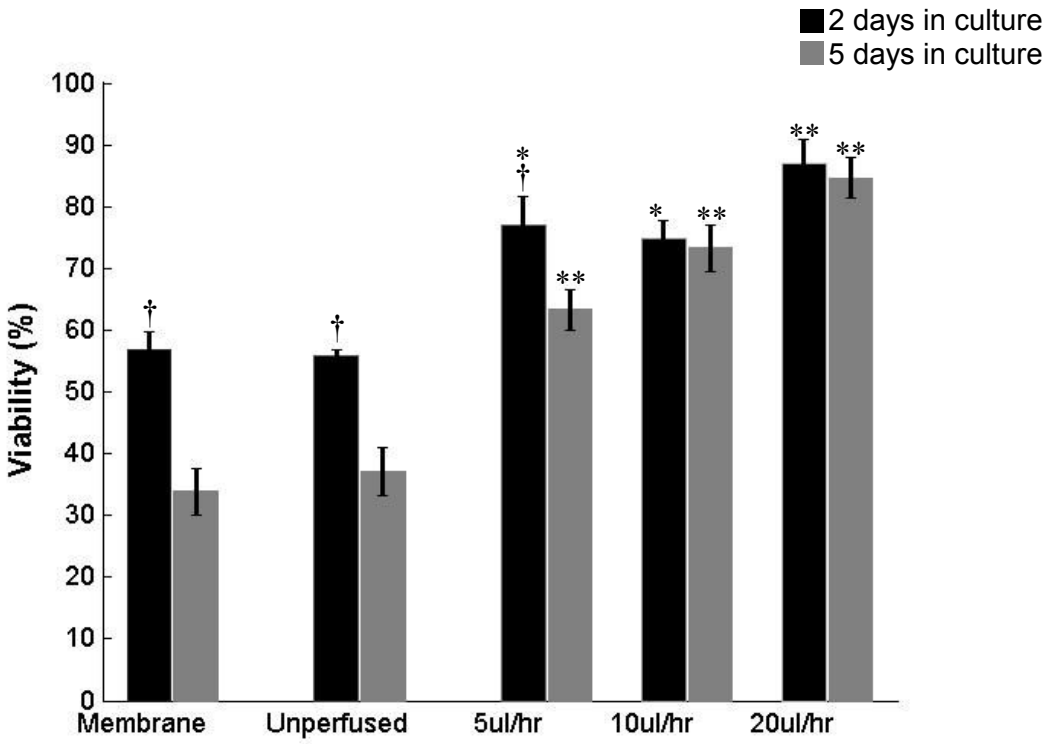

Figure 7.1: Viability of culture after 2 days and 5 days *in vitro*.
The viability of the perfused cultures at 5DIV versus 2DIV decreases much less at 20µl/hr flow rate compared to viability at 5µl/hr flow-rate, thus indicating 20µl/hr to be optimal flow rate to culture viable 700µm thick brain slices for long-term. Image shows viability assessment after 2DIV and 5DIV (Mean±SEM, n=3-4). A two way ANOVA test followed by Tukey's multiple comparison test was used to evaluate statistical significance. (†) indicates $p<0.01$ significant change in viability at 2DIV compared to 5DIV for the same culture condition (i.e., perfused at a given flow rate, unperfused, membrane). (**) indicates $p<0.01$ for viability compared to viability of unperfused and membrane controls for same day of perfusion. (*) indicate $p<0.05$ for viability compared to unperfused and membrane controls for same day of perfusion.

Organotypic organization of thick cortical slice cultures

To evaluate the morphological organization of the cultures, I fixed them after 5 day perfusion experiments in 2% paraformaldehyde in 0.5X phosphate buffered saline (PBS). This concentration of fixing solution helped to maintain the osmolarity and pH of the tissue that are important parameters in determining cell health and size. The tissue was sliced perpendicular to its diameter into 20-50µm thick slices to reveal its thickness.

I also prepared specimens from freshly cut and fixed tissue as a baseline to compare with cultured slices. The tissue was stained with H&E stain using standard protocols and was mounted on gelatin slides to observe the specimen using bright field microscope. Several cell types of characteristic morphology like pyramidal cells and star-shaped cells could be identified in the baseline specimen indicating organotypic nature of the culture [8]. These cell types could also be identified in perfused cultures. Further, perfused cultures showed similar cell density and cell sizes as baseline preparations while they were compromised in the unperfused control cultures. Evidently, the unperfused culture on the gold grid shows lesser cell density in the deeper layers of tissue. In membrane insert cultures, the cell density and size were found to be seriously compromised (figure 7.2).

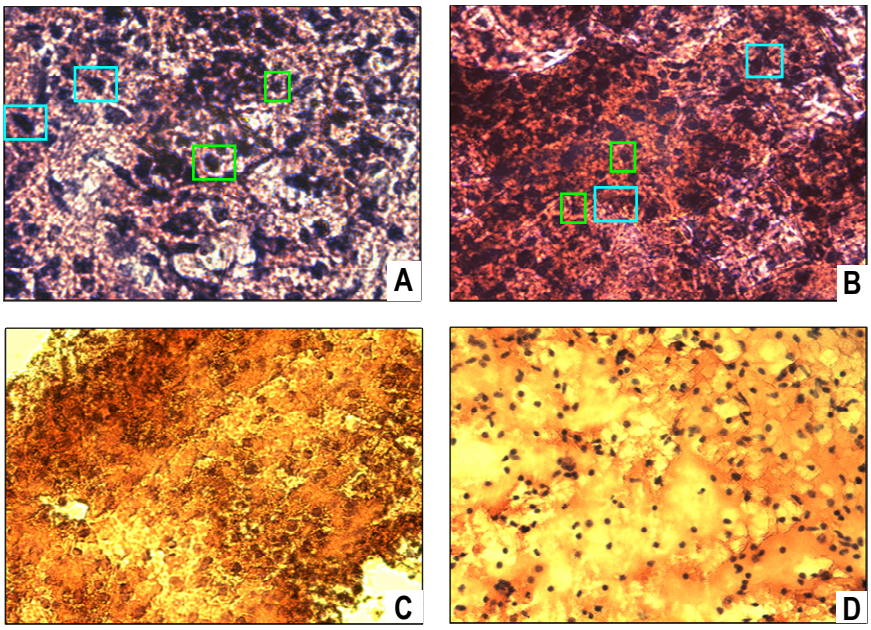

Figure 7.2: **Morphology Assessment**.
[A] Baseline* tissue showing common cell types found in cortex, for example, pyramidal cells(cyan squares), star-shaped astrocytes(green squares), etc. **[B]** Perfused cultured slice after 5DIV shows similar cell densities and cell shapes. These cultures also show characteristic cortical cells like pyramidal cells (cyan squares) and star-shaped astrocytes (green squares), etc. **[C]** Unperfused control slice culture after 5 DIV shows reduced cell density approximately in the middle layers of the tissue **[D]** Unperfused membrane insert culture** shows compromised health of cells and reduced cell sizes and cell densities.
* Baseline: Freshly cut tissue and stained and/or fixed to assess the viability and the morphology at cellular level in the beginning of the experiment.
** membrane insert culture means culture as described by Stoppini, 1991

Thickness preservation

I measured thickness of the cultures using specimens prepared with H&E staining. To evaluate change in thickness due to fixing medium, I cut fresh cortical slices of various thicknesses (from 250µm to 700µm) and fixed them using 2% paraformaldehyde in 0.5X PBS. The fixed tissue was sliced into thin slices along its thickness, stained with H&E and mounted on gelatin slides. With a calibrated field of view, I observed less than 10% change in thickness of these slices. Using this method, I observed that thickness is

preserved better in perfused cultures compared to the membrane insert cultures (figure 7.3).

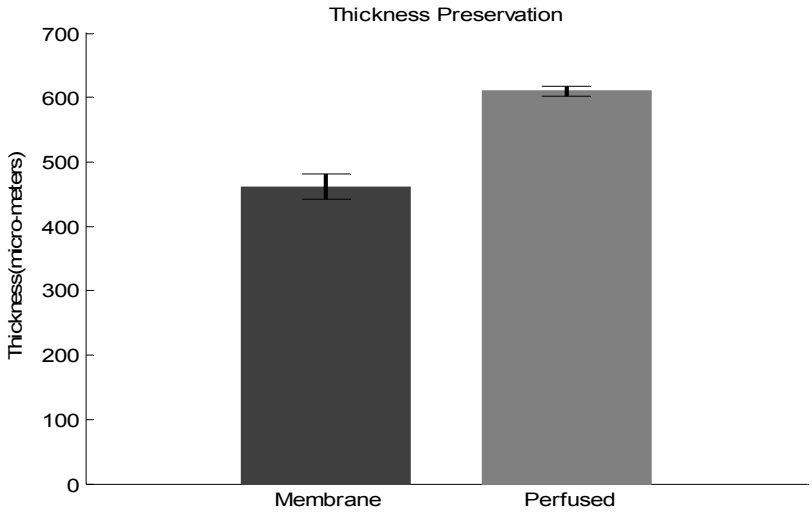

Figure 7.3: **Maintenance of thickness of culture after 5 DIV.** **[A]** Baseline* **[B]** Perfused cultured slice after 5DIV **[C]** Unperfused control slice culture after 5 DIV **[D]** Unperfused static membrane culture**

* Baseline: Tissue cut freshly and stained and/or fixed to assess the viability and the morphology at cellular level in the beginning of the experiment.

** Static membrane culture means culture as described by Stoppini, 1991.

Electrophysiological activity of cultured thick brain slices

Further, I attempted to record functional activity from the perfused slice cultures. Using a single micro-wire electrode, I probed the cultures at different randomly chosen places throughout their thickness. Most of the activity could be recorded by chemically evoking action potentials by addition of 120mM KCl in the culture bath. There was no evident relation of activity recording as a function of thickness. However, the amplitude of the recorded signal depended on the electrode's position relative to spontaneously firing neurons.

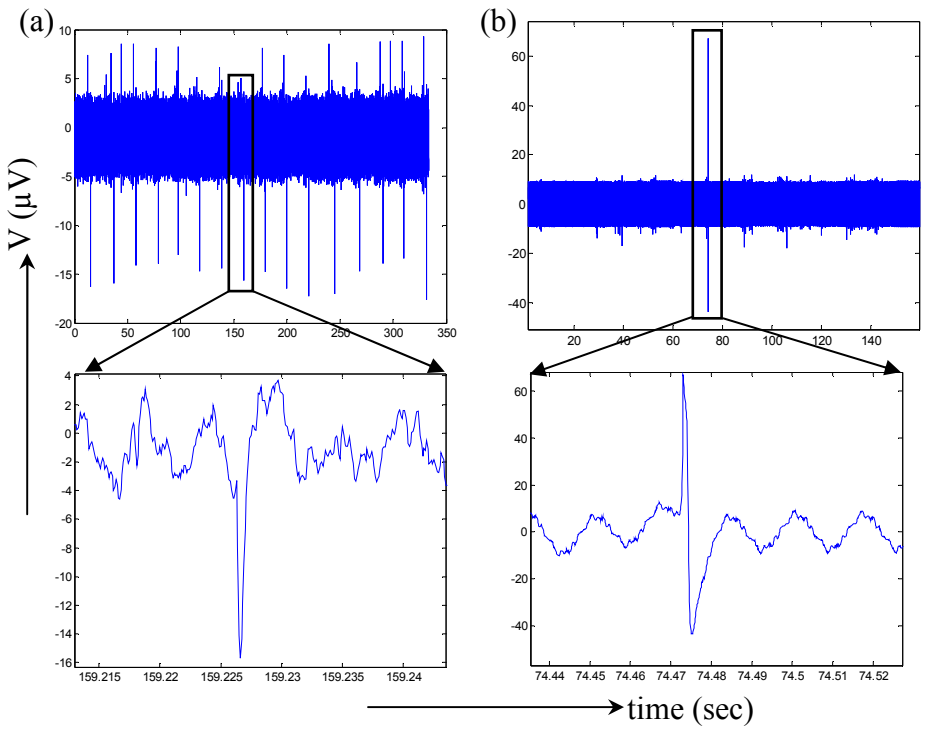

Figure 7.4: Activity traces from cultured slices after 5 DIV. Either spontaneous or chemically evoked activity could be recorded in 75% of the cultured slices. There were different amplitudes of recorded activity traces resulting from relative position of electrode to the firing neurons.

DISCUSSION AND CONCLUSIONS

Here I described characteristic organotypic morphology and activity properties of the viable thick brain slice cultures. Our perfusion method allowed ample supply of nutrients and oxygen throughout the tissue that resulted in increased viability (> 80%) of tissue even after 5 days in culture. However, the viability was decreased over time from 2DIV to 5DIV. The decrease in viability of perfused slices over time could be explained by slowly dying cells that might have released chemicals from the cut surfaces of the tissue. I believe that the viability of the unperfused cultures decreased dramatically after 5 DIV compared to perfused slices for two reasons: one, dying cut cells release harmful

chemicals that can diffuse in the tissue and trigger cell death in the adjacent tissue areas [62, 66], and second, the cells in the deeper layers of the tissue do not get sufficient nutrient and oxygen supply, resulting in starvation of tissue and leading to apoptosis (figure 7.2c, d). On the other hand, in the perfused tissue using our perfusion paradigm, there is sufficient supply of nutrients throughout the thickness of the tissue. Further, due to one way flow (from bottom to top of infusion chamber) of the nutrient medium and domination of convection over diffusion process, the harmful chemicals are washed away resulting in less harm to the adjacent cell layers in the tissue. Together, these are expected to result in much greater viability of the perfused cultures compared to the unperfused cultures.

Further, I noticed increased thickness maintained in perfused cultures compared to unperfused ones. This could be explained by additional mechanical support on the sides of the tissue by the biocompatible walls of the infusion chamber. Confinement of tissue in the infusion chamber prevented any lateral spreading of tissue, unlike membrane insert based cultures. This resulted in better preservation of thickness of the tissue. However, even the perfused tissue thinned down by 100μm after 5 DIV. This could be explained by considering washing away of dead cells from the culture volume that died initially during the cutting process. A more comprehensive study will be required to better understand this observation.

I also could record spontaneously or chemically evoked activity from cultured slices. This indicates their usefulness in electrophysiology and pharmacological studies. However, these recordings were done using a single microwire electrode. A more comprehensive examination could be done using multielectrode arrays [26, 28, 29].

Viable slices can be easily obtained from young animals, however recently there is emerging evidence that it is possible to obtain healthy organotypic slices from adult animals [62, 64, 116]. Hence, our culturing technique could be used to culture thicker organotypic slices from other parts of the brain that are traditionally cultured using the membrane insert method, for example cerebellum [40], striatum [9], spinal cord [50, 94, 115], olfactory epithelium [43], thalamus [81] and cortex [26, 63], other rodent species (rat) and from a range of ages (post-natal day 11–16). These thick organotypic cultures may benefit a wide spectrum of neuroscience investigations including learning and memory [7, 13, 16, 19, 23, 25, 31, 64, 84, 39], development [43, 63, 81, 88, 94, 105], traumatic brain injury [82], regeneration [78, 94, 116], effect of pharmacological agents on network properties and drug addiction [86], ischemia studies [87, 95], and so on.

CHAPTER 8

THICK BRAIN SLICE CULTURING METHOD AND THE CULTURE CHAMBER: RECOMMENDATIONS

In the previous two chapters, I described fabrication, characterization and validation of a perfusion enabled culturing chamber that provides three dimensional flow of oxygenated nutrient medium through the thick tissue cultures. Further, I used this device to culture 700µm thick brain slice cultures for five days *in vitro*. In this chapter I make some recommendations for future work on this project.

OPTIMIZATION OF PERFUSION PARADIGM

I tested continuous flow rates (5, 10, 20, 30µl/hr) to evaluate amenable flow rates to brain tissue's mechanical strength and viability. The results of my experiments indicate that forced perfusion at flow-rates ≤ 20µl/hr supports viable organotypic cortical slice cultures while higher flow rates are detrimental to the tissue health. The viability of the cultures may be further characterized for additional flow rates 15µl/hr and 25µl/hr to complete the spectrum of flow rate optimization studies. Additionally, I used continuous perfusion of the nutrient medium. Currently tested flow rates indicate that approximately three culture volume exchanges of oxygenated nutrient medium per hour are optimal for enhanced viability of the tissue. Other studies describe secretion of neurotrophic factors by glial cells that are necessary for normal functioning of neurons. It is unknown whether current flow rates provide sufficient time for such neuron-glia life supporting material

exchange. I did not attempt any study to characterize the necessity of supplying neurotrophic factors and their effect on viability. Thus, a more detailed study using pulsatile flow compared to continuous flow may be necessary to optimize nutrient supply in more detail while allowing sufficient time for physiologic neuron-glial interactions. Further, measurements of oxygen level at various heights of the specimen at different flow rates may be a helpful parameter to optimize the perfusion paradigm (flow rates, continuous versus pulsatile flow) [28].

QUANTITATIVE ANALYSIS OF ORGANOTYPIC ORGANIZATION

In the current study, I characterized morphological organization and recording of electrical activity from these cultures only qualitatively. Although H&E staining tells much about the cellular organization, size and cell types based on their morphology, a more detailed organotypic characterization, effect of perfusion on survival of neurons and astrocytes, and physiologic network organization of neurons and astrocytes requires detailed studies using immunostaining methods. A quantitative study of dendritic structures, cell types (inhibitory, excitory, pyramidal, astrocytes) and cellular organization in the characteristic layer structure of the cortex is desired to authenticate detailed organotypic organization of these cultures.

CHARACTERIZATION OF THICK BRAIN SLICE CULTURES FOR LONGER-TERM

In the current studies I examined viability of thick brain slice cultures only for five days *in vitro*. Optimization of viable cultures for longer term may be desired in some experimental paradigms. Currently, viability of cultures is tested at two time points,

2DIV and 5DIV. My experiments indicated various levels of decrease in viability from 2DIV to 5DIV at different flow rates. To optimize the perfusion paradigm for long-term viable cultures, it is desired to characterize the viability of cultures at more time points.

QUANTITATIVE ANALYSIS OF ELECTROPHYSIOLOGY

I used only one microwire electrode to probe functional activity of the culture. A multisite recording at different heights of the culture is desired to authenticate reliable recordability from the cultures. Ideally, patch clamp recordings would be best to validate their spontaneous, electrically or chemically evoked electrical properties compared to established preparations such as acute slices, or dissociated tissue culture. To use these cultures for targeted recording and excitability for 3D hybrot projects, it is required to be able to reliably record and electrically stimulate at the targeted layers of cortex. It may be required to use tetanic stimulation of layer V/VI and determine synaptic responses in layer II/III to authenticate successful use of these cultures for learning and memory model development [4].

CHARACTERIZATION OF 1MM THICK BRAIN SLICES

I tested only 700μm thick and 3mm in diameter brain slice cultures for these studies. Optimization of 1mm thick preparations may facilitate viable cultures of the entire thickness of adult mouse brains. To achieve this goal, it will be required to change the dimensions of the culture chamber. Additionally, longer term characterization of viability, thickness, organotypic organization and functional activity may be required to consolidate this study.

MODIFICATIONS OF CULTURING CHAMBER

The current version of culturing chamber has a gold grid as a porous seat to support cultures and as an infusion port of nutrients. The currently used gold grid has 40% transparency to the infused medium resulting in formation of microjets (figure 6.3). A microporous membrane (millipore membrane inserts) may be a more amenable tissue seat and perfusion substrate due to uniformly distributed smaller pores resulting in diffused and uniform flow pressure on tissue surface. Further, these membranes are shown to be of high strength, biocompatible, and support tissue adhesion as neurons naturally attach to them [114].

APPENDIX A

A STEP-BY-STEP USER MANUAL TO OPERATE CUSTOM MADE MULTIPHOTON MICROSCOPE

Note: The procedure to switch on the microscope should be followed sequentially as mentioned below. It is required to follow this procedure step-by-step as given below to make sure that computer recognizes the National instruments chassis as its slave – a condition for successful operation of the microscope and its software control.

ROUTING THE LASER BEAM TO THE MICROSCOPE

1. Switch on the Ti:saph (pulsed) laser at least 30 minutes prior to starting the imaging session to obtain stabilized laser power that translates to the quality of the images.
2. Check using a spectrometer that the femtosecond laser is “mode locked”.
3. Flip the routing mirror in front of the femtosecond laser box aperture to switch path of the laser beam from the Zeiss 510META microscope to the custom-made microscope.
4. Measure the laser power at the focal plane of the objective lens using power meter and adjust it between a range of 20–40mW using wave-plate (circular dial) to obtain good images.

SWITCHING ON THE MICROSCOPE PARTS

5. Switch on the power supply of the scanning mirrors. The driving boards of the scanning mirror are installed in a commercially available box. On the side of that

box, notice if both the LEDs have turned to green color. When the power supply is turned on, it takes 3 seconds for the LEDs to turn green from orange.

6. Switch on the power supply of the NI-chassis containing the interfacing cards. Notice if all the four LEDs are glowing on the front panel of the chassis.
7. Switch on the computer.
8. The green color of all the chassis LEDs ensures that computer has recognized chassis as its “slave”.
9. Switch on the power supply of the preamplifier first. It is required to switch it on before the power supply of the detector to avoid damage to the detector system and the preamplifier.
10. Now switch on the detector (PMT) power supply. The correct power needed to operate the PMT is stored on the memory of its power supply. Hit “recall” button twice to supply power to a custom-made high-voltage circuit (enclosed in a custom box) of the PMT. Do not touch high-voltage wires (thick red wire; it carries 1250V!!).
11. Switch on the Z-control power supply from the Corvus controller.
12. Start the custom-written LabView software. A user interface will appear.
13. The MXI-interface code will recognize the interface cards to operate the microscope remotely via the software.
14. Place the test specimen under the objective lens. Make sure that the BG glass filter and the appropriate band-pass filters are present in the path before the liquid-light guide.

15. After visual inspection of the specimen, bring the dichroic mirror cube in the center to route the fluorescent signal to the detector. Pull the mirror (sliding rod on the upper right side of the trinocular) out of the laser beam path.

OPERATING THE SOFTWARE FOR IMAGING

16. Figure A.1 and its caption show the essential six-steps to set the software to obtain a 512x512 pixel image.
17. Do not change the scan mirror parameters until familiar with their meaning, that is, how do they translates to scan driving waveform generated from these inputs! (Ideally, these should not be in direct control of the user. I wanted to modify it for more intuitive user inputs that translate in the "background LabView code" to the appropriate settings for the raster scan. I suggest incorporation of this feature in the software as an essential near term goal.) Inappropriate settings may lead to damage of the scanning mirrors due to discontinuous waveform that inappropriate settings will generate.
18. Other operations, such as, time-lapse, 2D imaging, z-stack (3D) imaging, can also be done using appropriate settings from "step 2" (on the image A.1). The corresponding desired inputs for the z-step settings, the time-lapse settings, and the XY position settings can be done from the "Z-series control panel", the "time-lapse control panel" and the "position control panel", respectively.
19. Always set the "PMT VOLTAGE" to zero before stopping the software.
20. Always press "stop" or "stop all" button before quitting LabView. Otherwise, the scanning mirrors will keep running due to the stored waveforms on the FIFO memory of the digital-to-analog cards. The commands "stop" or "stop all" force

all the buffers, the counters, the clocks, and the memories on all the interfacing cards to be clear to use them again in the next scanning/imaging session.

21. After stopping and quitting the program, NEVER save any changes asked by the prompt window on the LabView software.
22. Always, first stop the PMT power supply and then the preamplifier supply.
23. Switch off the chassis before switching off the computer to avoid failure of its recognition as a “slave” by the computer during its next session.
24. Make sure that the power supply for the driving boards of the scanning mirrors is off before you leave.

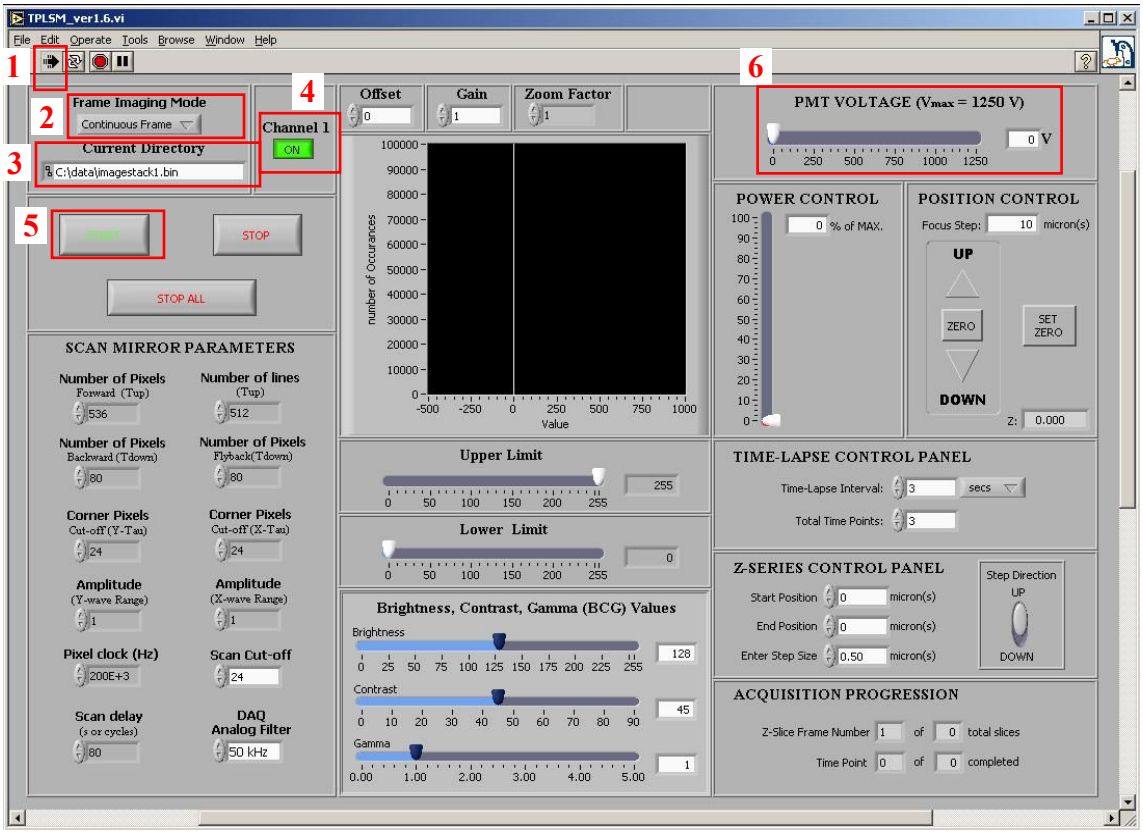

Figure A.1. User interface of software to operate custom built multiphoton microscope.
[1] Initialize software [2] Select operation mode [3] Enter file/directory name [4] Hit “channel 1” to “ON” [5] Hit “Start” [6] Increase PMT gain (PMT voltage). Adjust PMT gain to obtain desire intensity of the image.

APPENDIX B

A TROUBLE-SHOOTING MANUAL TO FOR THE CUSTOM MADE MULTIPHOTON MICROSCOPE

I'M NOT GETTING AN IMAGE!

There can be several reasons for not getting an image with the custom made multiphoton microscope. Check the following list:

1. First of all check that the pulsed laser is mode-locked and it is routed to the custom-made microscope by a flip mirror.
2. Make sure that the laser beam is reaching at the focal plane. You can do so by using a special fluorescent detection card excited by the infra-red laser light. If it is not reaching at the focal plane, check if the mirror in the trinocular (slider on its right hand side) is pulled out. Again, check if the laser beam is reaching at the focal plane now. If it is still not reaching at the focal plane, further inspection of laser beam route will be required to ascertain that system is not misaligned.
3. If the laser beam is reaching at the focal plane, then check if the dichroic mirror is in place. It is required to be in a position directly above the objective lens to route the beam towards detector.
4. Make sure that the detector and the preamplifier power supply is on.
5. Check if you are using the right emission filters and the excitation wavelength for your fluorophore.
6. Take a test image using a test slide such as a pollen grain slide.

THE SOFTWARE IS NOT STARTING!

Sometimes, due to its previous history of stopping the system inappropriately, the software may not work.

1. Try restarting the system. Each and everything!
2. If you have switched on the computer before the chassis, the chassis will not communicate with the computer. This can be tested from the color of the four LEDs on the front side of the chassis (green, if it was recognized by computer; orange: if it is not recognized by computer). In this case, restarting the chassis followed by restarting the computer will solve the problem.
3. Software still may not start due to MXI-interface failure if the chassis was not powered on before the computer. Switch off the chassis and wait for 5 minutes. There is a large capacitor in the chassis that takes time to discharge. Hurrying up to restart the chassis and the computer system will not help.

APPENDIX C

A DETAILED PROTOCOL TO SET-UP FLUIDIC SYSTEM AND THICK BRAIN SLICE CULTURING METHOD

SETTING UP THE FLUIDIC SYSTEM

1. Test all the gold grid devices to confirm proper adhesion of the gold grid to its orifice in the infusion chamber.
2. Choose appropriate FEP membrane lids to fit them snugly on the withdrawal chamber.
3. Change the FEP membrane of each lid every time a new experiment is started.
4. Clean the infusion and the withdrawal capillary tubing with ethanol followed by deionized water at least 4-5 times.
5. Make sure there is no leak or blockage in the microcapillary tubing. Test for the possible leaks at each connector by flushing deionized water using a syringe.
6. Autoclave all the parts, including the experiment platform (stand on which chambers are secured tight during experiment).
7. Fix the capillary infusion and the withdrawal tubing to the infusion and the withdrawal ports of the devices inside a sterile laminar flow hood.
8. Fill the HBS solution in the withdrawal side syringes and the nutrient medium in the infusion side syringes. Attach these syringes to the infusion and the withdrawal lines.
9. Make sure that there are no air bubbles in these lines at this time.
10. Cover the chambers with the teflon lids to avoid any accidental unsterility.

11. Set the syringe-pump at the appropriate flow settings.
12. Carefully fix the syringes on the infusion and the withdrawal sides.
13. Run a test flow at a flow rate ~1ml/hr to test for any potential leaks.
14. Fix any leaks in the lines at this point. Sometimes, it may require repeating the entire process depending on the leak spots and the leak severity. Any leaks will ruin the experiment by invalidating the set flow rate, and/or by the infection.
15. Once assured that there are no leaks and the system works in infusion/withdrawal flow conditions, stop the flow and check for any bubbles in the infusion line once more.
16. Remove the teflon lid and aspirate all the medium in the infusion and the withdrawal chamber very carefully with a micro-pipette without damaging the gold grid and its adhesion to the device orifice.
17. Pour 20µl of laminin in the infusion chamber. Due to surface tension, it may look like a drop sitting in the infusion chamber. The excess of laminin will exit to the withdrawal chamber upon closing the chamber with the teflon lid. This will ensure coating of gold-grid and the interior walls of the infusion chamber with laminin properly. Leave the enclosed chambers in the sterile hood and prepare for harvesting of the tissue slices. To obtain good anchoring of tissue with the chamber, it is required to coat the chamber with laminin atleast 30-40 minutes before transferring the tissue in it.
18. Prepare the gold grid chamber and the membrane insert culture dishes (35 mm cultures dishes) for the control experiments. Coat them with the laminin and fill the culture bath to ensure diffusion based supply of nutrients to these cultures.

Use 35mm diameter teflon membranes to prevent evaporation and infection while allowing gaseous exchange.

HARVESTING AND PLATING THE BRAIN SLICES

19. Autoclave all the required dissection instruments. Warning: Never use any unsterile tools or media to handle the tissue! The following procedure needs to be completed in only a few minutes to ensure high viability of the tissue just after the slicing.
20. Following the NIH rules euthanize one mouse pup (P11-P15) at a time and remove its brain from its skull quickly (~1 min or less).
21. Transfer the brain in the chilled nutrient medium and wait for 30 seconds to 1 minute. This step helps to reduce the metabolic activity of the tissue due to reduced temperature and make the tissue slightly stiffer (brain is very delicate gel-like tissue otherwise) which eases the tissue slicing.
22. During the wait time, make all the tools ready for separating the tissue slices under a dissection microscope.
23. Cut the brain into two hemispheres using a micro-knife. Keep one hemisphere in the chilled nutrient medium and transfer the other half quickly to the tissue chopper disc. Make sure that the tissue chopper is preset for the desire slice thickness and a sterile blade is secured in place.
24. Using appropriate coordinates, cut tangential, saggital or coronal cortical slices of desired thickness.
25. Gently transfer the tissue in the chilled nutrient medium.

26. Similarly slice the other hemispehere too and transfer it to the chilled nutrient medium. (From harvesting brain to cutting slices should not take more than 3-5 minutes) to ensure high viability tissue to start with.
27. Using two blunt microspatulas, separate the slices and leave them in the chilled nutrient medium.
28. Using a biopsy tool of appropriate diameter (same as infusion chamber for best fit), cut the slices into round discs. Transfer these round discs of slices to a new dish containing the chilled nutrient medium and enclose it with a teflon lid to transfer the tissue to the laminar hood to ensure sterility. Remove the teflon lid from the culture chamber.
29. Very gently remove any excess laminin in the infusion chamber.
30. Using two flat microspatuals, gently transfer the tissue to the infusion chamber. Make sure that there are no micro-cuts accidentally happened to the tissue during this time. The micro-cuts will form path of low resistance for the infused medium resulting in hampering of perfusion of medium “thorough” the tissue thickness.
31. Fill the withdrawal chamber with the nutrient medium and close the chamber with a teflon lid.
32. Start the nutrient medium flow from the syringe pump immediately.
33. Transfer the tissue in the control experiment chambers and the membrane insert chamber that are floating on the nutrient medium. Close the culture dishes with the appropriate teflon lids.

34. Gently transfer the perfusion set-up and the control cultures in the culture incubator that is set at 5% CO_2, 9% O_2, 65% relative humidity and 35ºC temperature.
35. Clean the dissection hood and discard the biohazards appropriately.
36. After completing the experiments, clean the capillary tubing and chambers immediately with deionized water till all the medium is clearly exited from them. Leaving them even for a couple of hours without cleaning allows contents of the nutrient medium to dry and block them. Similarly clean the chambers and preferably store them in deionized water till next use. This not only helps to prevent blocking of the grid with tiny particles or molecules, but also helps to keep the hydrophobic nature of PDMS (manifold material) low. This ensures slightly reduced experimental set-up time for next experiment.

APPENDIX D

LABELING AND IMAGING THE BRAIN SLICE CULTURES FOR VIABILITY ASSESSMENT AND ORGANOTYPIC ORGANIZATION

LABELING THE CULTURE FOR THE VIABILITY ASSESSMENT

1. Take out appropriate number of the aliquots of the propidium iodide and the hoechst stains and keep them in light-tight condition in the laminar flow hood. Allow them to thaw and adjust to the room temperature.
2. Gently transfer the set-up to the laminar hood without hindering/disturbing the perfusion equipment.
3. Mix one aliquot of each, hoechst and propidium iodide, in 200µl (per culture chamber) nutrient medium. The nutrient medium should be equilibrated with the incubator environment. It is advised to use the same nutrient medium preparation to avoid any pH or osmolarity shock to the culture.
4. Remove the teflon lid from the culture chamber very gently to ensure that no harm is done to the tissue.
5. Aspirate medium from the withdrawal chamber and pour the fluorescent dye mixed the nutrient medium.
6. Close the chamber and transfer the set-up to the incubator and wait for at least 40 minutes to 1 hour to ensure intake of the dyes by the entire thickness of the tissue.
7. Prepare for imaging.

FIXING THE BRAIN SLICES AND STAINING THEM WITH H&E

8. After imaging, the slices are transferred to a 2% paraformaldehyde solution made in 0.5X phosphate buffer solution (pH 7.4).
9. Before transferring the slices in the fixing medium, the pH and the osmolarity of the nutrient medium in the culture bath should be measured and adjust to the same value as of the fixing solution.
10. The tissue should be stored at 4ºC for at least 24 hours before slicing it into thin axial slices for H&E staining.
11. The fixed slices can be cut into thin axial (perpendicular to its diameter) either using the tissue chopper or the cryostat depending on required thinness of the axial tissue slice.
12. The thin perpendicular slices show entire thickness of the tissue. They are mounted on the gelatin slides and are left overnight to dry and adhere to the slide.
13. Using the automatic machine in core histology facility, several slides can be labeled with H&E at once following the standard procedure.
14. The labeled slides are taken out of the xylene solution (a medium used during H&E staining) and are covered with coverslips to prepare for imaging with a regular brightfield microscope.

APPENDIX E

DATA ANALYSIS USING THE IMAGE-J SOFTWARE

The data was imported in the ImageJ software – available for free from the NIH website: http://rsb.info.nih.gov/ij/. I downloaded several important and relevant plugins. Some of the relevant plugins for the viability data processing are: “LSM reader”, “Stacks”, and “AVI reader”.

The data was imported in the ImageJ software using the “LSM reader” plugin. The data from the two detector channels, one for the hoechst label and the other for the propidium iodide label, open up in the two different image windows. The data is cleaned to remove the background noise and to increase contrast for the entire stack, wherever needed. The cleaned data is then converted to a binary data set using the “adjust threshold” command. This command allows adjustment of the threshold based on pixel intensity. The nuclei in the out-of-focus planes are fainter and appear smaller in size compare to those that are in the focal plane. The “adjust threshold” command allows to select nuclei that are in the same plane based on their intensity. After obtaining a binary image, the command “analyze particles” is used to adjust the range of the size of the particles to be counted. This command returns detailed analysis of the particles and their size distribution. One flaw in this analysis is that when the two nuclei are very close, the binary image converts it into a single unit and the software counts them as single entity. However, the number of such nuclei is only fractional part of the total number of nuclei.

The data was visually inspected for each frame of stack to omit possibility of wrong threshold criterion that may result from automated threshold by software.

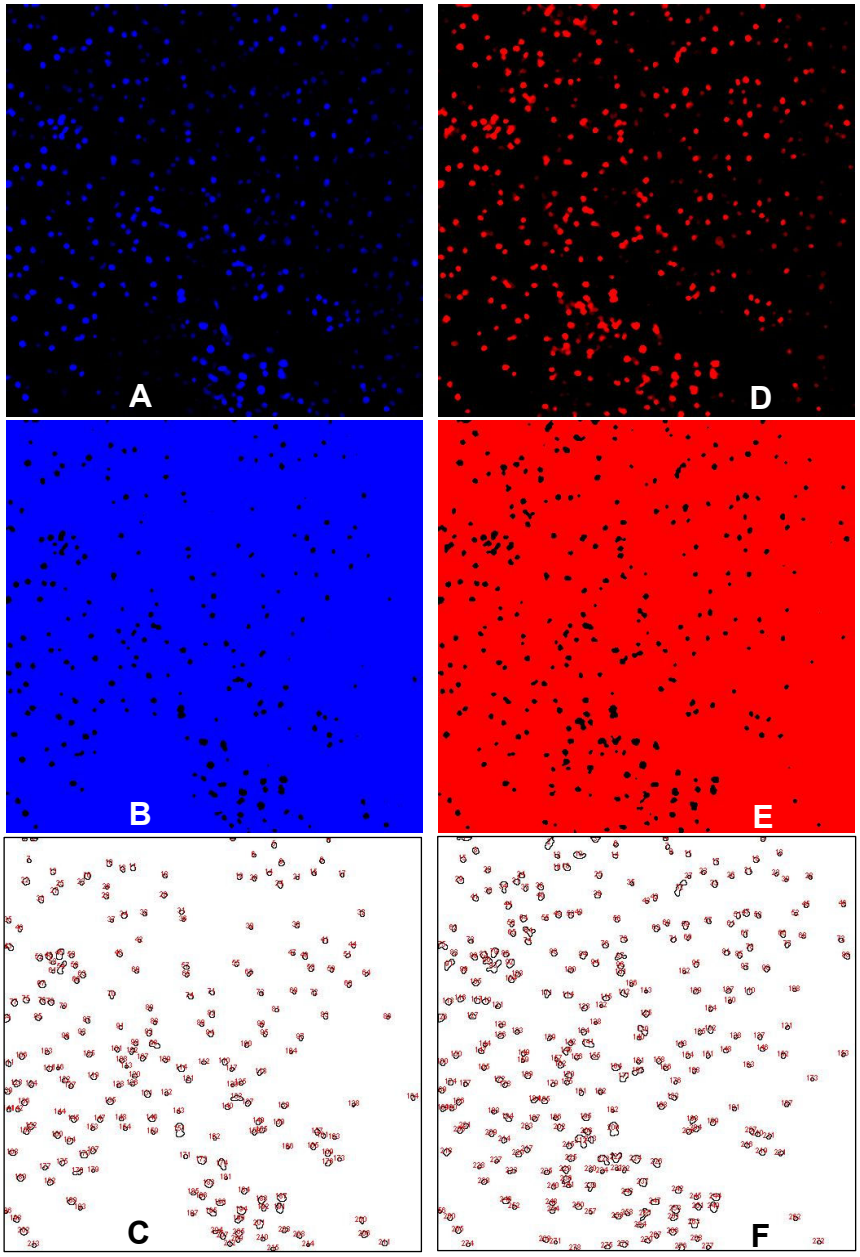

Figure E.1. An Example of data analysis using ImageJ software.
Data was collected in two different detector channels: Blue (Hoechst) and Red (Propidium iodide) **[A]** A frame of cleaned data from a control slice culture (5DIV experiments). **[B]** To avoid double time counting the data was thresholded to count nuclei in the focal same plane. The nuclei that are in deeper plane appear fainter and smaller in size in the current plane. **[C]** Reliable counting of nuclei by the software. **[D,E,F]** Similar analysis for data from other detection channel (propidium iodide) for the same sample and same focal plane.

APPENDIX F

PUBLISHED WORKS

Custom-made multiphoton microscope for long-term imaging of neuronal cultures to explore structural and functional plasticity.

Komal Rambani, Mark C. Booth, Edgar Brown, Ivan Raikov, and Steve M. Potter, Proc. SPIE Vol. 5700, p. 102-108, Multiphoton Microscopy in the Biomedical Sciences V., 2005.

We use dissociated cultures of E-18 rat cortical neurons to study how they process the information. To correlate the electrophysiological data with corresponding network structure, we observe effects of the stimuli on the structural changes in this culture using multiphoton microscopy. To keep our 2D and 3D cultures alive for long-term studies, it is necessary to protect them against photodamage. At the same time, we need a flexible microscope design to accommodate our multielectrode arrays (MEAs) electrophysiological station. We have constructed a custom-designed multiphoton microscope based on design of Tsai et al. The microscope is optimized for the two-photon mode to collect maximum possible fluorescent signal using minimum excitation laser intensity. Special attention is paid to get uniformly illuminated images and the ability to use the entire bandwidth of the pulsed laser (700-1000 nm) with the same set of optical components. Flexibility of the design will allow us to easily change or incorporate other optical components suitable for different experimental needs. This microscope will allow us to do electrophysiology and imaging concurrently while maintaining the optimum temperature and CO2 levels.

Keywords: Multiphoton microscope, long-term imaging, learning *in vitro*, cortical neuronal networks.

Maintaining Viable Thick Cortical Slices by Perfusion of Nutrient Medium

Komal Rambani, Jelena Vukasinovic, Ari Glezer, Steve M. Potter, Society for Neuroscience, Atlanta, 2006.

Brain slice cultures are valuable *in vitro* models for various electrophysiological, morphological, pharmacological, and ischemia studies. These include roller tube method (Gahwiler, *J. Neurosci. Meth.,* 1981) and static cultures in which brain slices are grown on permeable membranes (Stoppini, *J. Neurosci. Meth.,* 1991). With these methods, the nutrient medium reaches cells across the thickness of the slice by diffusion and the slice thins down from 500µm thickness to around 150µm within two days. Culturing thick brain slices (> 400µm) has been a challenge due to necrosis in the middle of the slice due to ischemia. We hypothesize that perfusion of oxygenated nutrient medium will allow better viability of thick brain slices. We have developed a simple closed-loop infusion-withdrawal type microfluidic chamber to allow perfusion of 700µm tangential or transverse cortical slices (Vukasinovic, *Proc. BIO2006*). The chamber is covered with a teflon membrane lid to allow sterility and gaseous exchange with incubator (Potter, *J. Neurosci. Meth., 2001)*. The infusion and withdrawal of medium is done at the same flow-rate via syringe pump and teflon µ-capillary tubing that connect the µ-fluidic chamber to the medium-containing syringes. The µ-fluidic system is kept in a humidified incubator maintained at 9% O_2, 5% CO_2 and 65% humidity. The infusion capillary tubing

contains an aerator and a one-way check valve to allow equilibrium of nutrient medium with the incubator environment and to ensure smooth flux of fluid that reaches the tissue. The design of this system requires the infused medium to pass through the thickness of the tissue that is supported on a porous gold grid before reaching withdrawal chamber, which encourages perfusion of oxygenated nutrient medium at all levels of tissue throughout its thickness. The viability of the tissue was assessed by propidium iodide and Hoechst fluorescent probes and multiphoton microscopy. We have observed better viability in perfused cortical slices compared to the unperfused slices at different flow rates of oxygenated nutrient medium. Further, confinement of tissue in infusion chamber helps to preserve the thickness of tissue better compared to Stoppini's method. The development of thick organotypic cortical brain slices will prove to be very useful model for various studies requiring multiple layers of the cortex, especially when cut tangential to the cortical surface.

Keywords: Organotypic brain slices, Thick Cortical slice cultures, microfluidic system

REFERENCES

[1] AKTURK, S., GU, X., KIMMEL, M., WANG, Z., and TREBINO, R., "Measuring Spatio-Temporal Pulse Distortions Using Grenouille," Commercial and Biomedical Applications of Ultrafast Lasers VII, 2005.

[2] ARAYA R., JIANG J., EISENTHAL K. B., and YUSTE R., "The spine neck filters membrane potentials," PNAS, 103, 17961-17966, 2006.

[3] ARAYA R., EISENTHAL K. B., and YUSTE R., "Dendritic spines linearize the summation of excitatory potentials," PNAS 10, 1073, 2006

[4] ARONIADOU, V. A., and KELLER A., "Mechanisms of LTP Induction in Rat Motor Cortex *in vitro*," *Cereb. Cortex.,* 5, 353-362, 1995.

[5] BAKER R. E., CORNER M. A., and PELT J., "Spontaneous neuronal discharge patterns in developing organotypic mega-co-cultures of neonatal rat cerebral cortex," Brain Res, 1101, 29-35, 2006.

[6] BAKKUM, D. J., SHKOLNIK, A. C., BEN-ARY, G., GAMBLEN, P., DEMARSE, T. B. and POTTER, S. M., "Removing some 'A' from AI: Embodied Cultured Networks," Embodied Artificial Intelligence. Iida, F., Pfeifer, R., Steels, L. and Kuniyoshi, Y. New York, Springer. 3139: 130-145, 2004.

[7] BARRIA, A. and MALINOW, R., "NMDA receptor subunit composition controls synaptic plasticity by regulating binding to CaMKII," Neuron, 48, 289–301, 2005.

[8] BEACH, R.L., BATHGATE, S.L. and COTMAN, C.W., "Identification of cell types in rat hippocampal slices maintained in organotypic cultures," Brain Res., 255, 3–20, 1982.

[9] BECQ, H., BOSLER, O., GEFFARD, M., ENJALBERT, A. and HERMAN, J.P., "Anatomical and functional reconstruction of the nigrostriatal system *in vitro*: selective innervation of the striatum by dopaminergic neurons," J. Neurosci. Res., 58, 553–566, 1999.

[10] BENEDIKTSSON, A.M., SCHACHTELE, S.J., GREEN, S.H. and DAILEY, M.E., "Ballistic labeling and dynamic imaging of astrocytes in organotypic hippocampal slice cultures," J. Neurosci. Methods, 141, 41–53, 2005.

[11] BINDOKAS V. P., LEE C. C., COLMERS W. F., and MILLER R. J., "Changes in Mitochondrial Function Resulting from Synaptic Activity in the Rat Hippocampal Slice," J. Neurosci., 18(12), 4570-4587, 1998.

[12] BREWER, G. J., and COTMAN C.W., "Survival and growth of hippocampal neurons in defined medium at low density – advantages of a sandwich culture technique or low oxygen," Brain Research, 494, 65-74, 1989.

[13] BUCHS, P.A., and MULLER, D., "Induction of long-term potentiation is associated with major ultrastructural changes of activated synapses," Proc. Natl. Acad. Sci., 93, 8040–8045, 1996.

[14] CHAO, Z. C., BAKKUM, D. J., WAGENAAR, D. A., and POTTER, S. M., "Effects of random external background stimulation on network synaptic stability after Tetanization: A Modeling Study," Neuroinformatics, 3(3), 263-280, 2005.

[15] CHEUSS V, YASUDA R, SOBCZYK A, and SVOBODA K., "Nonlinear [Ca2+] Signaling in Dendrites and Spines Caused by Activity-Dependent Depression of Ca2+ Extrusion," *J Neurosci.,* **26**, 8183 -8194, 2006.

[16] COLLIN, C., MIYAGUCHI, K., and SEGAL, M., "Dendritic spine density and LTP induction in cultured hippocampal slices," J. Neurophysiol 77, 1614–1623, 1997.

[17] COLTMAN, B.W., EARLEY, E.M., SHAHAR, A., DUDEK, F.E. and IDE, C.F., "Factors influencing mossy fiber collateral sprouting in organotypic slice cultures of neonatal mouse hippocampus," J. Comp. Neurol., 362, 209–222, 1995.

[18] DAVE, A. S., and MARGOLIASH, D., "Song Replay During Sleep and Computational Rules for Sensorimotor Vocal Learning," *Science,* Vol. 290. no. 5492, pp. 812 – 816, 2000.

[19] DEBANNE, D., GAHWILER, B.H., and THOMPSON, S.M., "Cooperative interactions in the induction of long-term potentiation and depression of synaptic excitation between hippocampal CA3–CA1 cell pairs *in vitro*," Proc. Natl. Acad. Sci., 93, 11225–11230, 1996.

[20] DEMARSE, T. B., WAGENAAR, D. A., BLAU, A. W. and POTTER, S. M., "The Neurally Controlled Animat: Biological Brains Acting with Simulated Bodies," Autonomous Robots, 11, 305-310, 2001.

[21] DEMARSE, T. B., WAGENAAR, D. A., BLAU, A. W., and POTTER, S. M., "Interfacing neuronal cultures to a computer generated virtual world," Proc. 7th Joint Symposium on Neural Computation, USC, 36-42, 2000.

[22] DENK, W., STRICKLER, J. H., and WEBB, W. W., "Two photon laser scanning fluorescence microscopy," Science, 248, 73-76, 1990.

[23] DE PAOLA, V., ARBER, S. and CARONI, P., "AMPA receptors regulate dynamic equilibrium of presynaptic terminals in mature hippocampal networks," Nat. Neurosci., 6, 491–500, 2003.

[24] DE PAOLA V, HOLTMAAT A, KNOTT G, SONG S, WILBRECHT L, CARONI P, and SVOBODA K., "Cell type-specific structural plasticity of axonal branches and boutons in the adult neocortex," *Neuron,* **49**, 861 -875, 2006.

[25] DE SIMONI, A., GRIESINGER, C.B., and EDWARDS, F.A., "Development of rat CA1 neurones in acute versus organotypic slices: role of experience in synaptic morphology and activity," J. Physiol., 550, 135–147, 2003.

[26] DONG, H.W. and BUONOMANO, D.V., "A technique for repeated recordings in cortical organotypic slices," J. Neurosci. Methods, 146, 69–75, 2005.

[27] DOUPE, A. J., SOLIS, M. M., KIMPO, R., and BOETTIGER C. A., "Cellular, Circuit, and Synaptic Mechanisms in Song Learning," Ann. N.Y. Acad. Sci., **1016**, 495-523, 2004

[28] EGERT, U., OKUJENI,S., NISCH, W., BOVEN K.H., RUDORF R., GOTTSCHLICH N., and STETT, A., "Optimized Oxygen Availability and Signal-to-Noise Ratio in Brain Slice Recordings with Perforated Microelectrode Arrays," 5th International Meeting on Substrate-Integrated Micro Electrode Arrays, Reutlingen, 2006.

[29] EGERT U, HECK, D, and AERTSEN, A., "2-dimensional monitoring of spiking networks in acute brain slices," Exp Brain Res, 142, 268-274, 2002.

[30] EHRENGRUBER, M.U. ET AL., "Recombinant Semliki Forest virus and Sindbis virus efficiently infect neurons in hippocampal slice cultures," Proc. Natl. Acad. Sci. USA, 96, 7041–7046, 1999.

[31] ENGERT, F. and BONHOEFFER, T., "Dendritic spine changes associated with hippocampal long-term synaptic plasticity," Nature, 399, 66–70, 1999.

[32] FELDMAN D. E. and KNUDSEN, E. I., "An Anatomical Basis for Visual Calibration of the Auditory Space Map in the Barn Owl's Midbrain," J. Neurosci., Volume 17 (17), pp. 6820-6837, 1997.

[33] FELSEN, G., TOURYAN, J., HAN, F., and DAN, Y. , "Cortical sensitivity to visual features in natural scenes," PLoS Biol., 3 (10), e342., 2005.

[34] FU, Y., Djupsund, K., GAO, H., HAYDEN, B., SHEN, K., and Dan, Y. "Temporal specificity in the cortical plasticity of visual space representation," *Science,* 296, 2002.

[35] GAHWILER, B.H., "Organotypic monolayer cultures of nervous tissue," J. Neurosci. Methods, 4, 329–342, 1981.

[36] GAHWILER, B.H., "Organotypic cultures of neural tissue," Trends. Neurosci., 11, 484–489, 1988.

[37] GAHWILER, B.H., CAPOGNA, M., DEBANNE, D., MCKINNEY, R.A. and THOMPSON, S.M., "Organotypic slice cultures: a technique has come of age," Trends Neurosci., 20, 471–477, 1997.

[38] GAHWILER, B.H., "Nerve cells in culture: the extraordinary discovery by Ross Granville Harrison," Brain. Res. Bull., 50, 343–344, 1999.

[39] GALIMBERTI, I. ET AL., "Long-term rearrangements of hippocampal mossy fiber terminal connectivity in the adult regulated by experience," Neuron, 50, 749–763, 2006.

[40] GIANINAZZI, C. ET AL., "Apoptosis of hippocampal neurons in organotypic slice culture models: direct effect of bacteria revisited," J. Neuropathol. Exp. Neurol., 63, 610–617, 2004.

[41] GHOUMARI, A.M. ET AL., "Mifepristone (RU486) protects Purkinje cells from cell death in organotypic slice cultures of postnatal rat and mouse cerebellum," Proc. Natl. Acad. Sci. USA, 100, 7953–7958, 2003.

[42] GLOVER, C.P., BIENEMANN, A.S., HEYWOOD, D.J., COSGRAVE, A.S. and UNEY, J.B., "Adenoviral-mediated, high-level, cell-specific transgene expression: a SYN1-WPRE cassette mediates increased transgene expression with no loss of neuron specificity," Mol. Ther., 5, 509–516, 2002.

[43] GONG, Q., LIU, W.L., SRODON, M., FOSTER, T.D. and SHIPLEY, M.T., "Olfactory epithelial organotypic slice cultures: a useful tool for investigating olfactory neural development," Int. J. Dev. Neurosci., 14, 841–852, 1996.

[44] GÖPPERT-MAYER M., "Über Elementarakte mit zwei Quantensprüngen," Ann Phys, 9, 273-295, 1931.

[45] GU X., AKTURK, S., SHREENATH, A., CAO, Q., and TREBINO, R., "The Measurement of Ultrashort Light - Simple Devices, Complex Pulses," XFemtosecond Laser Spectroscopy, ed. P. Hannaford, Springer Science Business Media, Inc., 2005.

[46] HARRISON, R.G., "Observations on the living developing nerve fiber," Proc. Soc. Exp. Biol. Med., 4, 140–143, 1907.

[47] HARRISON, R.G., "The outgrowth of the nerve fiber as a mode of protoplasmic movement," J. Exp. Zoo., 142, 5–73, 1959.

[48] HEINEMANN, U. ET AL., "Cell death and metabolic activity during epileptiform discharges and status epilepticus in the hippocampus," Prog. Brain Res., 135, 197–210, 2002.

[49] HEINEMANN, U. ET AL., "Coupling of electrical and metabolic activity during epileptiform discharges," Epilepsia, 43 (5), 168–173, 2002.

[50] HILTON, K.J., BATESON, A.N. and KING, A.E., "A model of organotypic rat spinal slice culture and biolistic transfection to elucidate factors that drive the preprotachykinin-A promoter," Brain. Res. Rev., 46, 191–203, 2004.

[51] HOGUE, M.J., "Human fetal brain cells in tissue cultures: their identification and motility," J. Exp. Zool., 106, 85–107, 2006.

[52] HOLTMAAT A, WILBRECHT L, KNOTT GW, WELKER E, and SVOBODA K., "Experience-dependent and cell-type-specific spine growth in the neocortex," *Nature,* **441**, 979 -983, 2006.

[53] IKEGAYA Y., AARON G., COSSART R., ARONOV D., LAMPL I., FERSTER D., and YUSTE R., **"**Synfire Chains and Cortical Songs: Temporal Modules of Cortical Activity," Science, 304 (5670), 559-564, 2004.

[54] IYER, V., LOSAVIO, B.E., and SAGGAU, P., "Compensation of spatial and temporal dispersion for acousto-optic multiphoton laser-scanning microscopy," J. Biomed Opt., 8(3), 460-71, 2003.

[55] JOHANSSON' B.B., and BELICHENKO P.V,. "Neuronal Plasticity and Dendritic Spines: Effect of Environmental Enrichment on Intact and Postischemic Rat Brain," *Journal of Cerebral Blood Flow and Metabolism,* **22,** 89–96, 2002.

[56] KAKEGAWA, W., TSUZUKI, K., YOSHIDA, Y., KAMEYAMA, K. and OZAWA, S., "Input- and subunit-specific AMPA receptor trafficking underlying long-term potentiation at hippocampal CA3 synapses," Eur. J. Neurosci., 20, 101–110, 2004.

[57] KARPOVA AY, TERVO DGR, GRAY NW, and SVOBODA K., "Rapid and Reversible Chemical Inactivation of Synaptic Transmission in Genetically Targeted Neurons," *Neuron,* **48**, 727 -737, 2005.

[58] KESHISHIAN, H. ROSS HARRISON'S, "The outgrowth of the nerve fiber as a mode of protoplasmic movement," J. Exp. Zool A Comp. Exp. Biol., 301, 201–203, 2004.

[59] KIM, J.A. ET AL., "Cytoskeleton disruption causes apoptotic degeneration of dentate granule cells in hippocampal slice cultures," Neuropharmacology, 42, 1109–1118, 2002.

[60] KLAPSTEIN G. J. and COLMERS W. F., "Neuropeptide Y Suppresses Epileptiform Activity in Rat Hippocampus *In Vitro*," J Neurophysiol, 78,1651-1661, 1997.

[61] KOVACS, R. ET AL., "Free radical-mediated cell damage after experimental status epilepticus in hippocampal slice cultures," J. Neurophysiol, 88, 2909–2918, 2002.

[62] KRASSIOUKOV, A.V. ET AL., "An *in vitro* model of neurotrauma in organotypic spinal cord cultures from adult mice," Brain Res. Brain Res. Protoc., 10, 60–68, 2002.

[63] LETINIC, K., ZONCU, R. and RAKIC, P., "Origin of GABAergic neurons in the human neocortex," Nature, 417, 645–649, 2002.

[64] LEUTGEB, J.K., FREY, J.U. and BEHNISCH, T., "LTP in cultured hippocampal-entorhinal cortex slices from young adult (P25–30) rats," J. Neurosci. Methods, 130, 19–32, 2003.

[65] LI, Z. ET AL., "Synaptic vesicle recycling studied in transgenic mice expressing synaptopHluorin," Proc. Natl. Acad. Sci. USA, 102, 6131–6136, 2005.

[66] Li and McIlwain. Maintenance of resting potentials in slices of mammalian cerebral cortex and other tissue *in vitro*. Journal of physiology, London 139:178-190, 1957.

[67] LIM C., BLUME, H. W., MADSEN J. R., and SAPER C. B., "Connections of the hippocampal formation in humans: I. The mossy fiber pathway," The Journal of Comparative Neurology, 385 (3), 325 – 351, 1998.

[68] LINKE, R., HEIMRICH, B. and FROTSCHER, M., "Axonal regeneration of identified septohippocampal projection neurons *in vitro,"* Neuroscience, 68, 1–4, 1995.

[69] Lo, D.C., McAllister, A.K. and Katz, L.C., "Neuronal transfection in brain slices using particle-mediated gene transfer," Neuron, 13, 1263–1268, 1994.

[70] London, J.A., Biegel, D. and PACHTER, J.S., "Neurocytopathic effects of beta-amyloid-stimulated monocytes: a potential mechanism for central nervous system damage in Alzheimer disease," Proc. Natl. Acad. Sci. USA, 93, 4147–4152, 1996.

[71] LUKSCH H., GAUGER B., and WAGNER H., "A Candidate Pathway for a Visual Instructional Signal to the Barn Owl's Auditory System," J. Neurosci., 20:RC70:1-4, 2000.

[72] LUNDSTROM, K. ET AL., "Semliki Forest virus vectors: efficient vehicles for *in vitro* and *in vivo* gene delivery," FEBS Lett., 504, 99–103, 2001.

[73] LUNDSTROM, K., ABENAVOLI, A., MALGAROLI, A. and EHRENGRUBER, M.U., "Novel Semliki Forest virus vectors with reduced cytotoxicity and temperature sensitivity for long-term enhancement of transgene expression," Mol. Ther., 7, 202–209, 2003.

[74] MACLEAN J., WATSON B., AARON G., and YUSTE R, "Internal Dynamics Determine the Cortical Response to Thalamic Stimulation," Neuron, 48, 811–823, 2005.

[75] MACLEAN JN, FENSTERMAKER V, WATSON BO, and YUSTE R., "A visual thalamocortical slice." Nat Methods., 3(2),129-34, 2006.

[76] MAJEWSKA, A., YIU G., and YUSTE R., "A custom-made two-photon microscope and deconvolution system," Pflugers Arch, 441(2-3), 398-408, 2000.

[77] MALETIC-SAVATIC, M., MALINOW, R., and SVOBODA, K., "Rapid dendritic morphogenesis in CA1 hippocampal dendrites induced by synaptic activity," Science 283, 1923–1927, 1999.

[78] MCALLISTER, A.K., LO, D.C. and KATZ, L.C., "Neurotrophins regulate dendritic growth in developing visual cortex," Neuron, 15, 791–803, 1995.

[79] MCALLISTER, A.K. "Biolistic transfection of cultured organotypic brain slices," Methods Mol. Biol., 245, 197–206, 2004.

[80] MIYAGUCHI, K., MAEDA, Y., COLLIN, C. and SIHAG, R.K., "Gene transfer into hippocampal slice cultures with an adenovirus vector driven by cytomegalovirus promoter: stable co-expression of green fluorescent protein and lacZ genes," Brain Res. Bull., 51, 195–202, 2000.

[81] MOLNAR, Z. and BLAKEMORE, C., "Development of signals influencing the growth and termination of thalamocortical axons in organotypic culture," Exp. Neurol., 156, 363–393, 1999.

[82] MORONI, F. ET AL. , "Poly(ADP-ribose) polymerase inhibitors attenuate necrotic but not apoptotic neuronal death in experimental models of cerebral ischemia," Cell Death Differ., 8, 921–932, 2001.

[83] MTCHEDLISHVILI, Z. and KAPUR, J., "High-affinity, slowly desensitizing GABAA receptors mediate tonic inhibition in hippocampal dentate granule cells," Mol. Pharmacol., 69, 564–575, 2006.

[84] NAGERL, U.V., EBERHORN, N., CAMBRIDGE, S.B. and BONHOEFFER, T., "Bidirectional activity-dependent morphological plasticity in hippocampal neurons," Neuron, 44, 759–767, 2004.

[85] NAUMANN, T., LINKE, R. and FROTSCHER, M., "Fine structure of rat septohippocampal neurons: I. Identification of septohippocampal projection neurons by retrograde tracing combined with electron microscopic immunocytochemistry and intracellular staining," J. Comp. Neurol., 325, 207–218, 1992.

[86] NEISEWANDER, J.L., BAKER, D.A., FUCHS, R.A., TRAN-NGUYEN, L.T.L., PALMER, A., and MARSHALL, J.F., "Fos protein expression and cocaine-seeking behavior in rats after exposure to a cocaine self-administration environment," J. Neurosci., 20, 798-805, (2000).

[87] NEWELL, D.W., BARTH, A., PAPERMASTER, V. and MALOUF, A.T., "Glutamate and non-glutamate receptor mediated toxicity caused by oxygen and glucose deprivation in organotypic hippocampal cultures," J. Neurosci., 15, 7702–7711, 1995.

[88] NIKONENKO, I. ET AL., "Integrins are involved in synaptogenesis, cell spreading, and adhesion in the postnatal brain," Brain Res. Dev. Brain Res., 140, 185–194, 2003.

[89] NIKOLENKO, V., NEMET, B.A., and YUSTE, R., "A two-photon and second-harmonic microscope," Methods, 30(1), 3-15, 2003.

[90] NORABERG, J. ET AL., "Organotypic hippocampal slice cultures for studies of brain damage, neuroprotection and neurorepair," Curr. Drug Targets CNS Neurol. Disord., 4, 435–452, 2005.

[91] NORABERG, J., KRISTENSEN, B.W. and ZIMMER, J., "Markers for neuronal degeneration in organotypic slice cultures," Brain Res. Brain Res. Protoc., 3, 278–290, 1999.

[92] NURIYA M., JIANG J., NEMET B., EISENTHAL K. B., and YUSTE R., **"**Imaging membrane potential in dendritic spines," PNAS 103, 786-790, 2006.

[93] O'BRIEN, J.A., HOLT, M., WHITESIDE, G., LUMMIS, S.C. and HASTINGS, M.H., "Modifications to the hand-held gene gun: improvements for *in vitro* biolistic transfection of organotypic neuronal tissue," J. Neurosci. Methods, 112, 57–64, 2001.

[94] OISHI, Y., BARATTA, J., ROBERTSON, R.T. and STEWARD, O., "Assessment of factors regulating axon growth between the cortex and spinal cord in organotypic co-cultures: effects of age and neurotrophic factors," J. Neurotrauma, 21, 339–356, 2004.

[95] PEREZ VELAZQUEZ, J.L., FRANTSEVA, M.V. and CARLEN, P.L., "*In vitro* ischemia promotes glutamate-mediated free radical generation and intracellular calcium accumulation in hippocampal pyramidal neurons," J. Neurosci., 17, 9085–9094, 1997.

[96] PORTERA-CAILLIAU C, WEIMER RM, PAOLA VD, CARONI P, and SVOBODA K., "Diverse Modes of Axon Elaboration in the Developing Neocortex," *PLoS Biol,* **3**, e272, 2005.

[97] POTTER, S.M., and DEMARSE, T. B., "A new approach to neural cell culture for long-term studies," J. Neurosci. Methods, 110,17-24, 2001.

[98] POTTER, S. M., FRASER, S. E. and PINE, J., "Animat in a Petri Dish: Cultured Neural Networks for Studying Neural Computation," Proc. 4th Joint Symposium on Neural Computation, UCSD, 167-174, 1997.

[99] POTTER, S. M., "Vital Imaging: two photons are better than one," Curr. Biol., 6(12), 1595-1598, 1996.

[100] POTTER, S. M., "Distributed processing in cultured neuronal networks," Prog. Brain Res., 130, 49-62, 2001.

[101] POTTER, S. M., "Two-photon microscopy for 4D imaging of living neurons," Imaging in Neuroscience and Development: A Laboratory Manual. Yuste, R. and Konnerth, Cold Spring Harbor Laboratory Press, 2004.

[102] POTTER, S. M., WAGENAAR, D. A. and DEMARSE, T. B., "Closing the Loop: Stimulation Feedback Systems for Embodied MEA Cultures. Advances in Network Electrophysiology Using Multi-Electrode Arrays." Taketani, M. and Baudry, M. New York, Kluwer, 2006.

[103] POTTER, S. M. WAGENAAR, D. A., MADHAVAN, R., and DEMARSE, T. B., "Long-term bidirectional neuron interfaces for robotic control, and *in vitro* learning studies," Engineering in Medicine and Biology, 25th Annual International Conference of the IEEE, Cancun, 2003.

[104] POZZO MILLER LD, NK MAHANTY, JA CONNOR and DMD LANDIS, "Spontaneous pyramidal cell death in organotypic slice cultures from rat hippocampus is prevented by glutamate receptor antagonists," Neuroscience, 63, 471-487, 1994.

[105] RAINETEAU, O., RIETSCHIN, L., GRADWOHL, G., GUILLEMOT, F. and GAHWILER, B.H., "Neurogenesis in hippocampal slice cultures," Mol. Cell. Neurosci., 26, 241–250, 2004.

[106] RATHENBERG, J., NEVIAN, T. and WITZEMANN, V., "High-efficiency transfection of individual neurons using modified electrophysiology techniques," J. Neurosci. Methods, 126, 91–98, 2003.

[107] SAKATA, J. T., and BRAINARD, M. S., "Real-time contributions of auditory feedback to avian vocal motor control," J. Neurosci. **26**, 9619-9628, 2006.

[108] SCHMIDT, H. ET AL., "Organotypic hippocampal cultures. A model of brain tissue damage in *Streptococcus pneumoniae* meningitis," J. Neuroimmunol., 113, 30–39, 2001.

[109] SHEPHERD GMG, and SVOBODA K., "Laminar and columnar organization of ascending excitatory projections to layer 2/3 pyramidal neurons in rat barrel cortex," *J. Neurosci.,* **25**, 5670 -5679, 2005.

[110] SHEPHERD GMG, STEPANYANTS A, BUREAU I, CHKLOVSKII DB, and SVOBODA K., "Geometric and functional organization of cortical circuits," *Nat Neurosci.,* **8**, 782 -790, 2005.

[111] SIMONI, A. D., and YU, L.M., " Preparation of organotypic hippocampal slice cultures: interface method." Nature Protocols 1, 1439 – 1445, 2006.

[112] SOBCZYK A, SCHEUSS V, and SVOBODA K., "NMDA receptor subunit-dependent [Ca2+] signaling in individual hippocampal dendritic spines," *J. Neurosci.,* **25**, 6037 -6046, 2005 .

[113] SOELLER, C. and CANNELL, M. B., "Construction of a 2-photon microscope and optimization of illumination pulse duration," Pflugers Arch European Journal Of Physiology, 432, 555-561, 1996.

[114] STOPPINI, L., BUCHS, P.A. and MULLER, D., "A simple method for organotypic cultures of nervous tissue," J. Neurosci. Methods 37, 173–182, 1991.

[115] TAKUMA, H., SAKURAI, M. and KANAZAWA, I., "*In vitro* formation of corticospinal synapses in an organotypic slice co-culture," Neuroscience 109, 359–370, 2002.

[116] TOM, V.J., DOLLER, C.M., MALOUF, A.T. and SILVER, J., "Astrocyte-associated fibronectin is critical for axonal regeneration in adult white matter," J. Neurosci., 24, 9282–9290, 2004.

[117] TRULLIER, O., and MEYER, J. A., "Animat navigation using a cognitive graph," Biol Cybern, 83(3), 271-85, 2000.

[118] TSAI P.S., NISHIMURA, N, YODER, E.J., DOLNICK, E.M., WHITE, G.A., and KLEINFELD, D., "Principles, design and construction of a two-photon laser scanning microscope for *in vitro* and in vivo brain imaging," In vivo optical imaging of brain, CRC Press, 2002.

[119] VUKASINOVIC J., and GLEZER A., " A microperfusion chamber for neuronal cultures," Proceedings of Bio2006, 1-2, 2006.

[120] WAGENAAR, D. A., PINE, J. and POTTER, S. M., "An extremely rich repertoire of bursting patterns during the development of cortical cultures," BMC Neuroscience, 7(11), 2006.

[121] WAGENAAR, D. A., MADHAVAN, R., PINE, J., and POTTER, S. M., "Controlling bursting in cortical cultures with closed-loop multi-electrode stimulation," J. Neuroscience 25: 680-688, 2005.

[122] WAGENAAR, D. A., and POTTER, S. M., "A versatile all-channel stimulator for electrode arrays, with real-time control," Journal of Neural Engineering, 1, 39-45, 2004.

[123] WAGENAAR, D. A., PINE, J., and POTTER, S. M., "Effective parameters for stimulation of dissociated cultures using multi-electrode arrays," Journal of Neuroscience Methods, 138, 27-37, 2004.

[124] WAGENAAR, D. A. and POTTER, S. M., "Real-time multi-channel stimulus artifact suppression by local curve fitting," J. Neurosci. Methods, 120, 113-120, 2002.

[125] WAGENAAR, D. A., PINE, J., and POTTER, S. M., "Searching for plasticity in dissociated cortical cultures on multi-electrode arrays," Journal of Negative Results in BioMedicine, 5,16, 2006.

[126] WOKOSIN, D. L., AMOS, B. G. and WHITE, J. G., "Detection sensitivity enhancements for fluorescence imaging with multi-photon excitation microscopy," *IEEE EMBS,* **20**, 1707-1714, 1998.

[127] YAMAMOTO M., "Electrical activity in thin sections from the mammalian brain maintained in chemically defined media *in vitro*," Journal of Neurochemistry 13, 1333-1343, 1966.